PUBLICATIONS OF THE ASTRONOMICAL SOCIETY OF THE PACIFIC, 111:1049–1087, 1999 September

Invited Review

Massive Stars: Their Environment and Formation

GUIDO GARAY
Departamento de Astronomía, Universidad de Chile, Casilla 36-D, Santiago, Chile
AND
SUSANA LIZANO
Instituto de Astronomía, UNAM, Apdo. Postal 70-264, 04510 México, D.F., México

Received 1999 May 6; accepted 1999 May 7

ABSTRACT. Cloud environment is thought to play a critical role in determining the mechanism of formation of massive stars. In this contribution we review the physical characteristics of the environment around recently formed massive stars. Particular emphasis is given to recent high angular resolution observations which have improved our knowledge of the physical conditions and kinematics of compact regions of ionized gas and of dense and hot molecular cores associated with luminous O and B stars. We will show that this large body of data, gathered during the last decade, has allowed significant progress in the understanding of the physical processes that take place during the formation and early evolution of massive stars.

1. INTRODUCTION

Massive stars in our Galaxy are born predominantly within the dense cores of giant molecular clouds. This premise is strongly supported by a wealth of observations which show that hallmarks of newly formed massive stars, such as compact regions of ionized gas, are intimately associated with warm and dense regions of molecular gas (Churchwell, Walmsley, & Cesaroni 1990; Cesaroni et al. 1991; Plume, Jaffe, & Evans 1992). It remains unclear, however, how the actual formation of massive stars takes place. In the current paradigm of the formation of low-mass stars (Shu, Adams, & Lizano 1987; Shu et al. 1993), the central region of a dense core begins to condense quasi-statically through the process of ambipolar diffusion. As the magnetic pressure support decreases, the central region reaches an unstable quasi-equilibrium state in which the thermal pressure alone supports the core against its self-gravity. This stage marks the initial condition for dynamical collapse. After becoming gravitationally unstable, the core undergoes a phase of free-fall isothermal collapse. As ensuing major evolutionary stages, the model predicts (*a*) an accretion stage, characterized by the presence of a central protostar and a circumstellar disk surrounded by an infalling envelope of dust and gas; (*b*) a phase in which the protostar deposits linear and angular momentum, and mechanical energy into its surroundings through jets and molecular outflows; and finally (*c*) a relatively more advanced phase in which the protostar settles onto the zero-age main sequence (ZAMS), increasing its luminosity. Although this paradigm has been very successful in explaining what is observationally known about the formation of low-mass stars (cf. Lada 1991), its applicability to the formation of massive stars is arguable. The evolutionary timescales of high-mass stars are much shorter than for low-mass stars. Massive stars are expected to affect their environment very soon after a stellar core has formed since their Kelvin-Helmholtz timescale ($\leq 10^4$ yr for an O star) is short compared with all other relevant evolutionary timescales. They begin burning hydrogen and reach the main sequence before they stop accreting matter from the surrounding protostellar envelopes. The formation of a massive disk, and hence the appearance of molecular outflows and jets, in the accretion phase is thus not clear. In addition, in stage *c*, the massive star starts to produce an appreciable output of UV photons and possibly develops strong winds which will drastically affect the physical conditions, structure, and chemistry of their surroundings. Since in this stage the massive star ionizes its surroundings, giving rise to a small region of ionized gas, this phase is usually referred as the ultracompact H II region phase.

An understanding of the physical processes that dominate during the early stages of formation of massive stars and their influence back on the molecular gas out of which they formed requires a detailed knowledge of the physical conditions of the environment prior to and after the formation of the star. Until recently, the observational evidence concerning the process of formation of massive stars was, however, scarce. Many questions remain unanswered, such

as: What is the basic unit within a molecular cloud that will give birth to a massive star? Are massive stars surrounded by disks? Is the bipolar outflow phase seen in low-mass stars also present in the formation of high-mass stars? How is the environment around newly formed massive stars affected by their strong radiation and winds? What is the connection between massive stars and masers? Are the different maser species signposts of different evolutionary stages? Are massive stars formed by accretion processes or by stellar mergers? The difficulties in determining the physical conditions of the gas during the formation and early evolution of an individual massive star are not only due to their rapid evolution, but also to some observational disadvantages. Massive stars are born deeply embedded within molecular cores, hence the process of star formation is obscured by the dust that surrounds them, and it cannot be investigated at optical wavelengths. In addition, massive stars are usually born in clusters or groups, hence their individual studies are usually afflicted by confusion, particularly because they are found at greater distances from the Sun than the sites of low-mass star formation.

O and B stars emit the bulk of their radiation at wavelengths shorter than the Lyman continuum limit which ionizes the dense molecular gas producing compact H II regions. In addition, circumstellar dust surrounding the region of ionized gas absorbs all the stellar radiation, either directly or after being processed in the nebula, producing compact regions of warm dust that reemit the absorbed energy in the far-infrared. Hence, the study of the environment around young massive stars would be better performed through observations of its ionized, atomic, and molecular constituents at infrared, millimeter, and radio wavelengths where the opacity of the dust and gas is considerably smaller. The advent of aperture synthesis radio telescopes has provided high angular resolution, sensitivity, and spectral resolution and has opened up this field for investigation. A wealth of new observations of ultracompact H II regions, photodissociation regions, cocoons of warm dust, hot molecular cores, and maser emission are providing important data about the physical conditions and kinematics of the ionized and molecular gas very close to newly formed stars and therefore partial answers to the questions posed above are beginning to emerge.

In this article we review the results of recent high spatial resolution observations of high-mass star-forming regions which have significantly contributed to the understanding of the physical conditions and dynamics, of both the ionized and molecular gas, in the immediate vicinity of recently formed massive stars. The review is organized as follows. In § 2 we present recent observational data on the physical conditions and kinematics of compact H II regions. Compact H II regions tell us about the locations where massive stars form. They also provide information about the circumstances under which massive stars form. Do massive stars form in the densest part of molecular clouds? Do massive stars form in a highly clustered way? A number of problems that have been raised by these observations is also discussed. For instance, radio continuum surveys of our Galaxy have shown the presence of a considerable number of ultracompact H II regions, with radii in the range from $\sim$0.02 to $\sim$0.2 pc (Wood & Churchwell 1989a; Kurtz, Churchwell, & Wood 1994). Assuming that the age of these compact H II regions corresponds to their dynamical ages, then their small sizes would imply that they are very young objects. The large number of ultracompact (UC) H II regions predicted to exist in our Galaxy and their short dynamical ages pose a problem: *the rate of massive star formation appears to be much greater than other indicators suggest* (Wood & Churchwell 1989b; Churchwell 1990). In § 3 we discuss the characteristics of the molecular gas around massive stars. Particular emphasis is placed on recent high angular resolution ammonia observations which have shown the presence of very dense, warm, and compact structures of molecular gas near massive stars (Garay, Moran, & Rodríguez 1993a; Cesaroni et al. 1994a; Gómez, Garay, & Lizano 1995). We address questions such as: Are the dense and warm ammonia clumps remnants of the process of collapse and fragmentation of a molecular core or rather the product of the interaction of the stellar winds and UV radiation from the luminous newly formed star with the surrounding natal molecular gas? Are they the basic units of massive molecular clouds that produce massive stars? In § 4 we discuss results from recent observations of masers which are powerful signposts of active massive star formation. These masers provide information about the physical conditions and kinematics of the gas surrounding massive stars on scales of 10–10^3 AU. In § 5 we discuss how massive stars may form. First we bring together the results presented in previous sections with other important observational results not dealt before which set the observational constraints for possible models. Then we discuss the role of different physical processes in the formation of massive stars, and finally a formation scenario is proposed. A summary is presented in § 6. The observed properties and models of the circumstellar dust cocoons associated with compact H II regions are not covered in this article but are nicely discussed in the thorough reviews of newly formed stars and their environments given by Churchwell (1990, 1991, 1993).

2. COMPACT H II REGIONS

Young massive stars emit copious Lyman continuum photons which excite their surroundings, giving rise to dense and small regions of ionized gas. These regions, called compact H II regions, are characterized by having high emission measures which make them very bright at radio

wavelengths. Hence they act as powerful radio beacons of newly formed stars that are still embedded in their natal molecular clouds. In the first part of this section we summarize what is known about the morphologies, physical conditions, and kinematics of compact H II regions determined from high angular resolution radio observations. In the second part we describe theoretical models that have been proposed to explain the observed and derived properties of compact H II regions.

2.1. Physical Parameters

Most of the physical parameters of compact regions of ionized gas are determined from observations at radio wavelengths. By modeling the observed radio continuum spectrum as due to free-free emission arising from an isothermal and homogeneous region of ionized gas, the electron temperature and emission measure can be determined from the optically thick and thin portions of the spectrum, respectively (cf. Gordon 1988). In addition, if the geometry and the distance to the compact H II region are known, its physical size and the average electron density can be derived (Mezger & Henderson 1967). The electron temperature can also be determined from observations of radio recombination lines (cf. Brown, Lockman, & Knapp 1978).

The regions of ionized gas around recently formed massive stars have diameters, L, between 0.005 and 0.5 pc, electron densities, n_e, between 2×10^3 and 3×10^5 cm^{-3}, and emission measures, EM, in the range from 2×10^6 to 1×10^9 pc cm^{-6}. These physical parameters are significantly correlated, as shown in Figure 1, which presents plots of the electron density and emission measure against diameter for a large sample of compact H II regions. The data were taken from the surveys of compact H II regions of Wood & Churchwell (1989a; *squares*) and Garay et al. (1993b; *circles*) and from the high angular resolution observations of compact H II regions within the Sgr B2 and W49A massive star-forming regions of Gaume et al. (1995a; *pentagons*) and De Pree, Mehringer, & Goss (1997; *triangles*), respectively. Least-squares linear fits (*solid lines*) to the trends give $n_e = 7.8 \times 10^2 L^{-1.19 \pm 0.05}$ and $\mathrm{EM} = 6.3 \times 10^5 L^{-1.53 \pm 0.09}$, where L is in pc, n_e is in cm^{-3}, and EM is in pc cm^{-6}. Since EM is proportional to $n_e^2 L$, these two relations are not independent of each other. In what follows we will discuss only the electron density versus size relationship.

Assuming that the distribution of spectral types (and hence of the ionization characteristics) among the stars exciting compact H II regions is independent of the initial conditions of the surrounding medium, then n_e should be on average proportional to $L^{-3/2}$. A feasible explanation for the shallower observed power-law index is that on average ultracompact ($L < 0.05$ pc) H II regions are excited by stars with lower luminosities (hence lower number of ionizing photons) than those exciting compact ($0.05 < L < 0.5$ pc) H II regions. This hypothesis is supported by Figure 2, which plots the rate of ionizing photons, N_u, versus the diameter of all H II regions plotted in Figure 1 and of the H II regions in the survey of Kurtz et al. (1994; *stars*). It clearly shows that UC H II regions are excited by less luminous stars than those exciting compact H II regions. It could also be possible that some of the UC H II regions in the surveys of Wood & Churchwell (1989a) and Kurtz et al. (1994) do not contain luminous embedded stars but are instead externally ionized objects, corresponding to the denser structures within a larger, inhomogeneous H II region that is excited by a single luminous star. This possibility is sustained by the fact that practically all the interstellar media has a clumpy structure (cf. Hartquist & Dyson 1993). The number of ionizing photons required to excite the ultracompact source is, in this case, smaller than the total number actually emitted by the star by a factor of $\Omega/4\pi$, where Ω is the solid angle subtended by the UC clump from the star. Thus, the spectral type derived from the radio observations of the UC H II region corresponds to a lower limit of the true spectral type of the external exciting star. An alternative explanation for the observed power-law index is that interstellar dust within UC H II regions absorbs an important fraction of the ionizing photons.

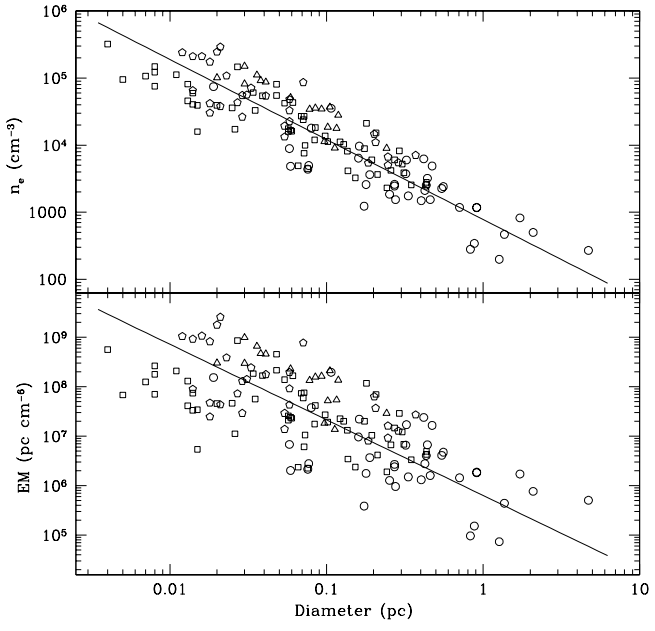

FIG. 1.—Relationship between physical parameters of compact and ultracompact H II regions. *Top*: Electron density vs. diameter. *Bottom*: Emission measure vs. diameter. The lines are least-squares linear fits to the data points (*squares*: Wood & Churchwell 1989a; *circles*: Garay et al. 1993b; *pentagons*: Gaume et al. 1995a; *triangles*: De Pree et al. 1997).

Radio continuum observations with high angular resolution show that compact regions of ionized gas exhibit a variety of morphologies (cf. Wood & Churchwell 1989a;

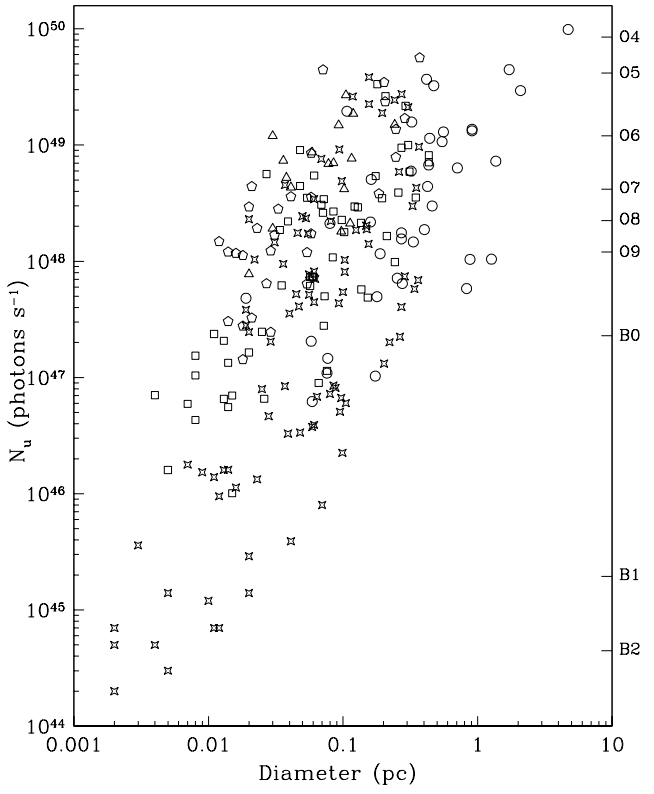

FIG. 2.—Ionizing photon rate vs. diameter relationship for compact and ultracompact H II regions (*stars*: Kurtz et al. 1994; all other symbols same as in Fig. 1). Marked on the right axis is the number of ionizing photons emitted by ZAMS stars with spectral types from B2 to O4.

Garay et al. 1993b; Kurtz et al. 1994). From a survey of 75 compact H II regions, Wood & Churchwell (1989a) found that 20% have cometary shapes—characterized by exhibiting a bright compact head and a diffuse extended tail—16% show core-halo morphologies, 4% exhibit shell structures, 17% have irregular or multiple-peaked brightness distributions, and 43% are spherical or unresolved. Radio continuum maps of the prototype cometary (G34.3+0.15; Reid & Ho 1985; Garay, Rodríguez, & van Gorkom 1986), shell (G45.07+0.13; Turner & Matthews 1984), and bipolar (Campbell 1984) compact H II regions are shown in Figure 3. As noted by Wood & Churchwell (1989a) and Fey et al. (1992), the morphology of a source determined through radio synthesis observations depends not only on its intrinsic brightness distribution but on the response (synthesized beam) of the telescope. Thus, the classification depends on the sensitivity of the instrument to different size scales. In particular, objects classified as irregular or multiple peaked with very high angular resolution have been found to be bright substructures within more extended structures as observed with coarser angular resolution (cf. Garay et al. 1993b; Kurtz et al. 1999a). These could correspond to the externally ionized globules discussed above. The intrinsic morphology of the ionized gas, on the other hand, depends on the characteristics of both the exciting star and of the environment, as well as on their interaction. In § 2.3 we discuss theoretical models that have been proposed to explain the morphologies of compact H II regions.

2.2. Kinematics

Motions of the ionized gas within H II regions may be shaped by the density structure of the ambient medium, by stellar winds, and/or by the motion of the exciting star with respect to the ambient medium. To determine the relative contribution of these processes, a detailed knowledge of the velocity field across H II regions is required. Information about the kinematics of compact H II regions can be directly derived from observations of radio recombination lines, which yield the systemic velocity and the line width of the ionized gas. In this section we first discuss the observed characteristics of the integrated line profiles from compact H II regions, which provide information about the global properties of the motions, and then the characteristics of the velocity field across compact H II regions of different morphological types determined from observations with high angular resolution.

2.2.1. Global Motions

The spectral broadening of recombination lines from H II regions includes three main components (cf. Gordon 1988): (1) thermal broadening, $\Delta v_{\rm th}$,

$$\Delta v_{\rm th} = \left(8 \ln 2 \, \frac{kT_e}{m_{\rm H}}\right)^{1/2} = 21.4 \left(\frac{T_e}{10^4 \ {\rm K}}\right)^{1/2} \ {\rm km \ s^{-1}} \ , \quad (1)$$

where T_e is the electron temperature, k is Boltzmann's constant, and $m_{\rm H}$ is the mass of the hydrogen atom; (2) broadening due to electron impacts, Δv_i, given by

$$\Delta v_i = 4.3 \left(\frac{n}{100}\right)^{7.4} \left(\frac{10^4 \ {\rm K}}{T_e}\right)^{0.1} \left(\frac{n_e}{10^4 \ {\rm cm^{-3}}}\right) {\rm km \ s^{-1}} \ , \quad (2)$$

where n is the principal quantum number of the recombination line; and finally (3) nonthermal broadening, $\Delta v_{\rm nt}$, which might be produced by blending of emission, within an observing beam, from gas at different flow velocities (microturbulence) or large-scale velocity fields (macroturbulence). In general, the line profile will be a Voigt function, corresponding to the convolution of a Gaussian profile and a Lorentzian profile due to impact broadening. If pressure broadening is not important, which at the physical conditions of compact H II regions is a good aproximation for recombination lines with $n \leq 100$, the observed line

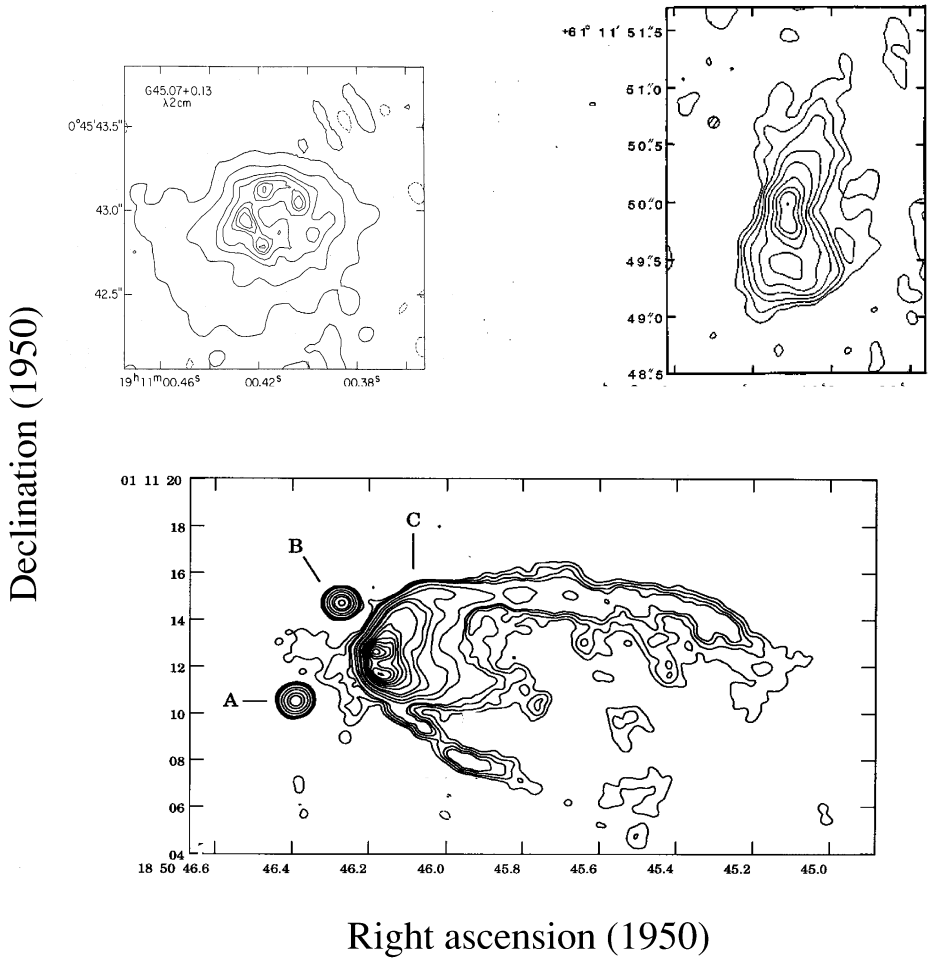

FIG. 3.—Morphologies of ultracompact H II regions. *Top right*: Radio continuum emission of the bipolar source NGC 7538 (Campbell 1984). *Top left*: Radio continuum emission of the shell source G45.07+0.13 (Turner & Matthews 1984). *Bottom*: Radio continuum emission of the cometary source G34.3+0.15 (Gaume et al. 1994).

profile, $\Delta v_{\rm obs}$, is roughly Gaussian, and we may write

$$\Delta v_{\rm obs} = (\Delta v_{\rm th}^2 + \Delta v_i^2 + \Delta v_{\rm nt}^2)^{1/2} . \quad (3)$$

The observed parameters of radio recombination lines from compact H II regions are distinctly different from those of larger regions. In particular, the line widths of compact H II regions are considerable broader than those of diffuse H II regions. This is illustrated in the upper panel of Figure 4, which plots the observed line width of recombination lines against diameter for three classes of H II regions: compact (*stars*), typical (*squares*), and extended (*triangles*). As representative of typical and extended H II regions we used, respectively, the sample of 36 objects observed by Churchwell et al. (1978) in the H109α line and the sample of 23 low-density objects (mainly Sharpless regions) observed by Garay & Rodríguez (1983) in the H125α line. The sample of compact H II regions, listed in Table 1, consists of all compact (diameters less than 0.5 pc) regions of ionized gas observed to date with high angular resolution in either the H66α or H76α lines, which are the most commonly observed lines with present interferometric instruments. In order to show which is the dominant mechanism that produces the broad lines in compact H II regions, plotted in the middle and lower panels of Figure 4 are the thermal and nonthermal line widths against the diameters of all H II regions. The thermal and pressure broadening widths were computed from equations (1) and (2), respectively, using the electron temperatures derived from the radio recombination line observations and the electron densities derived from the radio continuum observations. The nonthermal widths were then computed from these and the observed line widths, using equation (3). Figure 4 clearly shows that the most important source of line broadening in compact H II regions is of nonthermal origin, the thermal line widths being roughly the same in all samples.

The nonthermal broadening of the lines may be either due to large scale systematic motions of the ionized gas or

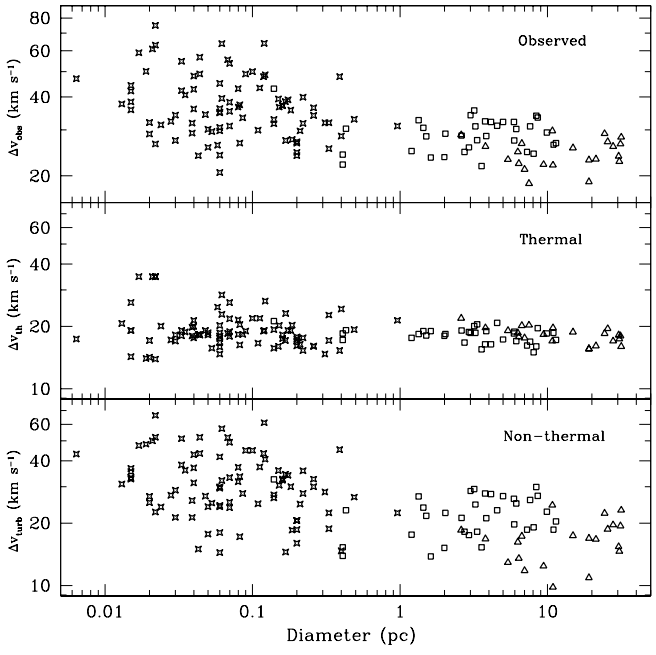

FIG. 4.—Line width vs. diameter relationship for H II regions. *Triangles*: extended H II regions (Garay & Rodríguez 1983); *squares*: typical H II regions (Churchwell et al. 1978); *stars*: compact and ultracompact H II regions (Table 1). *Top*: Observed line width. *Middle*: Thermal line width. *Bottom*: Nonthermal line width.

due to turbulence, namely, the motions of small-scale eddies within the compact H II region. Possible sources of turbulence in H II regions are the expansion of dense, small-scale structures of gas into less dense surrounding medium; champagne flows; stellar winds; and magnetic turbulence (Arons & Max 1975). As can be seen in the lower panel of Figure 4, the nonthermal line width of H II regions decreases as the size increases. Explanations for this trend have not yet been given. Two possible models that could explain this behavior are photoevaporation from massive circumstellar disks (Hollenbach et al. 1994; Yorke & Welz 1996; Richling & Yorke 1997) and mass loading from clumps embedded within UC H II regions (Dyson, Williams, & Redman 1995; Lizano et al. 1996; see discussion in § 2.5). In the photoevaporated disk case, the line width close to the disk would reflect rotation plus expansion motions of the ionized gas, whereas at larger distances it would reflect only expanding motions. In the photoevaporation from clumps model, the photoevaporated material that is fed into the flow is expected to increase the mean velocity dispersion of the region of ionized gas. Since the amount of incorporated photoevaporated gas is proportional to the number of ionizing photons, the observed trend could be due to the geometric dilution of the ionizing photons with distance. None of these models has, however, made explicit predictions regarding the dependence of line width with distance, and further theoretical work is needed in this area. The photoevaporated disk explanation may find support with the high angular resolution recombination line observations of the complex W49A massive star-forming region which reveal that the H II regions with the broader line widths exhibit also larger spectral indices (De Pree et al. 1997). The broad line sources have spectral indices in the range between 0.3 and 1.0, consistent with those expected for ionized wind sources (Panagia & Felli 1975).

2.2.2. *Motions within Individual Regions*

High angular resolution observations of radio recombination line emission are now making it possible to map the line center velocity and line width across compact H II regions and therefore allowing one to investigate the kinematics of the ionized gas within individual regions. Detailed observations of the physical conditions and kinematics of the ionized gas within compact H II regions have been presented by Garay et al. (1986), Gaume & Claussen (1990), Zijlstra et al. (1990), Wood & Churchwell (1991), Garay, Lizano, & Gómez (1994), Afflerbach et al. (1994), and De Pree et al. (1994). In what follows we only discuss the observed characteristics of the velocity fields in compact H II regions with bipolar morphologies since, as will be argued below, they provide information of an important evolutionary stage of massive stars.

Compact H II regions with bipolar radio continuum morphologies have been found in only a handful of cases: NGC 7538 IRS 1 (Campbell 1984; Turner & Matthews 1984), NGC 6334A (Rodríguez, Cantó, & Moran 1988), G45.48 + 0.13 (Garay et al. 1993b), and W49A-A (De Pree et al. 1997). The radio continuum emission from the core of NGC 7538 IRS 1 shows a double lobe structure, with lobes separated by $\sim$600 AU. The prototype region, NGC 6334A, exhibits a bright compact central region, having a shell appearance, and extended symmetrical lobes of lower brightness. Campbell (1984) and Rodríguez et al. (1988) suggested that the bipolar morphology results from the confinement of the ionized gas by a flattened structure of neutral gas and dust. Radio recombination line observations of bipolar, or elongated, H II regions have revealed that the line center velocity exhibits a steep gradient along their symmetry axis. The observed morphology and kinematics suggest that the ionized material in these sources is undergoing a high-velocity bipolar outflow. The highly elongated H II region K3-50A exhibits a change in the H76α line center velocity of $\sim$56 km s^{-1} over a linear distance of $\sim$0.37 pc, implying a velocity gradient along the major axis of $\sim$150 km s^{-1} pc^{-1} (De Pree et al. 1994). Similarly, the H76α and H92α line center velocity of the NGC 6334A region exhibits a velocity gradient along the axis of symmetry of the lobes (De Pree et al. 1995a), suggesting that the lobes correspond to the two halves of a collimated outflow from a central star. An outflow velocity of $\sim$30 km s^{-1} is

TABLE 1

PARAMETERS OF COMPACT H II REGIONS

Source	Diameter (pc)	n_e (10^4 cm^{-3})	Δv (km s^{-1})	Line	T_e (K)	Reference
DR 21A	0.05	2.7	30.1	H76α	7200	1
DR 21B	0.06	3.0	30.6	H76α	7540	1
DR 21C	0.07	3.0	31.0	H76α	7010	1
DR 21D	0.05	2.3	25.7	H76α	7550	1
DR 21E	0.08	0.8	43.0	H76α	10100	1
DR 21F	0.10	0.5	50.0	H76α	10480	1
G5.89−0.39	0.12	2.7	64.0	H76α	8000	2
G5.89−0.39A	0.044	23.7	49.0	H76α	7200	3
G5.89−0.39B	0.044	23.7	56.7	H76α	7200	3
G10.62−0.38	0.048	15.6	34.3	H76α	8000	3
G11.94−0.62	0.043	6.1	23.9	H76α	7300	3
G29.96−0.02	0.109	4.4	29.9	H76α	6000	3
G30.54+0.0A	0.167	1.8	38.4	H76α	6400	3
G34.3+0.2	0.068	13.0	55.5	H76α	7500	4
G35.20−1.74	0.039	8.6	31.8	H76α	7100	3
G45.07+0.13	0.040	16.0	48.1	H76α	8700	4
G45.12+0.13	0.119	11.3	47.8	H76α	7900	3
GM 24	0.04	3.8	42.8	H76α	10000	5
K3-50A	0.09	7.9	49.0	H76α	7900	6
K3-50C1	0.06	3.8	35.0	H76α	7100	6
NGC 6334A	0.20	0.31	23.9	H76α	6900	7
NGC 6334F	0.02	3.8	32.0	H76α	6400	7
W3A	0.40	0.84	28.4	H76α	12900	1
W3B	0.186	1.7	27.5	H76α	9000	1
W3C	0.082	1.96	26.7	H76α	9100	1
W3(OH)	0.015	13.0	42.1	H76α	8000	8
W49S-K	0.22	2.2	39.9	H76α	6800	8
W51d	0.20	2.0	27.0	H76α	6600	8
W51e	0.33	1.0	25.4	H76α	6400	8
G10.6−0.4	0.086	3.9	33.3	H66α	7300	8
G19.6−0.2A	0.053	2.4	29.5	H66α	5400	8
G20.1−0.1A	0.039	2.9	29.1	H66α	8600	8
G34.3+0.2	0.033	10.0	54.7	H66α	8000	4
G45.07+0.13	0.033	12.0	42.3	H66α	7100	4
M17 UC1	0.0064	33.	47.0	H66α	6600	9
N7538 IRS 1 N	0.0026	10.	180.0	H66α	15000	10
N7538 IRS 1 S	0.0025	10.	180.0	H66α	15000	10
Sgr N K1	0.024	12.0	31.3	H66α	8800	11,12
Sgr N K3	0.013	28.0	37.6	H66α	9400	11,12
Sgr N K4	0.04	7.7	36.0	H66α	6800	11,12
Sgr N K5	0.21	2.8	29.7	H66α	5900	11,12
Sgr N K6	0.39	2.0	47.8	H66α	5100	11,12
Sgr N L	0.22	3.4	31.7	H66α	5100	11,12
Sgr N L13.30	0.06	3.4	20.6	H66α	4700	11,12
Sgr N R	0.31	1.0	31.9	H66α	4700	11,12
Sgr A1	0.26	3.3	36.4	H66α	5700	11,13
Sgr A2	0.06	4.4	29.7	H66α	6700	11,13
Sgr B	0.035	12.7	40.7	H66α	7700	11,13
Sgr B9.89	0.019	6.2	50.1	H66α	4300	11,13
Sgr B9.96	0.022	5.5	26.5	H66α	4200	11,13
Sgr B9.99	0.028	5.4	32.3	H66α	6500	11,13
Sgr B10.06	0.015	8.5	35.7	H66α	4500	11,13
Sgr B10.10	0.020	6.5	28.9	H66α	4400	11,13
Sgr C	0.03	6.2	27.3	H66α	6300	11,13
Sgr D	0.03	8.4	34.1	H66α	7200	11,13
Sgr E	0.06	9.4	34.8	H66α	7000	11,13
Sgr F1	0.021	26.0	61.	H66α	26400	11,13
Sgr F2	0.022	22.0	75.	H66α	26400	11,13
Sgr F3	0.022	43.0	63.	H66α	26400	11,13

TABLE 1—*Continued*

Source	Diameter (pc)	n_e (10^4 cm^{-3})	Δv (km s^{-1})	Line	T_e (K)	Reference
Sgr F4.....	0.017	26.0	59.	H66α	26400	11,13
Sgr G	0.015	26.0	44.3	H66α	14900	11,13
Sgr H	0.06	13.0	45.1	H66α	6100	11,13
Sgr I.....	0.08	8.3	36.6	H66α	7300	11,13
Sgr J.....	0.26	1.7	34.0	H66α	5600	11,13
Sgr Y.....	0.06	3.0	24.0	H66α	5500	11,13
Sgr Z	0.20	1.3	24.6	H66α	5700	11,13
W49A	0.070	5.5	53.7	H66α	10400	14
W49B	0.062	4.5	63.9	H66α	17600	14
W49C	0.062	6.0	39.5	H66α	11500	14
W49D	0.070	5.6	38.2	H66α	7800	14
W49F	0.058	5.5	26.2	H66α	13400	14
W49G1.....	0.112	3.4	43.3	H66α	10500	14
W49G2.....	0.122	3.3	48.6	H66α	15400	14
W49G3.....	0.160	3.1	37.0	H66α	7200	14
W49G4.....	0.140	3.1	32.8	H66α	8100	14
W49G5.....	0.152	3.0	36.6	H66α	8900	14
W49I	0.182	1.1	35.6	H66α	8000	14
W49J	0.168	1.7	27.3	H66α	11700	14
W49L	0.96	0.4	31.0	H66α	10000	14
W49M	0.160	1.2	37.1	H66α	6700	14
W49N	0.070	2.3	35.3	H66α	14900	14
W49O	0.082	5.0	37.3	H66α	5800	14
W49S.....	0.174	1.9	39.0	H66α	8000	14
W3(OH).....	0.015	13.0	38.3	H66α	8000	8

REFERENCES.—(1) Roelfsema 1987; (2) Zijlstra et al. 1990; (3) Wood & Churchwell 1989a; (4) Garay, Rodríguez, & van Gorkom 1986; (5) Roth et al. 1988; (6) De Pree et al. 1994; (7) De Pree et al. 1995a; (8) Garay, Reid, & Moran 1985; (9) Johnson, De Pree, & Goss 1998; (10) Gaume et al. 1995b; (11) Gaume et al. 1995a; (12) De Pree et al. 1995c; (13) De Pree et al. 1996; (14) De Pree, Mehringer, & Goss 1997.

derived. The largest mass motions of ionized gas detected so far are observed toward the core of the NGC 7538 IRS 1 compact H II region. Gaume et al. (1995b) detected extremely wide H66α line profiles, of $\sim$180 km s^{-1} (FWHM), implying the presence of substantial mass motions. They suggest that the motions trace a stellar wind outflow and photoevaporation of nearby clumpy neutral material. These results are particularly relevant for the study of the formation process of massive stars, since they provide definitive evidence for the presence of collimated ionized bipolar outflows. In addition, they may be implying that massive disks, which could collimate the wind, are formed during the process of collapse of massive stars.

2.3. Theoretical Models

This section presents an overview of the theoretical models proposed to explain the characteristics of the compact H II regions. We place particular emphasis on the model predictions regarding the morphologies and kinematics of the ionized gas and their confrontation with observations.

2.3.1. *Classical Expansion*

Because of the difference in pressure between the ionized gas and the surrounding neutral gas, H II regions are expected to expand in the neutral ambient medium. The classical analysis of the expansion of H II regions (cf. Spitzer 1978; Dyson & Williams 1980) assumes that the ambient medium is homogeneous in density and temperature and neglects the role of stellar winds. The expansion in this case is characterized by two main phases. In the initial stage, which starts when the young massive star embedded in a molecular cloud begins to produce UV photons, an ionization front is formed which moves rapidly outward through the ambient medium. This phase of expansion comes to an end when the number of photoionizations within the ionized region equals the number of recombinations. At this point the H II region fills a region with a radius R_S^0, called the Strömgren radius, given by (Strömgren 1939)

$$R_S^0 = 0.032\left(\frac{N_u}{10^{49}\ \mathrm{s}^{-1}}\right)^{1/3}\left(\frac{10^5\ \mathrm{cm}^{-3}}{n_0}\right)^{2/3}\ \mathrm{pc}\ , \qquad (4)$$

where n_0 is the initial density of the ionized gas ($=2n_{\mathrm{H}_2}$, where n_{H_2} is the molecular density of the ambient gas), and

N_u is the rate of ionizing photons emitted by the exciting star. This initial phase is rapid and short-lived. The characteristic time, t_S, in which the Strömgren radius is reached is given by

$$t_S = \frac{1}{n_0 \alpha_B} ,$$

where α_B is the recombination coefficient excluding captures to the ground level. For an O7 ZAMS star, which has an output of UV photons of 4×10^{48} s^{-1} (Panagia 1973), born in a medium with an ambient density of 10^5 cm^{-3}, the Strömgren radius, of 0.015 pc, is reached in $\sim$1 yr. This, however, should only be taken as a fiducial value since it is likely that the star turns on its output of UV photons in a lapse of time considerably larger than this.

Afterward, the heated gas will expand and form a shock front that moves out through the neutral gas. The rate of expansion of the H II region during this phase is then determined by the interaction between the ionization and shock fronts. In this phase the radius, R_i, of the H II region increases with time, t, as (cf. Spitzer 1978)

$$R_i = R_S^0 \left(1 + \frac{7 C_{II} t}{4 R_S^0}\right)^{4/7} , \quad (5)$$

where C_{II} is the sound speed in the ionized gas. The expansion stalls when the hot, but lower density, ionized gas reaches pressure equilibrium with the surrounding cool ambient medium. The final equilibrium radius of the H II region, R_f, is (Dyson & Williams 1980)

$$R_f = \left(\frac{2T_e}{T_0}\right)^{2/3} R_S^0 ,$$

where T_0 is the temperature of the ambient gas. Using equation (4), the equilibrium radius can be written as

$$R_f = 1.1 \left(\frac{N_u}{10^{49}\ \mathrm{s}^{-1}}\right)^{1/3} \left(\frac{T_e}{10^4\ \mathrm{K}}\right)^{2/3} \left(\frac{100\ \mathrm{K}}{T_0}\right)^{2/3} \times \left(\frac{10^5\ \mathrm{cm}^{-3}}{n_0}\right)^{2/3} \mathrm{pc} , \quad (6)$$

and is reached in a lapse of time, t_{eq},

$$t_{eq} \leq 7.6 \times 10^5 \left(\frac{N_u}{10^{49}\ \mathrm{s}^{-1}}\right)^{1/3} \left(\frac{10^5\ \mathrm{cm}^{-3}}{n_0}\right)^{2/3} \times \left(\frac{T_e}{10^4\ \mathrm{K}}\right)^{2/3} \left(\frac{100\ \mathrm{K}}{T_0}\right)^{7/6} \mathrm{yr} . \quad (7)$$

The upper limit arises because in the derivation of equation (5) the pressure of the ambient gas has been neglected.

2.3.2. *Stellar Winds*

The expansion due to the gradient in pressure is not, however, the only way in which the interstellar medium around a young massive star can be set in motion. Luminous, massive stars are known to possess strong stellar winds, and it is possible that the interstellar gas motions are dominated by the wind energy and momentum. Thus, winds may play an important role in the dynamical evolution of compact regions of ionized gas. In fact, stellar winds (Castor, McCray, & Weaver 1975; Shull 1980) have been proposed as the main mechanism for producing the shell morphologies observed in UC H II regions. Another mechanism that could produce a shell structure is radiation pressure on dust grains (Kahn 1974), but this has been shown to be less important than stellar winds (Turner & Matthews 1984).

Massive stars have powerful winds which are expected to cause a considerable impact on their environment as they deposit momentum and mechanical energy into the interstellar medium (Van Buren 1985). It is not known, however, when the wind phenomenon begins in massive stars. Probably well before a stellar wind is set into motion, bipolar outflows produced in the formation process will have a major input of mechanical energy and momentum. Assuming that the dynamical effects of the wind are important from the very beginning of the compact H II region phase, then the evolution proceeds roughly as follows. The interaction of the stellar wind with the interstellar medium produces a dense shell of circumstellar gas that expands away from the star. This shell is exposed to the UV radiation from the recently formed star; thus it will be either totally or partially ionized. The evolution of the H II region is thus closely tied to the evolution of the circumstellar shell. When the shell is driven by the pressure of the hot bubble of shocked stellar wind, the radius of the shell, R_{sh}, increases with time as (Castor et al. 1975)

$$R_{sh} = 0.042 \left(\frac{L_w}{10^{36}\ \mathrm{ergs\ s}^{-1}}\right)^{1/5} \times \left(\frac{n_0}{10^5\ \mathrm{cm}^{-3}}\right)^{-1/5} \left(\frac{t}{10^3\ \mathrm{yr}}\right)^{3/5} \mathrm{pc} , \quad (8)$$

where L_w is the wind mechanical luminosity. The velocity of expansion of the shell, V_{sh}, is then

$$V_{sh} = 24.7 \left(\frac{L_w}{10^{36}\ \mathrm{ergs\ s}^{-1}}\right)^{1/5} \times \left(\frac{n_0}{10^5\ \mathrm{cm}^{-3}}\right)^{-1/5} \left(\frac{t}{10^3\ \mathrm{yr}}\right)^{-2/5} \mathrm{km\ s}^{-1} . \quad (9)$$

UC H II regions with shell or ring structures, determined from observations with high angular resolution, have been

reported by Turner & Matthews (1984) and by Garay et al. (1986). Turner & Matthews (1984) concluded that while the observed shell-like morphologies can be well explained as due to the action of stellar winds, the radiation pressure model faces several difficulties. In particular, the morphology and velocity structure of the G45.07+0.13 compact H II region, observed with 0".4 angular resolution, is well modeled by a ring of ionized gas expanding with a velocity of ~ 10 km s^{-1} driven by the wind of a star with a mechanical luminosity of $\sim 1 \times 10^{35}$ ergs s^{-1} (Garay et al. 1986). Acord, Churchwell, & Wood (1998) and Kawamura & Masson (1998) measured the angular expansion rate of the shell-like UC H II regions G5.89−0.39 and W3(OH), respectively, deriving dynamical ages of ~ 600 and ~ 2300 yr. In the case of G5.89−0.39, assuming that the wind mechanical luminosity of the O6 central exciting star is $\sim 3 \times 10^{36}$ ergs s^{-1} (cf. Van Buren 1985) and that the density of the ambient medium is in the range 10^7–10^8 cm^{-3} (Harvey et al. 1994), then the observed shell radius and expansion velocity can be explained by the simple stellar wind model if the nebula is very young, $\sim 5 \times 10^2$ yr, consistent with the derived dynamical age. In the case of the W3(OH) object, Kawamura & Masson (1998) find that there is sufficient ram pressure from the stellar wind to sustain the shell structure. All these observations attest that winds are present from a very early stage in the evolution of newly formed stars.

The question that arises is: Under what conditions is the wind dynamically more important than the classical expansion due to the difference in pressure between the ionized gas and ambient medium? This has been investigated by Shull (1980) and by Garay et al. (1994), who studied the conditions under which a stellar wind in a medium with density gradients remains confined inside the flow driven by the difference in pressure alone. Shull (1980) concluded that the wind is more important when

$$\left(\frac{L_w}{10^{36}\ \mathrm{ergs\ s^{-1}}}\right) > 0.33\left(\frac{N_u}{10^{49}\ \mathrm{s^{-1}}}\right)^{2/3}\left(\frac{n_0}{10^5\ \mathrm{cm^{-3}}}\right)^{-1/3}.$$

The observational data that could permit one to test this theoretical prediction are not yet available, mainly due to the difficulty of deriving wind mechanical luminosities.

The classical expansion and the stellar wind models predict that H II regions should have spherically symmetric morphologies, and hence they do not adequately explain most of the observed morphologies. In what follows we will discuss models that have been proposed to explain nonspherical morphological types.

2.3.3. *Champagne Flows*

Champagne models assume that the medium in which a massive star is born is not uniform but has strong density gradients, which give rise to an H II region that expands supersonically away from the high-density region in a so-called champagne flow (Tenorio-Tagle 1979; Bodenheimer, Tenorio-Tagle, & Yorke 1979). As for the classical model, the evolution of the region of ionized gas is characterized by two main phases. In the initial stage, the ionization front rushes rapidly into the ambient medium. If the density falls off faster than $r^{-3/2}$, the ionization front in the direction of decreasing density is not trapped and the whole zone facing the low-density region becomes ionized (Franco, Tenorio-Tagle, & Bodenheimer 1990). The large pressure gradient left behind by the ionization front induces the formation of a strong shock which moves supersonically into the ionized low-density medium. This marks the beginning of the second stage of evolution, in which the ionized gas begins to stream away toward the direction of decreasing density.

Theoretical radio continuum maps of H II regions in the champagne phase, namely, when an expanding H II region within a molecular cloud reaches the cloud's edge, have been presented by Yorke, Tenorio-Tagle, & Bodenheimer (1983). The simulations show that during this phase the resulting configuration is a blister-type H II region, which is ionization bounded on the high-density side and density bounded on the side of outward champagne flow. The morphology of the ionized gas is roughly shaped like an opened fan. Numerical calculations of the velocity structure of the ionized gas during the champagne phase show that the ionized material is accelerated in the direction away from the molecular cloud to a relatively high velocity, up to several times its sound speed (Yorke, Tenorio-Tagle, & Bodenheimer 1984). Although the velocity increases with increasing distance from the cloud and can attain values in excess of 30 km s^{-1}, the average velocity of the ionized gas, integrated over the whole H II region, is shifted by a small amount (≤ 5 km s^{-1}) with respect to the velocity of the molecular cloud.

A clear demonstration of the presence of champagne flows associated with compact H II regions has been provided by high angular resolution observations of radio recombination line emission, which have permitted determination of the velocity structure across the compact sources. The two fan-shaped G32.80+0.19B and G61.48+0.09B1 compact H II regions exhibit striking gradients in the velocity of the ionized gas running along of the symmetry axis of the cometary-like structures, the velocity increasing smoothly from the head leading edge to the tail, by ~ 8 and 12 km s^{-1}, respectively (Garay et al. 1994). The observed velocity fields and morphologies, which are in good agreement with those predicted by the champagne model, combined with the similar velocities of the ionized gas at the head position and of the molecular gas, imply that these regions are undergoing champagne flows. Toward the compact H II region W3(OH), Keto et al. (1995) detected in the bright region of ionized gas a velocity gradient of 12 km

s^{-1}, as well as weak radio continuum emission aligned with the velocity gradient and extending away from the high-density gas immediately around the newly formed star. They interpret these observations as indicating that the W3(OH) H II region is undergoing a supersonic champagne flow (see also Sams, Moran, & Reid 1996). The shift in the recombination line velocity with principal quantum number observed toward this source (Berulis & Ershow 1983; Welch & Marr 1987), which is not explained within the classical model, is succesfully modeled in terms of blending of emission from gas at different velocities and densities within the champagne flow model.

2.3.4. *Bow Shocks*

An alternative hypothesis proposed to explain cometary morphologies is that cometary H II regions correspond to bow shocks supported by the stellar wind of an ionizing star that is moving supersonically through the ambient molecular cloud (Van Buren et al. 1990; MacLow et al. 1991). The bow shock model is able to explain fine observational aspects in the morphology of certain cometary H II regions, such as limb brightening and/or that the emission pinches back down to the symmetry axis, which are not easily explained within the champagne models. The characteristic size of a cometary H II region in the bow shock model is provided by the distance in front of the star where the terminal wind shock occurs. This distance, $l_{\rm bs}$, where the momentum flux in the wind equals the ram pressure of the ambient medium, is (Van Buren et al. 1990)

$$l_{\rm bs} = 0.015\left(\frac{\dot{M}_*}{10^{-6}\ M_\odot\ {\rm yr}^{-1}}\right)^{1/2}\left(\frac{v_w}{10^3\ {\rm km\ s}^{-1}}\right)^{1/2} \times \left(\frac{n_0}{10^5\ {\rm cm}^{-3}}\right)^{-1/2}\left(\frac{v_*}{10\ {\rm km\ s}^{-1}}\right)^{-1} \times \left(\frac{\mu_{\rm H}}{1.4}\right)^{-1/2}\ {\rm pc}\ , \quad (10)$$

where $\dot{M}_*$ is the stellar wind mass-loss rate, v_w is the wind terminal velocity, v_* is the velocity of the star relative to the molecular cloud, and $\mu_{\rm H}$ is the mean mass per hydrogen nucleus.

Detailed models of the expected velocity structure of the ionized gas for the bow shock hypothesis have been presented by Van Buren & MacLow (1992). As discussed previously, both the champagne and bow shock models reproduce well the observed morphology of cometary H II regions. The main differences between these two models concern the predictions about the kinematical properties of the ionized gas and lifetimes. The bow shock model predicts that the velocity gradient should be steeper in the head than in the tail, whereas in the champagne model the largest gradients are expected in the tail, where the gas is accelerated out the nozzle. In addition, contrary to the champagne flow model, the bow shock model predicts that the line widths should be broader along the leading edge of the ionization front than they are behind. Finally, the champagne flow model predicts that the velocity of the ionized gas near the coma of the cometary structure should be at rest with respect to the molecular gas velocity, whereas the bow shock model predicts it should be moving with the velocity of the star. Cometary H II regions for which the observations seem to be best explained by a bow shock model are G29.96−0.02 (Wood & Churchwell 1991; Van Buren & Mac Low 1992; Afflerbach et al. 1994) and G13.87+0.28 (Garay et al. 1994). Fey et al. (1995), and Lumsden & Hoare (1996) have however questioned the bow shock interpretation for G29.96−0.02, arguing in favor of a champagne flow. These contradictory results reflect the difficulty in observationally discriminating between the bow shock and champagne models.

Other models that have been proposed to explain cometary regions include supersonic Strömgren regions (Raga 1986), distorted magnetic H II regions (Gaume & Mutel 1987), and distorted stellar wind bubbles (Mac Low & McCray 1988).

2.4. Clustering and Clumpiness

Many compact H II regions are often found in groups and/or in the vicinity of larger, diffuse H II regions (Habing & Israel 1979; Wood & Churchwell 1989a; Garay et al. 1993b; Tieftrunk et al. 1997). This is illustrated in Figure 5, which presents a 4.9 GHz image of the W3 Main star-forming region showing the presence of a cluster of internally ionized compact H II regions and therefore of the presence of a recently formed association of O and B stars (Colley 1980; Tieftrunk et al. 1997). There are more than 10 H II regions, with diameters ranging from 0.01 to 0.7 pc and excited by stars with spectral types ranging from B1 to O6, within a region of $\sim$2 pc in diameter. To investigate quantitatively the gregarious nature of compact H II regions, Garay et al. (1993b) observed with arcsecond angular resolution the radio continuum emission toward 16 highly luminous *IRAS* point sources known to be associated with compact H II regions detected with single-dish telescopes. They found that a large fraction of these sources, particularly the most luminous ones, exhibit complex radio morphologies which could be decomposed into multiple components, strongly supporting the premise that massive stars tend to be born in rich groups or clusters. They conclude that as many as 50% of the *IRAS* point sources associated with unresolved (by single-dish instruments) radio continuum sources might be excited by a cluster of young O and B stars rather than by a single star.

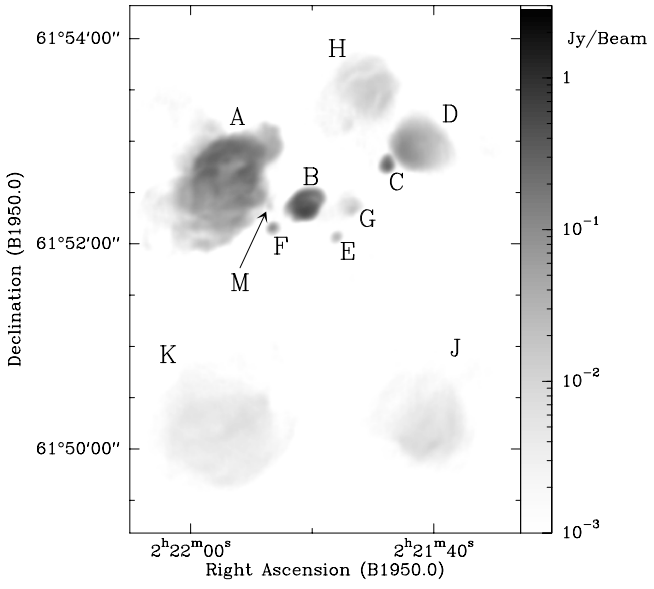

FIG. 5.—Map of the radio continuum emission, at 4.9 GHz, from the W3 massive star-forming region (taken from Tieftrunk et al. 1997).

The complex morphology of regions of ionized gas may not always, however, signal the presence of a cluster of O and B stars. The multiple-peaked or irregular morphologies of compact H II regions may well reflect the presence of density inhomogeneities within the ambient medium. Molecular clouds are known to be clumpy and highly inhomogeneous. In addition, the presence of clumps near recently formed stars might be further enhanced by the fragmentation process that is likely to take place during the gravitational collapse. The important question of whether the multiple compact components mark the location of young O stars or just the position of clumps of gas was first raised by Dreher et al. (1984). It is not clear yet what fraction of the UC H II regions associated with more diffuse H II regions truly corresponds to regions excited by an embedded star and which corresponds to dense clumps within an inhomogeneous region that is being externally excited by a single luminous star which ionizes both the compact region and the larger diffuse region.

2.5. Ages

Regions of ionized gas born in a medium of constant density are expected to expand into the ambient neutral gas at the sound speed of the ionized gas, until they reach pressure equilibrium with the ambient medium. Thus, if H II regions are smaller than R_f (see eq. [6]), then their sizes would indicate their ages. For instance, equation (5) shows that a region of ionized gas excited by an O7 star, born in a medium with a molecular ambient density of 10^5 cm^{-3}, would have expanded to a radius of 0.1 pc in a lapse of time of $\sim 2 \times 10^4$ yr. The small sizes of the UC H II regions ($R \leq 0.05$ pc) would then imply that they are very young objects, with lifetimes $\leq 5 \times 10^3$ yr.

Using the *IRAS* Point Source Catalog (PSC) and a color criterion that they propose selects UC H II regions, Wood & Churchwell (1989b) estimated that there are potentially $\sim$1650 UC H II regions within the disk of our Galaxy. Assuming that these objects have physical parameters similar to those actually derived for a small number of UC H II regions (namely, radii of $\sim$0.05 pc, number of ionizing photons of $\sim 4 \times 10^{48}$ s^{-1}; Wood & Churchwell 1989a) and that they are born in a medium with an ambient density of $\sim 10^5$ cm^{-3}, then their dynamical ages are typically $\sim 5 \times 10^3$ yr. The implied rate of massive star formation, $\psi \sim 0.3$ O stars yr^{-1}, is considerably larger than that estimated from other means. For instance, Güsten & Mezger (1983; see also Downes 1987) estimate that the star formation rate of OB stars ($10\ M_\odot < M < 60\ M_\odot$) is $\sim 0.82\ M_\odot$ yr^{-1}, which using an initial mass function weighted typical mass of 23 $M_\odot$ implies that $\psi \sim 4 \times 10^{-2}$ O stars yr^{-1}, about 10 times smaller than that derived under the above hypothesis. Note, however, that Codella, Felli, & Natale (1994a) found that 65% of a large ($\sim$450) sample of diffuse H II regions they studied are associated with *IRAS* point sources and satisfy the Wood & Churchwell color criterion. This criterion, therefore, selects compact as well as more diffuse H II regions, which may alleviate the problem.

Why do we see so many UC H II regions? Or phrasing it differently, Why are the ages of UC H II regions not consistent with their short dynamical ages? Wood & Churchwell concluded that the expansion of UC H II regions is inhibited by some mechanism, so that their small sizes do not necessarily indicate that they are extremely young. Several suggestions have been made to explain the lifetime paradox. Van Buren et al. (1990) proposed that most UC H II regions are excited by O stars that are in motion relative to the molecular cloud and that have formed a bow shock supported by its stellar wind (see § 2.3.4). Since bow shocks are static configurations, neither expanding nor contracting, UC H II regions would *live* as long as the moving star remains embedded within the molecular cloud. Hollenbach et al. (1994) proposed that newly formed OB stars are surrounded by a massive primordial disk which is photoevaporated by the UV photons from the star. The dense gas that is ionized close to the star, and that flows away from it, would then give rise to the observed UC H II region. The reservoir of dense gas within the disks may last for a million years or more, depending on the mass of the disk. Thus, UC H II regions could live much longer ($\sim 3 \times 10^5$ yr) than what their dynamical ages indicate because they are constantly being replenished by a dense circumstellar reservoir. Whereas the formation of accretion disks around massive young OB stars is expected given that molecular clouds have nonzero angular momentum, direct observational evi-

dence for its presence is scarce although beginning to emerge (see § 5.1.3).

Several authors (Dyson 1994; Dyson et al. 1995; Lizano & Cantó 1995; Lizano et al. 1996) have shown that the identification of the dynamical timescale with the age of compact H II regions is not suitable if the primordial ambient medium is clumpy. The presence of clumps near recently formed stars is expected because of the fragmentation process that takes place during the gravitational collapse. Dyson et al. (1995) investigated the interaction of the wind of a young massive star with the clumpy molecular gas and showed that mass loading due to the hydrodynamical ablation of clumps could result in long-lived UC H II regions. Lizano et al. (1996) showed that the mass injection from photoevaporated globules into a stellar wind causes trapping of the ionization front resulting in compact (0.1 pc) long-lived ($\sim 10^5$ yr) H II regions. Where both processes occur, Arthur & Lizano (1997) showed that photoevaporation dominates over ablation for self-gravitating clumps immersed in H II regions.

Alternatively, De Pree, Rodríguez, & Goss (1995b) (see also García-Segura & Franco 1996; Xie et al. 1996) suggest that the paradox finds a simple explanation if the physical conditions of the ambient medium are much denser and warmer than previously believed, resulting in very small equilibrium radii of the order of the size of UC H II regions. This hypothesis attains support on recent observations which show that the temperatures and densities of the molecular gas around UC H II regions are typically ~ 100 K and $\sim 1 \times 10^7$ cm^{-3}, respectively (see § 3.3). Under these conditions, the equilibrium radius of a region of ionized gas excited by an O9 star ($N_u = 1.2 \times 10^{48}$ s^{-1}) is just ~ 0.016 pc, and the time it takes to reach pressure equilibrium is $\sim 1 \times 10^4$ yr. Thus most UC H II regions could be objects that have already reached the equilibrium radius and hence be much older than what the dynamical age indicates. This possibility is further strengthened by the fact that a large fraction of UC H II regions are excited by stars emitting an output rate of ionizing photons smaller than that of an O9 star (see § 2.1) and therefore should have smaller equilibrium radii.

3. HOT MOLECULAR CORES

A wealth of observations have established that the presence of dense molecular gas toward regions of newly formed massive stars is quite common. For instance, a survey of emission in the CS($7 \rightarrow 6$) transition toward a large sample of star-forming regions associated with water masers show detection in $\sim 60\%$ of the cases (Plume et al. 1992). Since this transition has a critical density of $\sim 2 \times 10^7$ cm^{-3}, the detection of emission indicates the existence of very dense (n_{H_2}) $> 10^6$ cm^{-3}) gas within molecular cores. In addition to the high densities, observations of highly excited inversion transition lines of ammonia have shown that the presence of hot molecular gas, with temperatures in the range from 100 to 250 K, is also common (Mauersberger et al. 1986; Cesaroni, Walmsley, & Churchwell 1992). These observations, which were carried out using single-dish instruments, lack adequate angular resolution to determine the location of the hot and/or dense molecular emission with respect to the compact H II regions and to resolve its spatial structure and kinematics.

In this section we discuss the results of recent studies of dense and hot molecular emission, made with high angular resolution ($\leq 5''$), which have yielded information about their structure, physical properties, and kinematics (e.g., Heaton, Little, & Bishop 1989; Garay & Rodríguez 1990; Garay et al. 1993a; Cesaroni et al. 1994a, 1994b; Gómez et al. 1995; Garay et al. 1998; Cesaroni et al. 1998). These observations show that the hot ($T_K > 50$ K) and usually dense ($> 10^5$ cm^{-3}) molecular gas arises from small (< 0.1 pc) structures with masses in the range 10^2–3×10^2 $M_\odot$. We will refer to these structures as hot molecular cores. We note that although some authors use this term to imply the presence of an embedded object, we use it here just to refer to hot and compact structures of molecular gas regardless of whether they are internally or externally illuminated objects. Particular emphasis will be given to the physical and dynamical association between the hot cores and compact H II regions and to their evolutionary stage.

The high temperatures of hot cores increase evaporation of icy grain mantles, making the chemical processes in the vicinity of UC H II regions different from that in cold dark clouds. In particular, the gas phase is expected to be enriched with mantle constituents such as NH_3, H_2O, and CH_3OH. A comprehensive review of the observations and models of the chemistry in hot cores has been recently presented by van Dishoeck & Blake (1998). In dense, warm molecular cores the abundance of ammonia is considerably enhanced with respect to that in cold dark clouds (cf. Walmsley 1989, 1990). Thus, NH_3 lines, particularly those with high-excitation energy levels, have proved to be excellent tracers of the dense molecular gas around newly formed stars. Accordingly, most of the high angular resolution observations of compact cores have been made in lines of ammonia.

3.1. The Habitat: Massive Cores

Hot and dense molecular cores are not isolated entities but are compact features within larger, less dense, structures of molecular gas. Molecular clouds are known to be highly inhomogeneous clumpy entities exhibiting a hierarchy of structures with densities spanning several orders of magnitude (e.g., Wilson & Walmsley 1989; Blitz 1993). In this subsection we briefly summarize the characteristics and physical conditions of the molecular environment that sur-

rounds hot cores and compact regions of ionized gas derived from observations made with single-dish instruments (half-power beamwidth of typically 40″) which effectively provide the characteristics of the molecular emission averaged over spatial scales of typically ~ 1 pc. We assume that these data are representative of the conditions of massive cores (Caselli & Myers 1995). Massive cores are themselves not isolated entities but are found within giant molecular clouds (GMCs). They fill only a small fraction of the total GMC area and are concentrated in regions of active star formation. About 20% of the total gas in GMCs is found in the form of massive cores (cf. Tieftrunk et al. 1998a).

The derived parameters of massive cores depend on the molecular line used to trace them. Churchwell et al. (1990, hereafter CWC90) undertook a survey of ammonia emission in the (1, 1) and (2, 2) inversion transitions toward a large sample of compact H II regions, detecting emission toward 70% of them, implying that young regions of ionized gas are still embedded within massive cores, and deriving ammonia column densities of typically $\sim 10^{15}$ cm^{-2} and gas kinetic temperatures of typically 28 K. The line widths of the ammonia emission range between 1.5 and 4 km s^{-1}, with an average value of ~ 3.1 km s^{-1}. Since the thermal part of the line width amounts to only ~ 0.3 km s^{-1} (for $T_K \sim 28$ K), the line widths are largely dominated by nonthermal motions. Cesaroni et al. (1992) observed 16 massive cores associated with compact H II regions in the (4, 4) and (5, 5) transitions of NH_3, which are thought to trace warmer and denser gas than the (1, 1) and (2, 2) transitions, deriving rotational temperatures of typically ~ 46 K, ammonia column densities of typically 4×10^{16} cm^{-2}, and molecular densities of $\sim 10^6$ cm^{-3}. From observations of CS emission around compact regions of ionized gas, Cesaroni et al. (1991) found massive cores with densities of $\sim 10^6$ cm^{-3}, sizes of ~ 0.4 pc, and masses of $\sim 2 \times 10^3\ M_\odot$. In summary, the low angular resolution observations show that massive cores associated with regions of recent massive star formation have linear sizes between 0.3 and 1.0 pc, kinetic temperatures in the range 30–50 K, molecular densities in the range 2×10^4–3×10^6 cm^{-3}, and masses in the range 10^3–$3 \times 10^4\ M_\odot$. Caselli & Myers (1995) found that massive cores associated with embedded young stellar objects have physical properties almost identical to neighboring massive starless cores. Thus, these physical conditions are probably representative of massive cores in a phase prior to the formation of an OB cluster.

Since massive cores contain hot and dense structures, it is clear that the molecular gas within them is neither homogeneous nor isothermal. To determine how the physical and chemical conditions of the gas within a single massive core varies as a function of the distance from its center is a laborious task. It requires mapping in a variety of molecular transitions and with different angular resolutions. One of the most extensively scrutinized massive star-forming regions is G34.3+0.15, which has been observed with angular resolutions ranging from $\sim 2'$ (single dish) to $\sim 1''$ (aperture synthesis) and in several molecular transitions: at low angular resolutions (40″–130″) in lines of NH_3 (Heaton et al. 1985), at intermediate angular resolutions (20″–40″) in several rotational transitions of CO, HCO^+ and isotopes (Matthews et al. 1987; Heaton et al. 1993), and interferometrically in several lines of NH_3 (Andersson & Garay 1986; Heaton et al. 1989; Garay & Rodríguez 1990) and HCO^+, $H^{13}CN$, $HC^{15}N$, and SO (Carral & Welch 1992). The observed morphology of the molecular emission at different spatial scales and in different chemical probes is illustrated in Figure 6, which shows maps of (*top left*) NH_3 emission from observations with angular resolution of 2.2 (Heaton et al. 1985), (*top right*) HCO^+ emission with 6″ angular resolution (Carral & Welch 1992), and (*bottom right*) NH_3 emission with 1″ angular resolution (Heaton et al. 1989). At the largest linear scales, the ammonia observations trace an extended (diameter ~ 3.7 pc), cool ($T \sim 9$ K), low-density ($n_{H_2} \sim 5 \times 10^3$ cm^{-3}) *halo* surrounding a denser ($\sim 4 \times 10^4$ cm^{-3}) *core* having a diameter of ~ 1.7 pc (Heaton et al. 1985). The HCO^+ emission traces a warm ($T \geq 25$ K) structure of about 0.9 pc in diameter. The NH_3 and SO interferometric observations made with angular resolutions of $\sim 5''$ reveal the presence of a warm (~ 60 K), dense (6×10^5 cm^{-3}), and small (0.21×0.05 pc) substructure within the core, referred to as the *compact core*. At higher resolution ($\sim 1''$), Heaton et al. (1989) detected an

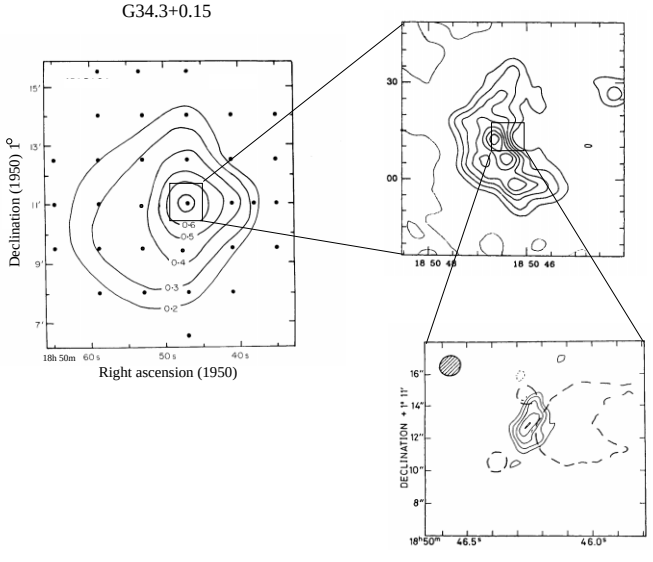

FIG. 6.—Maps of molecular emission from the G34.3+0.15 massive star-forming region at different angular resolutions. *Top left*: $NH_3(1, 1)$ emission with 2.2 resolution (Heaton et al. 1985). *Top right*: $HCO^+(1–0)$ emission with 6″ resolution (Carral & Welch 1992). *Bottom right*: $NH_3(3, 3)$ emission at 1″ resolution (Heaton et al. 1989). The dashed line corresponds to the lowest contour level of the 15 GHz emission from the bright cometary H II region.

ultracompact core which has a molecular hydrogen density of $\sim 4 \times 10^7$ cm^{-3} and a linear size of 0.05 × 0.02 pc. The hot ammonia emission from the UC dense core originates in a small region lying at the eastern edge and approximately delineating the leading edge of the UC cometary H II region. This morphology suggests that the emission from the UC core arises from molecular gas that has been compressed either by the expansion of the H II region, by stellar winds, or by the relative motions of an O star within the molecular cloud.

Using the data available on ammonia emission, which covers linear scales ranging from a few hundredths to a few parsecs, Garay & Rodríguez (1990) determined that the density and temperature of the molecular gas toward G34.3+0.15 decrease with distance from the peak continuum emission, r, as $r^{-1.7\pm0.4}$ and $r^{-0.6\pm0.1}$, respectively. Using HCO^+ data, Heaton et al. (1993) derived that the molecular density is constant out to a radius of 0.1 pc and decreases outward with radius as $r^{-2.1}$. Given the uncertanties in both determinations, such as in the adopted molecular abundances, the agreement is good. The density dependence with radius determined by Garay & Rodríguez (1990) is similar to that implied by Caselli & Myers (1995) for a large sample of massive dense cores, in the context of an equilibrium model of a dense core with thermal and nonthermal motions. They find that the density profile scales as $r^{-1.6}$ in massive dense cores and $r^{-1.1}$ in low-mass dense cores. Massive cores are, however, likely to be highly fragmented into filaments and dense clumps, thus the physical conditions derived assuming smooth density and temperature profiles should be taken only as representative of the bulk conditions of the clumpy emitting region. Whether the derived physical conditions of the G34.3+0.15 massive core are representative of that of the molecular gas in most of the massive cores forming massive stars has yet to be observationally established. In any case, the above observations clearly illustrate that hot cores are not isolated entities but are rather dense structures embedded in cooler, lower density, and more extended structures which dominate the emission detected in low angular resolution studies.

3.2. Association with Compact H II Regions

The study of the spatial distribution of the highly excited molecular emission relative to the thermal emission of the ionized gas on scales of less than 0.1 pc has began only recently, via high angular resolution observations of NH_3 made with the VLA (Heaton et al. 1989; Garay et al. 1993a; Cesaroni et al. 1994a; Gómez et al. 1995; Garay et al. 1998; Cesaroni et al. 1998), and CH_3CN made with the IRAM interferometer (Cesaroni et al 1994b; Olmi et al. 1996). These observations show that the highly excited emission arises from compact, hot molecular structures that are invariably located near, and in most cases are intimately associated with, compact H II regions. Hot cores are thus found in the immediate vicinity of newly formed massive stars. In some cases the observed line profiles appear in emission off to the side of the H II region and in absorption in front of it (cf. Keto, Ho, & Haschick 1987a; Garay & Rodríguez 1990; Gaume & Claussen 1990). In other cases the lines are only seen in absorption [W3(OH); Reid, Myers, & Bieging 1987; NGC 7538, Henkel, Wilson, & Johnston 1984], implying that the bulk of the dense molecular gas is located in front of the compact H II region. The intimate association is illustrated in Figure 7 which shows maps of the hot ammonia and radio continuum emission toward the G10.47+0.03 and G29.96−0.02 (Cesaroni et al. 1998) and G61.48+0.09 (Gómez et al. 1995) regions of young massive star formation. Not all compact H II regions are associated with dense and warm ammonia clumps, however. For instance, observations of the more than a dozen compact H II regions in the Sgr B2 region show that only two of them are associated with dense and hot ammonia clumps (Vogel, Genzel, & Palmer 1987; Gaume & Claussen 1990). Apparently, the dense ammonia gas in the other sources has been disrupted by the expansion of the H II region and/or outflows.

3.3. Physical Conditions

This section summarizes our knowledge of the physical conditions of the hot molecular gas found in the vicinity of UC H II regions. We concentrate the discussion on those sources for which the physical parameters have been determined from observations of inversion transitions of NH_3 made with high angular resolution. The most commonly observed line is the (3, 3) inversion transition, which effectively selects the warmer and higher density condensations within massive cores. In Table 2 we compile most of the data published to date of hot ammonia cores in regions of massive star formation, observed with high angular resolution. The term hot ammonia core is used here to refer to molecular structures with either ammonia line brightness temperatures and/or rotational temperatures between inversion transitions of ammonia ≥ 50 K. This criteria ensures that the kinetic temperature of the gas is greater than 50 K (Walmsley & Ungerechts 1983; Danby et al. 1988). These data show that hot ammonia cores have ammonia column densities as high as 10^{19} cm^{-2}, molecular hydrogen densities up to 7×10^7 cm^{-3}, and kinetic temperatures up to 250 K. Typically the hot ammonia emission originates from optically thick clumps with linear sizes of the order of 0.05 pc.

3.3.1. Temperatures

The kinetic temperature of molecular gas can be estimated from the rotational temperature between two tran-

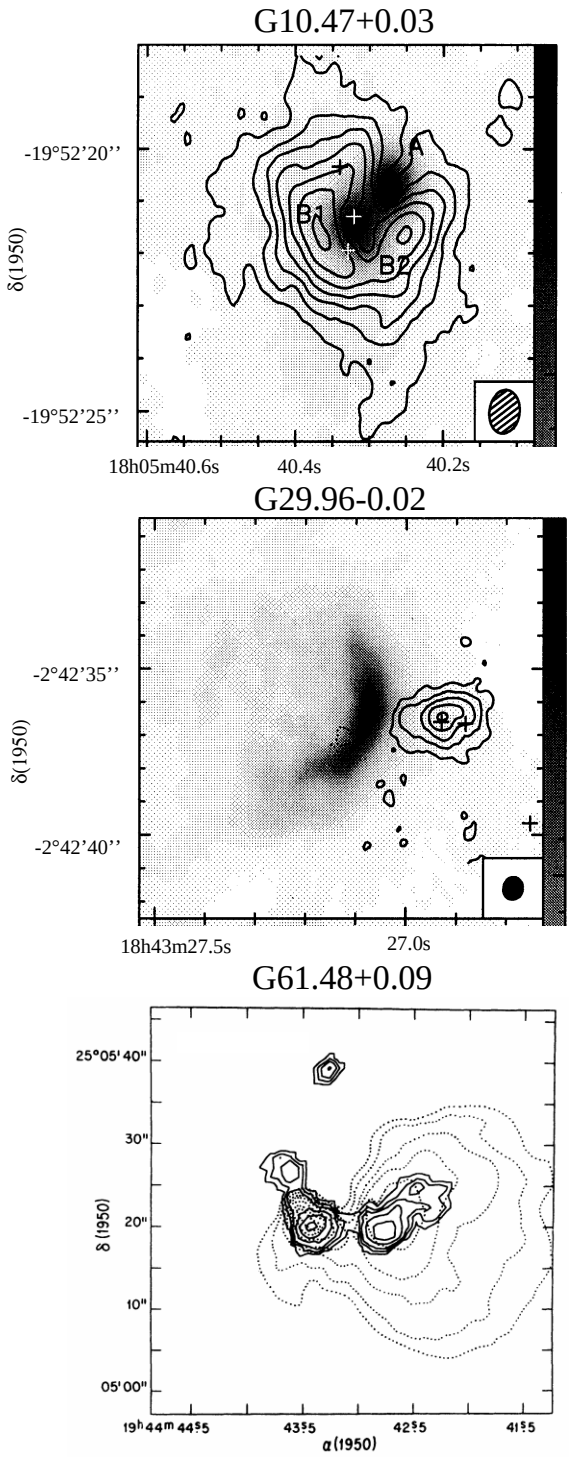

FIG. 7.—Association between ammonia emission from hot molecular gas and radio continuum emission from ionized gas, toward three regions of massive star formation. *Top*: G10.47+0.03 (Cesaroni et al. 1998). *Middle*: G29.96−0.02 (Cesaroni et al. 1998). *Bottom*: G61.48+0.09 (Gómez et al 1995). The radio continuum emission is represented in gray scale in the top and middle panels and by dashed lines in the lower panel. Ammonia emission is shown by the continuous lines.

sitions of a molecule, which can in turn be derived from the ratio of the optical depths of the transitions. The ammonia molecule is particularly convenient for this purpose because the optical depths of their inversion transitions can be directly derived from the observed intensity ratio of their hyperfine components. Observations of two inversion transition lines of ammonia permit one to determine the rotational temperature. For this reason the NH_3 molecule is known as a cosmic thermometer. Strictly, however, the NH_3 rotational temperature sets a lower limit to the kinetic temperature (Walmsley & Ungerechts 1983).

The kinetic temperatures of hot ammonia cores are typically $\sim$100 K and can be as high as 250 K. These temperatures are considerably higher than the kinetic temperatures of the $\sim$1 pc scale ambient medium (i.e., massive cores) that harbors compact H II regions, of typically 30 K (CWC90). The intimate association between hot ammonia cores and compact H II regions suggests that the heating of the molecular gas is most likely due to the strong radiation field from the luminous star (or stars) that excites the associated region of ionized gas. To be valid, this hypothesis requires that the total luminosity of the ammonia core be equal to or smaller than the total luminosity of the exciting star. In particular, for cores which are offset from the associated UC H II region, their luminosity should be smaller by a factor of $\Omega/4\pi$, where Ω is the solid angle subtended by the ammonia core from the ionizing star. The ammonia cores within the G32.80+0.19 and G61.48+0.09 (S88B) regions of star formation provide good examples of hot cores that are intimately associated with compact H II regions and have luminosities that can be fully explained as a result of heating by the nearby star which ionizes the H II region (Gómez et al. 1995).

Alternatively, hot ammonia cores may be heated by recently formed stars embedded at their centers and which have not yet produced a detectable ultracompact H II region. Cesaroni et al. (1994a) found that the hot ammonia cores within the G10.47+0.03 and G31.41+0.31 massive star-forming regions are offset from the nearby compact H II region and have luminosities in excess of the luminosity of the companion H II region, suggesting that the molecular gas in these cores is warmed by a luminous object that is embedded within the core and not by the star responsible for the ionization of the nearby compact H II region. The estimated core luminosities are however larger, by factors of $\sim$4–5, than the bolometric luminosity derived from the *IRAS* data, which is thought to be an upper limit—an inconsistency termed the "luminosity paradox." Later, Cesaroni et al. (1998) found that these cores are oblate and have strong temperature gradients and showed that the paradox was produced by the assumption of spherical geometry and emission at a single temperature. Finally, it is also possible that a nonnegligible contribution to the heating of cores could be provided by the input of mechani-

TABLE 2

HOT AMMONIA CORES[a]

Source	Distance (kpc)	Radius (pc)	Δv (km s^{-1})	N_{NH_3} (cm^{-2})	n_{H_2} (cm^{-3})	Mass[b] ($M_\odot$)	Reference
G5.89−0.39	4.0	0.2	8.0	9×10^{15}	6×10^{3}	30[m]	1
G9.62+0.19	5.7	0.066	5.1	1.6×10^{18}	1.2×10^{7}	164[v]	2
		0.040	4.3				2
G10.47+0.03	5.8	0.063	5.4	1.4×10^{19}	1.0×10^{7}	218[v]	2
		0.048	5.7				2
G10.47+0.03c	5.8	0.042	8.1	3.2×10^{18}	1.2×10^{7}	210[m]	3
		0.042	9.0				3
G19.61−0.23	3.5	0.026	9.5	2.4×10^{17}	9×10^{6}	25[m]	4
G29.96−0.02	7.4	0.072	7.6	1.7×10^{18}	1.3×10^{7}	138[v]	2
		0.038	4.3				2
G31.41+0.31	7.9	0.073	5.1	8.2×10^{18}	8.6×10^{6}	285[v]	2
		0.054	5.8				2
G32.80+0.19 S	13.	0.079	7.1	3×10^{16}	5×10^{4}	18[m]	5
G32.80+0.19 N	13.	0.10	4.8	5×10^{15}	7×10^{3}	10[m]	5
G32.80+0.19 M	13.	0.063	6.5				5
G34.26+0.15	3.8	0.015	7.5	7×10^{18}	7.0×10^{7}		6
		0.027	∼5	7×10^{18}	4.2×10^{7}	170[v]	7
G61.48 W	5.4	0.039	4.2	1×10^{16}	4×10^{4}	2[m]	5
G61.48 E	5.4	0.020	3.5	6×10^{15}	3×10^{4}	0.6[m]	5
Sgr B2 M	8.0	0.1	15.0	9×10^{17}	2×10^{5}	50[v]	8
Sgr B2 N	8.0	0.1	19.5	1×10^{20}	1×10^{7}	5000[v]	8
W3(H_2O)	2.2	0.006	4.2	1×10^{17}	4×10^{8}	18[m]	9
W3 IRS 5	2.3	0.03	5.6	1.5×10^{15}	$(1–4)\times10^{7}$	60–240[v]	10

[a] Parameters derived from observations of ammonia lines made with high angular resolution (VLA).

[b] In this column superscript "m" denotes molecular mass derived as in eq. (12) and superscript "v" denotes virial mass.

REFERENCES.—(1) Gómez et al. 1991; (2) Cesaroni et al. 1994a; (3) Garay, Moran, & Rodríguez 1993a; (4) Garay et al. 1998; (5) Gómez, Garay, & Lizano 1995; (6) Garay & Rodríguez 1990; (7) Heaton, Little, & Bishop 1989; (8) Vogel, Genzel, & Palmer 1987; (9) Wilson, Gaume, & Johnston 1993; (10) Tieftrunk, Gaume, & Wilson 1998b.

cal energy due to shocks, driven by either the expansion of the H II regions, stellar winds, or outflows. Since the expansion of the region of ionized gas drives a shock wave into the neutral gas, which sets it into motion outward, in this scenario the cores are most likely to be found along the edges of the associated compact H II region (cf. Keto & Ho 1989).

The temperature across ammonia cores has been mapped in only a few cases, most of which appear to be surrounding UC H II regions (Keto et al. 1987a; Garay & Rodríguez 1990; Garay et al. 1993a). These studies show a common feature: the presence of temperature gradients, with the temperatures being higher toward the associated UC H II region. In the G10.6−0.4 molecular core the kinetic temperature of the gas decreases with distance from the exciting star of the UC H II region, r, as $r^{-1/2}$, being ∼140 K at a distance of 0.05 pc and ∼54 K at 0.35 pc (Keto et al. 1987a). In the massive core G34.3+0.15 the rotational temperature varies as a function of the radial distance as $13(r/\mathrm{pc})^{-0.6}$ (see Fig. 8), having a value of ∼185 K at the position of the UC core ($r \sim 0.015$ pc; Garay & Rodríguez 1990). The rotational temperature of the ammonia structure associated with the G10.47+0.03 cluster of UC H II regions (Wood & Churchwell 1989a) changes with projected distance from the exciting stars as $r^{-0.4}$, increasing from ∼25 K in the outer parts of the halo (diameter of ∼0.25 pc) to ∼75 K at the center of the core (∼0.08 pc in size; Garay et al. 1993a). The observed gradients in temperature suggest that the molecular gas is heated via collisional excitation with hot dust, which in turn is heated by the absorption of radiation emitted by the central star. Scoville & Kwan (1976) worked out a simple model for this process and found that the dust temperature, T_D, at a distance r from an embedded star with luminosity, L_*, is

$$T_D = 65\left(\frac{0.1\ \mathrm{pc}}{r}\right)^{2/(4+\beta)}\left(\frac{L_*}{10^5\ L_\odot}\right)^{1/(4+\beta)}\left(\frac{0.1}{f}\right)^{1/(4+\beta)}\ \mathrm{K}\ , \tag{11}$$

where β is the power-law index of dust emissivity at far-infrared wavelengths and f is its value at 50 μm. The power-law indices of the temperature versus radius relationship derived from the observations are consistent with those predicted by this model and suggests that β is in the range from 0 to 1. In Figure 9 we plot the inferred temperature at a

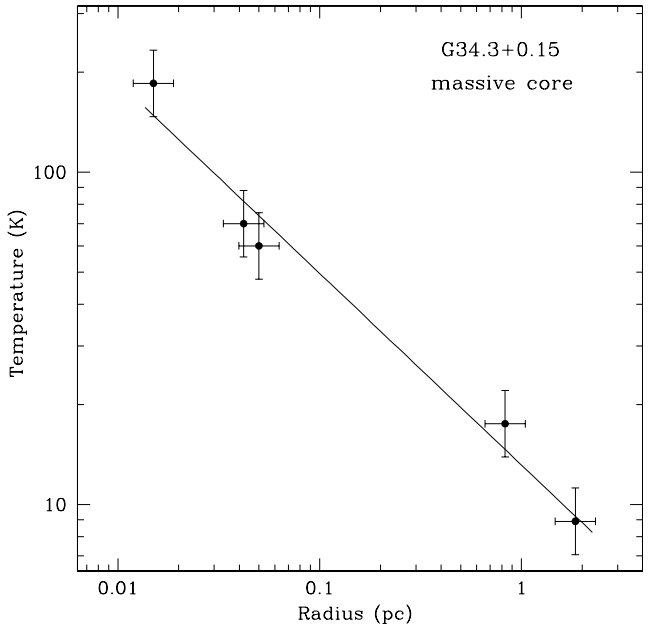

FIG. 8.—Rotational temperature of the ammonia gas toward the G34.3+0.15 massive star-forming region as a function of distance from the exciting central star or stars. The line is a least-squares linear fit to the data points.

distance of 0.1 pc from the central exciting star (or stars) as a function of luminosity for the four regions with reported temperature profiles with radius (G10.47+0.03, G10.6−0.4, G34.3+0.15, and Cepheus A). It shows that the temperature at a fixed distance from the central star increases with luminosity of the exciting star; a linear least-squares fit to the trend gives $T = 39(L_*/10^5\ L_\odot)^{0.4\pm0.2}$ K. Given the error in the exponent, and the fact that in most of the regions considered the heating is provided by a cluster of stars, rather than a single star, the observed trend is consistent with equation (11) and $\beta = 0$. The above results strongly argue that in these objects the embedded star or stars that ionizes the UC H II region also provides the bulk of the heating of the whole ammonia structures, including the hot cores.

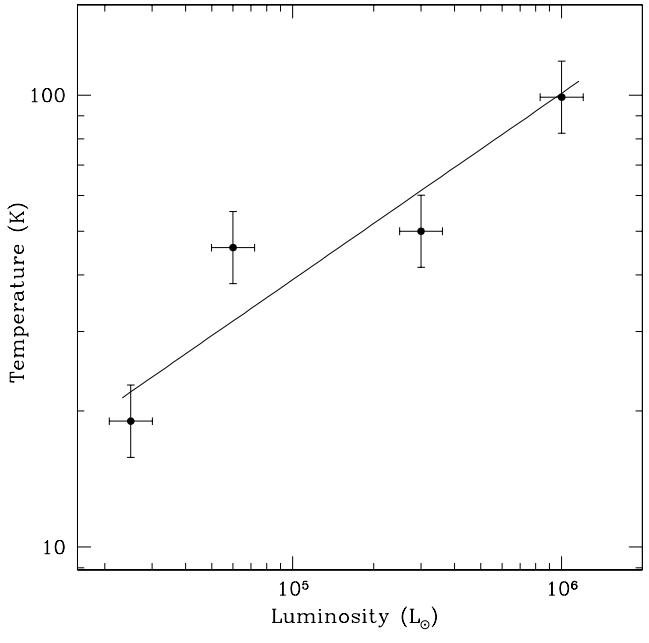

FIG. 9.—Molecular gas temperature at a fixed distance (0.1 pc) from the central exciting stars as a function of luminosity, for the four regions with reported temperature profiles with radius (see text). The line is a least-squares linear fit to the data points.

3.3.2. *Column Densities and Masses*

Assuming that all energy levels are populated according to LTE, the total column density of NH_3 can be derived once the optical depth, line width, rotational temperature, and excitation temperature of an inversion transition are known (see Ho & Townes 1983). The ammonia column densities of the compact ammonia cores range from $\sim 2 \times 10^{15}$ to $\sim 1 \times 10^{19}$ cm^{-2}. The large range of observed column densities may be due to evolutionary effects. As the region of ionized gas grows into the molecular environment and the molecular core expands, the NH_3 column density is expected to decrease. Hence objects with the larger column densities may correspond to the youngest ammonia cores.

The total mass of a spherical cloud of molecular gas can be determined from the derived ammonia column density, N_{NH_3}, and core radius, R, using the expression

$$M_{NH_3} = \mu_g m_{H_2} \left[\frac{H_2}{NH_3}\right] N_{NH_3} \pi R^2, \qquad (12)$$

where μ_g is the mean atomic weight of the gas (=1.36) and m_{H_2} is the mass of a hydrogen molecule. This approach requires an assumption about the $[NH_3/H_2]$ abundance ratio, which is the largest source of uncertainty of the method. The $[NH_3/H_2]$ ratio has been estimated to be between 10^{-7} for small, dark clouds (Ungerechts, Walmsley, & Winnewiser 1980) and 10^{-5} in the dense nucleus of the Orion molecular cloud (Genzel et al. 1982). The high temperature of the hot cores certainly increases the evaporation of icy mantles, making the chemical formation process in the vicinity of UC H II regions different from that in cold dark clouds. Thus, the gas phase is expected to be enriched with mantle constituents such as NH_3, CH_3OH, and H_2O although the precise amount of enrichment is difficult to estimate. For warm cores in massive molecular clouds the derived fractional ammonia abundances are typically $\sim 10^{-6}$ (e.g., Henkel, Wilson, & Mauersberger 1987).

Alternatively, the mass of the ammonia cores can be computed assuming that they are in virial equilibrium. For a

spherical core of radius R, the virial mass, $M_{\rm vir}$, in solar masses is

$$M_{\rm vir} = 210\beta(\Delta v)^2 R\ , \qquad (13)$$

where Δv is the line width in km s^{-1}, R is in pc, and β is a constant, of order unity, which depends on the density profile of the core ($\beta = 1$ for a uniform density core; $\beta = 0.90$ for one whose density varies as the inverse first power of the radius; MacLaren, Richardson, & Wolfendale 1988).

The molecular mass of the hot ammonia cores, computed using one of the two methods discussed above, ranges from about 1 to 300 $M_\odot$. Although the mass estimate can easily differ by an order of magnitude depending on the method used and its underlying assumptions, and hence should be taken with caution, the wide range of derived masses reflects physical differences among the cores. The less massive ($M < 30\ M_\odot$) and low-density ($n_{\rm H_2} < 5 \times 10^4$ cm^{-3}) cores (see Table 2), which are intimately associated with regions of ionized gas, appear to be different from the most massive ones. Gómez et al. (1995) suggest that they are probably clumps of remnant gas that are being heated externally by the exciting star of the H II region. We note that some of the cores listed in Table 2 have been observed in other molecular and continuum tracers, each of which might probe distinct regions of the core. In fact the mass estimated from millimeter and infrared continuum emission (see Kurtz et al. 1999b) are generally larger than those derived from the ammonia observations; the derived ratios of dust to molecular masses range from 0.5 to 90, with a geometric average of ~ 5.

3.3.3. Densities

The derived density of the hot ammonia cores, whose determination suffers the same difficulties as the mass determination, ranges from 1×10^4 to 7×10^7 cm^{-3}. The densest hot ammonia cores are thought to correspond to the cradles of massive stars, whereas the less dense hot cores are thought to correspond to structures representing the remnant molecular core material that has survived the powerful effects of the formation of a luminous star. However, whether the high densities are produced by the dynamical interaction between the newly formed star and the molecular core gas or reflect the initial conditions of dense fragments within the cores is still an open question. In some cases support for the first hypothesis is provided by (3, 3) ammonia observations which show that the dense gas emission arises also from the warmer parts of the cloud which are found very close to the heating source. The high densities may be produced either by compression from shocks associated with the expansion of the H II region or from bow shocks produced by the motions of the exciting star within the core.

The dependence of density with radius in ammonia cores has been investigated in a few cases. Keto et al. (1987a) found that the molecular hydrogen density in the G10.6−0.4 molecular core scales with radius roughly as r^{-2} and is 4×10^6 cm^{-3} within a centrally condensed structure of 0.05 pc in radius. In the G34.3+0.15 cloud the hydrogen molecular density is $\sim 7 \times 10^7$ cm^{-3} in the UC core (size of ~ 0.03 pc) and decreases outward as $n \propto r^{-1.7}$ (Garay & Rodríguez 1990). In the W51e8 ammonia core the column density scales with radius in a region of 0.04–0.3 pc as $r^{-1.0}$, implying a density dependence of $r^{-2.0}$ (Zhang & Ho 1997). The derived power-law index for the density distribution falls in the range between 3/2, predicted for gas collapsing to a point source that dominates the gravitational field (e.g., Shu 1977), and 2, expected for an isothermal sphere in hydrostatic equilibrium or a condensation of free-falling gas at constant speed. Whether or not these density dependences are representative of other massive cores remains to be investigated.

3.4. Line Widths

The line widths of the NH_3 emission from hot cores are remarkably wide, with values ranging from ~ 4 to ~ 10 km s^{-1}. They are broader than the typical ammonia line width of ~ 3 km s^{-1} observed by CWC90 toward massive cores associated with UC H II regions. We recall that the CWC90 observations sample regions of typically of ~ 1 pc in size which may contain hot cores. What is the origin of the broad line widths in hot ammonia cores? Thermal broadening is too small to explain the observed line widths. Even at the high kinetic temperature of hot cores, ~ 200 K, the thermal width is only ~ 0.7 km s^{-1}. Saturation broadening, due to large optical depths in the lines (see Ho 1972), is also insufficient. Although some saturation broadening is possible in the main lines, which generally have large opacities, a negligible contribution is expected for the satellite lines which also show very broad line widths. For example, the observed line widths of the ammonia emission from the G10.47+0.03 hot core are ~ 12 km s^{-1} in the main lines and ~ 9 km s^{-1} in the satellite lines (Garay et al. 1993a). The difference in line width, of ~ 3 km s^{-1}, can be ascribed to saturation effects in the main lines, but the large broadening observed in the satellite lines requires an additional explanation. We conclude that the large line width of the hot cores can be explained solely neither by its high kinetic temperature nor by its large optical depth. Most likely, the broad line widths are due to the presence of ordered or turbulent gas motions, which are believed to consist mainly of magnetohydrodynamic waves.

Several studies have shown that a significant correlation exist between the observed line width and size of molecular clouds (cf. Myers 1983 and references therein). To investigate whether or not the dense, hot, and compact molecular

structures fulfills such a relationship, we plot in Figure 10 the observed line width versus size for hot ammonia cores that are closely associated with compact H II regions. For comparison, also plotted are the values observed for dense cores in low-mass clouds (Myers 1983) and dense cores in massive clouds (Caselli & Myers 1995), which are denser and warmer than the cores within dark clouds. Figure 10 clearly shows that the line width–size relationship is not unique. At a given size, the hot ammonia cores have broader line widths than massive cloud cores, which in turn are broader than those in low-mass clouds. The shift in the line width versus size relationship observed for the three types of cores most likely reflects differences in the physical properties underlying this relation.

The physical basis for the Δv versus r relationship is still poorly understood, although the prevailing view is that the line broadening is magnetic in origin (Shu et al. 1987; Myers & Goodman 1988). Fuller & Myers (1992) concluded that the line width versus size relation observed for low-mass cores within dark clouds reflects the initial conditions for the formation of low-mass stars rather than being a consequence of star-core interaction. Similarly, Caselli & Myers (1995) concluded that the physical conditions observed in massive dense cores can also be considered part of the initial condition of the star formation process. It is then tempting to explain the observed differences in the Δv versus r relationship in terms of differences in the initial physical conditions of the different cores.

Assuming that the three types of cores are in virial equilibrium, the differences in line width at a fixed cloud size could be explained as due to differences in the molecular densities. Approximating the observed line width–size correlations by power-law relations $\Delta v = Cr^p$, where C and p are constants—different for each class of cores—and using equation (13) for the virial mass, it follows that $n_{H_2} \propto C^2/r^{2-2p}$. For cores with sizes in the 0.02–0.2 pc range (where a comparison of the ammonia data is appropriate) the average line width of low-mass cores, massive cores, and hot ammonia cores are roughly in the ratio 1:3:22, which would imply, if virialized, that their molecular densities are in the ratio 1:9:500. The average densities derived from the observations ($\sim 3 \times 10^4$ cm^{-3} for low-mass cores [Myers 1983], $\sim 2 \times 10^5$ cm^{-3} for massive cores [Caselli & Myers 1995], and $\sim 2 \times 10^7$ cm^{-3} for the hot ammonia cores) are in the ratio 1:7:700, close to those predicted from the observed shift in the line width–size relationship by the virial hypothesis. Note however that this simply recasts the problem of the shift in the Δv versus r relationship to the problem of what produces the high densities in hot ammonia cores. Larson (1981) suggested that the systematic differences in line width among the different types of cores may represent different amounts of evolution away from a "primordial" state of turbulence represented most closely by the low-mass cores. The more massive cores may have experienced more gravitational contraction than the low-mass cores, which would increase their virial velocities. However, this hypothesis predicts that the line width should increase as the radius decreases as $r^{-1/2}$ which is not observed.

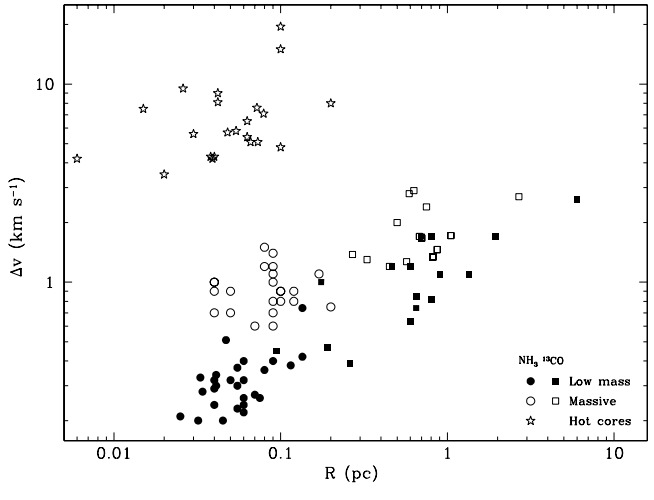

FIG. 10.—Observed line width vs. diameter relationship for dense molecular cores. *Filled circles and squares*: low-mass cores (Myers 1983); *open circles and squares*: massive cores (Caselli & Myers 1995); *stars*: hot cores.

To investigate in more detail the differences in the observed line width versus size relationship in terms of differences in physical parameters, it is convenient to separate the thermal and nonthermal contributions to the line width (cf. Myers 1983; Fuller & Myers 1987). Caselli & Myers (1995) found that for massive cores the nonthermal component of the line width, Δv_{nt}, depends on size as r^q with $q = 0.21 \pm 0.03$. On the other hand, Myers (1983) found that for low-mass cores $q \sim 0.53 \pm 0.07$. Caselli & Myers (1995) modeled these relations in terms of cloud structure and found that the difference in slopes is mainly due to differences in density structure. Cores in massive clouds are denser and have steeper density profiles than cores in low-mass clouds. We find that the nonthermal width of hot ammonia cores follows the trend $\Delta v_{nt} \sim r^{0.1 \pm 0.1}$. Even though the amount of data is small, implying that errors are large, it appears significant that the slope of the nonthermal line width–size relationship of hot ammonia cores is shallower than that of cores in massive clouds. It is thus tempting to suggest that the shallower slope of the hot ammonia cores imply that they are denser and have steeper density profiles than massive cores.

In the above discussion it was assumed that hot ammonia cores are in hydrostatic equilibrium, being supported against collapse by a nonthermal mechanism most likely of magnetic origin (Myers & Goodman 1988). In this picture, the hot cores might correspond to the basic units of massive star formation. The assumption of hydrostatic equilibrium

is debatable, however. As discussed in the preceding sections, the hot ammonia cores are likely to be battered by the winds and heated by the radiation from the luminous star that excites the nearby H II region. The broad line widths of the hot cores may then reflect molecular gas that is undergoing outflow motions, possibly driven by the expansion of the hot ionized gas around the newly formed stars. The hot ammonia gas would then be part of the heated and compressed region behind the shock front around a compact H II region. Clearly in this case the line widths cannot be used to derive virial masses. Whether the physical properties of the hot ammonia cores correspond to those of the initial process of the formation of massive stars or have been strongly affected by the presence of the intense UV fields and winds from the nearby stars remains to be investigated. On the other hand, the hot ammonia cores could be undergoing collapse. Interestingly, models of collapsing hot molecular cores assuming that they collapse from an initial singular logatropic density distribution can account for the large observed nonthermal line widths (Osorio, Lizano, & D'Alessio 1999; see § 5.2.2).

3.5. Kinematics

In this section we discuss the results of observations, made with high angular resolution, of the velocity field toward hot cores which permit one to resolve the structure of the motions across them and hence allow one to investigate the dynamics of the hot circumstellar molecular gas. A range of gas motions, involving either rotational, infalling, or outflowing motions, has been observed.

3.5.1. Infall

The first firm detection of an accretion flow of molecular gas onto newly formed massive stars was found in the case of G10.6−0.4, the brightest member of a complex of compact H II regions. From observations with moderate angular resolution (9″), Ho & Haschick (1986) found a rapidly rotating core embedded within a more extended, lower density, slowly rotating envelope. In addition, part of the molecular gas within the core is accreting onto the central H II region. The later result was confirmed by high angular resolution observations (0.″3) which show that the molecular gas close to the central H II region exhibits differential rotation and accelerating infall (Keto, Ho, & Haschick 1987a, 1988). These studies strongly suggest that the molecular gas within the core of G10.6−0.4 is gravitationally collapsing and spinning up as it approaches the central star. Similar spectroscopic signatures, indicating collapse and rotation motions possibly associated with the original accretion flows, were observed by Keto, Ho, & Reid (1987b) toward the W3(OH) and G34.3+0.15 regions of active star formation. All these cores have embedded UC H II regions showing that the central star has arrived on the main-sequence stage while the natal molecular gas is still undergoing gravitational collapse.

W51 is the other high-mass star-forming region where infall motions have been extensively studied. Rudolph et al. (1990) proposed that the entire W51 molecular cloud complex is in a state of gravitational collapse involving $4 \times 10^4\ M_\odot$. However, interferometric observations show that the contraction is confined to small ammonia condensations of only a few tenths of a parsec (Ho & Young 1996). The ammonia cores located near the "W51e" cluster of UC H II regions, which are excited by B0–B0.5 stars (Gaume, Johnston, & Wilson 1993), exhibit strong indications of infall and rotational motions (Zhang & Ho 1997; Zhang, Ho, & Ohashi 1998a). As in the case of the sources mentioned above, the W51e2 core is in a stage where the central star has already arrived on the main sequence with the surrounding gas still contracting onto the mass concentration at the center (Ho & Young 1996).

3.5.2. Expansion

Ammonia emission from dense molecular condensations associated with young massive stars indicating expansion motions have been reported in several cases (e.g., Vogel et al. 1987; Keto & Ho 1989; Gómez et al. 1991; Wood 1993; Garay et al. 1993a). In most of them the expansion motions are ascribed to the emergence of an expanding H II region which sweeps up the remnant ammonia gas into thin filaments and clumps. For example, toward the W33 Main region the NH_3 emission appears immediately surrounding regions of ionized gas, and their velocity structure indicates that the shells of molecular gas are expanding away from the H II regions (Keto & Ho 1989). These results suggest that the molecular emission arises from the compressed and heated gas behind the shock front driven by the expansion of the H II regions.

Alternatively, the expansion motions of warm ammonia structures may be produced by the presence of powerful outflows in the region. Toward the G5.89−0.39 UC H II region, which is associated with a rapid (total velocity of $\sim$60 km s^{-1}) bipolar outflow traced by OH maser features (Zijlstra et al. 1990) and with a more extended, massive, and energetic flow observed in CO (Harvey & Forveille 1988), the ammonia observations show the presence of a massive ($\sim$30 $M_\odot$) and warm ($\sim$90 K) molecular envelope that is undergoing expansion (Gómez et al. 1991; Wood 1993). Similarly, toward the DR 21 star-forming region the ammonia line emission traces hot shocked gas, corresponding to the remnant material that has survived a powerful outflow (Wilson et al. 1995).

3.5.3. Rotation

Ammonia structures within massive star-forming regions exhibiting the presence of rotational motions have been

reported in a few cases. Most of these structures have flattened morphologies and diameters greater than 0.1 pc, corresponding to interstellar, rather than circumstellar, disks. Jackson, Ho, & Haschick (1988) detected a molecular disk or toroid, of $\sim$0.3 pc in diameter, associated with the compact H II region NGC 6334F (Rodríguez, Cantó, & Moran 1982). The disk, of $\sim 30\ M_\odot$, is gravitationally bound and rotating about a central star of $\sim 30\ M_\odot$ that excites the compact H II region. Gaume & Claussen (1990) found that the ammonia condensation within the Sgr B2 Main H II complex (Vogel et al. 1987) is intimately associated with an ultracompact region of ionized gas (source F) which shows a shell or ringlike morphology. The ammonia core has an extent of $\sim$0.1 pc and exhibits a velocity gradient, roughly along a north-south direction, of $\sim$25 km s^{-1} across the source. They suggest that the ammonia structure delineates a molecular disk or torus, surrounding the Sgr B2 F H II region, that is rotating with a velocity of $\sim$11 km s^{-1}, implying a mass interior to the disk of $\sim 1400\ M_\odot$.

The first firm evidence from ammonia observations of the presence of a rotating circumstellar disk was presented by Zhang, Hunter, & Sridharan (1998b), who found that the flattened disklike structure around the young high-mass star IRAS 20126+4104 ($\mathscr{L} \sim 1.3 \times 10^4\ L_\odot$) exhibits a velocity gradient across the major axis. The motions of the disk, which has a radius of $\sim 5 \times 10^3$ AU, are consistent with Keplerian rotation around a 20 $M_\odot$ point mass.

3.6. Evolutionary States

Vogel et al. (1987) proposed that hot cores are produced during a relatively brief stage after the star begins to heat the surrounding medium. At a very early stage, dense material is still falling toward the star, while in the later stages, marked by the emergence of an expanding H II region, the dense gas is dispersed by outflows. In addition, as current theories of star formation assert (cf. Shu et al. 1987), one also expects to see rotating circumstellar disks. Thus, by studying the core kinematics, it should be possible to identify ammonia cores over a range of evolutionary stages, from cores undergoing accretion to condensations experiencing outflows. The observations described in the previous section permit one to identify an evolutionary sequence within observed ammonia cores. In the remaining of this section we incorporate in the discussion results obtained not only from ammonia observations but from other tracers of hot cores.

3.6.1. Collapse Phase

The existence of cores in a collapsing phase has been well established observationally (see § 3.5.1). The presence of infalling gas toward a central mass concentration is demonstrated by position-velocity diagrams which show the classic "C" or "O" shapes consistent with radial motions projected along the line of sight. The available infrared and radio data even allow one to distinguish different stages within the collapse phase. Ammonia cores with infall motions and with embedded UC H II regions, implying that a massive star has already formed at their centers, most likely mark the oldest stage of the collapse phase. Explanations in terms of pure free-fall collapse of the molecular gas toward the central star (or stars) are difficult, since the free-fall collapse time of the core, $\sim 10^4$ yr, is short compared with the timescale of formation of the luminous early-type OB stars at the center of the flow ($\sim 10^5$ yr). It has been suggested (e.g., Ho & Haschick 1986) that the molecular gas in the core is spiralling toward the compact H II regions, slowly falling but rapidly spinning up due to partial conservation of the angular momentum.

Cores in an earlier evolutionary stage are distinguished by being luminous but not associated with an UC H II region (e.g., Cesaroni et al. 1994a; Hunter et al. 1998; Molinari et al. 1998). They are characterized by having densities of $\sim 10^7$ cm^{-3}, sizes $L \sim 0.1$ pc, and temperatures $T > 100$ K. Walmsley (1995) proposed that these cores host inside a young massive OB-type star (or stars) that is still undergoing an intense accretion phase. The high mass accretion rate of the infalling material quenchs the development of an UC H II region (Yorke 1984), and the free-free emission from the ionized material is undetectable at centimeter wavelengths. The mass accretion rate is also large enough that the ram pressure of the infall could provide the force to prevent the expansion of an H II region. The minimum accretion rate needed to choke off an incipient H II region, $\dot{M}_{\rm crit}$, is

$$\dot{M}_{\rm crit} = 2\sqrt{\pi}\mu m_{\rm H}\left(\frac{N_u G M_*}{\alpha_B}\right)^{1/2}, \qquad (14)$$

where M_* is the mass of the central object, μ is the mean atomic weight, and G is the gravitational constant. We will refer to this type of objects as collapsing hot molecular cores (CHMCs) to distinguish them from other types of hot molecular cores. Osorio et al. (1999) modeled the spectrum of several CHMCs as massive envelopes accreting onto a young massive central B-type star (see § 5.2.2). In order to fit the data, accretion rates in the envelopes $\dot{M} > 5 \times 10^{-4}$ $M_\odot$ yr^{-1} are required, implying that the main heating agent is the accretion luminosity. The lifetime of these objects is short $\lesssim 10^5$ yr. The central star is expected to increase its mass by accretion up to $M_* \sim$ 30–40 $M_\odot$ until the radiation pressure onto dust grains reverses the infall in timescales of $\sim 10^4$ yr. Osorio et al. (1999) suggest that radiation pressure together with a stellar wind can help clear out the accreting flow. An UC H II region is then produced, its evolution being governed by the reversal of the accretion flow.

The fraction of the observed ammonia cores that are in the CHMC stage is debatable. Most of the luminous ammonia cores without radio emission reported so far have been found in the neighborhood of H II regions, and it is not clear how much of its heating is due to internal or external sources of energy. Recently, Kaufman, Hollenbach, & Tielens (1998) calculated the temperature structure of dense hot cores with either internal or external illumination. They find considerable differences in the temperature structure; internally heated cores can more easily produce large column densities ($N_{H_2} \geq 10^{23}$ cm^{-2}) of hot ($T > 100$ K) gas than externally heated cores. These results are important because they can be used to observationally discern between different types of hot cores.

A potential candidate of a molecular core in this evolutionary stage is object W51e8 in W51, which shows spectroscopic characteristics of infall of a centrally condensed cloud (Ho & Young 1996; Zhang & Ho 1997). Radio continuum emission is undetected at 3.6 cm at a sensitivity of less than 1 mJy (Gaume et al. 1993) and detected ($\sim$17 mJy) at 1.3 cm wavelengths. The spectral index is much stepper than the one expected for an optically thick H II region, suggesting that the flux density at 1.3 cm is dominated by dust emission (Zhang & Ho 1997). The lack of free-free emission associated with this object could be interpreted as due to the action of accreting matter which keeps the region of ionized gas close to the stellar radius and prevents its expansion. Strong evidence for the presence of a luminous molecular core that may be the precursor of an UC H II region is presented by Molinari et al. (1998), who found that the luminous ($\mathscr{L} \sim 1.6 \times 10^4$ $L_\odot$) *IRAS* source 23385+6053 is coincident with a 3.4 mm compact and massive ($M \sim 470$ $M_\odot$) core, but is undetected in the radio continuum and at mid-IR ($\lambda < 15$ μm) wavelengths. This core would then correspond to a "forerunner" of an UC H II region.

Finally, ammonia cores with inward motions implying the presence of a massive object, but underluminous at infrared wavelengths and without detectable free-free emission, would represent cores in the earliest possible collapse stage, contracting toward a central mass condensation but without yet giving rise to a luminous protostar. Compact ammonia cores that exhibit radial flows and that are not associated with detectable sources of radio continuum emission have been observed within the star-forming regions DR 21 (Keto 1990), G10.5+0.0 (Garay et al. 1993a), and NGC 6334 (Kraemer et al. 1997). Their kinetic temperatures are consistently smaller than those of ammonia cores associated with compact H II regions. To show that these objects are effectively in the earliest evolutionary stage of infall, undergoing gravitational collapse and accretion just prior to the formation of a massive protostar, and not in the CHMC phase, it is crucial to determine their infrared luminosity with high angular resolution.

The positive identification of a protostellar condensation after gravitational collapse has formed a massive stellar core but before nuclear reactions have set in remains one of the main goals of observers of young massive stars. Even though direct evidence of the process of collapse of a dense and compact molecular core leading to the formation of a single massive star has yet to be obtained, there is an increasing number of objects that may be tracing very early stages of massive star formation, as evidenced by their association to H_2O masers, bipolar molecular outflows, and/or warm dust emission but no detectable, or weak, thermal emission from ionized gas (e.g., objects G75.78+0.34 MM and NGC 6334F MM; Carral et al. 1997). Interestingly, several of these objects have been found located near the head of cometary UC H II regions (Hofner & Churchwell 1996; Carral et al. 1997). Other luminous ($L_{bol} > 10^3$ $L_\odot$) objects identified with massive protostellar objects without detectable levels of radio continuum free-free emission are G34.24+0.13 MM (Hunter at al. 1998) and the TW object (Wilner, Welch, & Foster 1995) which is also associated with H_2O masers, a bipolar outflow, and a jet of synchrotron emission (Reid et al. 1995).

3.6.2. *Expansion Phase*

The evidence for the existence of a late stage in which the ammonia condensations are undergoing outflowing motions is also compelling and has been presented in § 3.5.2. The outflowing motions are produced either by the expansion of the recently formed H II region or by the presence of molecular outflows. In several cases the hot ammonia emission appears surrounding the newly formed UC H II region, suggesting compression and heating by the ionization shock front at the boundary of the H II region. The shell-like structure of molecular clumps around the H II regions may represent the latest stage in the evolution of a warm molecular core, before it is disrupted by the expansion of the H II region. This hypothesis is supported by the fact that the densities of the ammonia cores projected toward H II regions are generally lower than those found located beyond UC H II regions. Thus, OB stars play an important role in the heating, increase in velocity dispersion, and finally the destruction of the massive cores that gave them birth.

3.6.3. *Initial Phase*

The first phase of the evolutionary sequence in the formation of a massive star, representing the initial condition for the actual phase of gravitational collapse, is thought to consist of a dense and compact molecular core. We will refer to this structure as a high-mass prestellar core. Unlike its counterpart in sites of low-mass star formation, namely,

the ammonia cores (Myers & Benson 1983), its physical characteristics are still unknown, although it must contain a mass of at least 20 $M_\odot$ within a region with a size ≤ 0.05 pc (McCaughrean & Stauffer 1994; Hillenbrand 1997). An important issue which has not yet been discerned is the temperature of such a massive prestellar core, namely, the temperature just before massive star formation.

Although different strategies have been applied in search of these objects, the inherent quiescent massive prestellar cores have been difficult to detect. A number of searches have been made using as targets UC H II regions. Given the tendency of O and B stars to form in clusters and the continuing process of star formation within an association, it is expected to find molecular structures that will give rise to the next generation of massive stars near UC H II regions. In fact, most of the known hot ammonia cores have been identified using this criteria, and thus a strong selection effect is associated with the current available sample. The nearby OB stars have enough radiative and mechanical luminosity to substantially alter the initial core conditions. Such an environment is thus considerably affected by the presence of the existing massive stars, and whether or not the physical conditions of the hot cores near UC H II regions represent the initial conditions of massive prestellar cores is debatable (cf. Stahler, Palla, & Ho 1999). Hot cores either contain a central star or have been heated by nearby massive stars, and therefore their physical characteristics are unlikely to reflect initial conditions. It is possible that at the expected high densities and low temperatures of high-mass prestellar cores molecules are frozen on dust grains and are significantly depleted in the gas phase, so that their detection cannot be easily achieved via molecular line observations. Thus, others have sought for compact, massive condensations of cold dust emission based on high spatial resolution observations in the millimeter and submillimeter wavelength range. In particular, Mezger et al. (1988) found half a dozen compact dust emission knots with masses between 10 and 60 $M_\odot$ embedded in the NGC 2024 star-forming region. Mezger et al. (1988) derived that the knots have high densities ($n_H \sim 10^8$–10^9 cm^{-3}), sizes from 0.003 to 0.03 pc, and dust temperatures of $\sim$16 K, and suggested that they correspond to isothermal massive protostellar condensations without luminous stellar cores. However, observations of CS($7 \rightarrow 6$) line emission showed that the dust knots are closely associated with molecular condensations with gas temperatures of $\sim$45 K, inconsistent with the 16 K derived from the dust emission, suggesting that the submillimeter continuum peaks contain heavily obscured luminous stellar cores (Moore et al. 1989). Another strategy adopted in the search for the molecular precursors of high-mass stars is to use as targets H_2O maser sources that are not associated with radio continuum sources (cf. Codella & Felli 1995). As will be discussed in § 4.1, water masers are powerful signposts of regions of massive star formation, and their detection almost guarantees the presence of high-mass stars. The most promising approach in the search of massive prestellar cores, and determination of their physical parameters and dynamics, will be through high angular resolution observations at submillimeter wavelengths in tracers of cold, high-density molecular gas, which is one of the main goals of the next-generation submillimeter arrays.

4. MASER EMISSION

Since the discovery of maser phenomenon in the interstellar medium 35 years ago (Weaver et al. 1965), several studies have shown that three molecules exhibit widespread and powerful maser emission in regions of active star formation: H_2O, OH, and CH_3OH. More recently, maser emission in molecular lines of H_2CO and NH_3 has been detected toward a few compact H II regions (Hofner et al. 1994; Pratap, Menten, & Snyder 1994; Kraemer & Jackson 1995). Besides acting as powerful signposts of active star formation, the intense maser emission provides a unique tool to probe the physical conditions and kinematics of these regions on scales of 10–10^3 AU. The purpose of this section is to shortly summarize what has been learned about the dynamics of these regions and the spatial and physical association to other tracers of massive star formation. For excellent reviews of maser theory and observations, see Reid & Moran (1981, 1988) and Elitzur (1982).

4.1. H_2O

Interstellar water masers are characterized by appearing in small clusters of features or centers of activity, with extents of $\sim$10–100 AU, and by exhibiting a wide spread in velocity, of $\sim$50–100 km s^{-1} (Genzel & Downes 1977; Genzel et al. 1978). From a survey of water emission in the 6_{16}–5_{23} rotational transition at 22 GHz toward compact H II regions, Churchwell et al. (1990) found that the frequency of ocurrence of water masers in the neighborhood of newly formed O and B stars to be $\sim$67%, demonstrating that water maser action is a common phenomenon in regions of star formation. H_2O masers have been found in young forming regions containing stars as massive as O7 down to at least B3, their luminosity being proportional to the total FIR luminosity of the region (Moran 1990; Palagi et al. 1993). However, the detailed relationship between the H_2O masers and individual stars in these regions has yet to be established. Hofner & Churchwell (1996) found that water masers associated with H II regions of cometary morphology always appear in clumps located near, yet offset from, the cometary arcs. In most cases the H_2O centers of activity are either undetectable at radio continuum wave-

lengths or associated to weak radio continuum sources. In some cases the water masers are associated with hot molecular cores, suggesting that they might mark the position of young protostellar objects.

Using VLBI techniques it is possible to study the H_2O centers of activity with milliarcsecond resolution allowing measurements of proper motions and radial velocities, thus providing velocity information in three dimensions. However, very few observations of this kind have been made so far. Most of the H_2O masers studied with VLBI reveal radial expansion from a single origin (Orion-KL: Genzel et al. 1981; Sgr B2: Reid et al. 1988), implying that the H_2O maser phenomenon is associated with mass outflows. Using the VLA, with angular resolution of 0.″08, Torrelles and collaborators have recently mapped the water maser emission toward three regions of star formation containing multiple O and B stars, radio continuum jets, and molecular outflows. They found that the H_2O masers exhibit a dichotomy in their spatial distribution with respect to that of the radio jet: they trace either outflows (masers oriented along the major axis of the radio jet) or disks around YSOs (masers distributed perpendicular to the major axis of the radio jet). The water masers in disklike distributions appear to surround a B star, and their motions indicate either rotation (W75[B], NGC 2071; Torrelles et al. 1997, 1998a) or a combination of rotation and contraction (Cepheus A; Torrelles et al. 1996, 1998b). These results are very important since they show the presence and yield the kinematics of disks at scales as small as 10 AU. The masers found along the continuum jet exhibit a close spatial and velocity correspondence with the outflowing molecular gas, showing that they are taking part in the bipolar outflow.

4.2. OH

Hydroxyl masers are known to be excellent indicators of UC H II regions. Surveys of OH maser emission, in the 1.665 GHz line, toward star-forming complexes show that the OH masers are always found associated with the densest and most compact H II region within the complex. The OH maser emission arises from spots with linear sizes of $\sim 10^{14}$ cm and are distributed typically over regions of $\sim 10^{16}$ cm. The OH maser spots are generally found projected on the face of the compact H II region (e.g., Garay, Reid, & Moran 1985; Gaume & Mutel 1987). Garay et al. (1985) found that in most cases the OH masers are redshifted from the velocity of the associated UC H II region and suggested that the OH maser probably lie in a remnant accreting envelope, outside the advancing ionization front of the H II region, that is still collapsing toward the recently formed star. However, in the case of W3(OH) the proper motions of the OH maser spots suggest that they are in an expanding molecular shell between the shock front and the ionization front from the H II region (Bloemhof, Reid, & Moran 1992).

4.3. CH_3OH

Fifteen years after the discovery of methanol maser emission (Barrett, Schwartz, & Waters 1971) it was recognized that maser action in methanol lines is a common phenomenon in regions of massive star formation (Menten et al. 1986). Numerous masing transitions of methanol have been observed at centimeter and millimeter wavelengths. The strongest masers at centimeter wavelengths arise from the J_2–J_1 series of E-type methanol at 25 GHz (Barrett, Ho, & Martin 1975; Menten et al. 1986); the 2_0–3_{-1} E transition at 12.2 GHz (Batrla et al. 1987; Norris et al. 1987); the 2_1–3_0 E and 9_2–10_1 A^+ transitions at 19.9 and 23.1 GHz (Wilson et al. 1984, 1985); and the 5_1–6_0 A^+ transition at 6.7 GHz (Menten 1991; McLeod & Gaylard 1992; Caswell et al. 1995a). In the millimeter regime strong emission has been found in the 5_{-1}–4_0 E transition at 84 GHz (Batrla & Menten 1988); the 8_0–7_1 A^+ transition at 95 GHz (Plambeck & Menten 1990); the 3_1–4_0 E transition at 107 GHz (Val'tts et al. 1995), and the J_0–J_{-1} series of E at 157 GHz (Slysh, Kalenskii, & Val'tts 1995).

Two types of methanol masers have been identified (Batrla et al. 1987; Menten 1991): Class I masers which show maser emission in the 4_{-1}–3_0 E, 7_0–6_1 A^+, 5_{-1}–3_0 E, 8_0–7_1 A^+, and J_2–J_1 E transitions, and Class II masers which show maser emission in the 2_0–3_{-1} E, 2_1–3_0 E, 5_1–6_0 A^+, 9_2–10_1 A^+, 7_{-1}–8_{-1} E, 6_2–5_3 A^-, and 6_2–5_3 A^+ transitions. None of the lines that mase in Class I sources also mase in Class II sources and vice versa. Class I sources are found in the general vicinity of massive star-forming regions, but are offset from compact H II regions, strong infrared sources, OH maser centers, and other indicators of the formation of high-mass stars. Plambeck & Menten (1990) suggested that Class I masers are associated with shock fronts, indicating the interface of interaction between mass outflows and dense ambient material. Alternatively, Class I masers may be associated with earlier phases of stellar evolution and may indicate the true protostars which are still accreting mass. In contrast, Class II masers are closely associated with OH interstellar masers and compact H II regions (Menten et al. 1988; Norris et al. 1988; Caswell, Vaile, & Forster 1995b). They are frequently found spatially distributed along lines or arcs, suggesting that they might be associated with either shock fronts, jets, or edge-on protoplanetary disks around the nascent star (Norris et al. 1988, 1993).

4.4. NH_3

The first detection of maser emission in the ammonia molecule was presented by Madden et al. (1986), who

reported maser emission in the $(J, K) = (9, 6)$ inversion transition toward four regions of active star formation (W51, NGC 7538, W49, and DR 21[OH]). Since then, NH_3 maser emission from the W51 region has been reported in several other inversion transitions (Mauersberger, Henkel, & Wilson 1987; Wilson & Henkel 1988; Wilson, Gaume, & Johnston 1991; Zhang & Ho 1995, 1997) and detected toward the G9.62+0.12 and NGC 6334 star-forming regions (Hofner et al. 1994; Kraemer & Jackson 1995).

The relationship between the NH_3 maser action and the birth of young massive stars has yet to be established. Pratap et al. (1991) found that the ammonia masers toward the W51e H II region are closely associated to, although not coincident with, the two ultracompact H II regions W51e1 and W51e2. On the other hand, toward the G9.62+0.12 H II complex the NH_3 maser is coincident with a weak continuum source and a water maser (Hofner et al. 1994). Although the number of sources studied is small, the NH_3 masers exhibit the same dichotomy in their spatial distribution as the H_2O masers, tracing either disks or outflows. For instance, in the NGC 7538 region the NH_3 masers are coincident with the core of the bipolar compact H II region, show a velocity gradient, and seem to arise in a thick rotating molecular disk surrounding IRS 1 (Gaume et al. 1991). Toward NGC 6334I, the NH_3 masers are located at the end of high-velocity bipolar outflows, suggesting that they are produced by shocks and mark the location where the molecular outflow jet impinges upon the ambient medium.

4.5. Relationship between Masers

The discussion presented in the previous sections shows that masers are frequently associated with bipolar outflows, infrared sources, and UC H II regions, demonstrating that they are closely associated with the early stages of O and B star formation. The physical association between masers and other signposts of high-mass star formation has however yet to be established. In general there is a good overall positional coincidence between the masers and dense molecular clumps seen in thermal emission lines (cf. Gaume et al. 1993). On the other hand, in the complex regions of star formation where maser emission has been detected in different molecular species, the maser spots do not appear to be coincident with each other. A good illustration of this is presented in Figure 11, which plots the position of H_2O, OH, CH_3OH, and NH_3 maser spots toward the G9.62+0.19 massive star-forming region (Hofner et al. 1994), showing that the maser spots are usually not coincident. These authors propose that the striking alignment of masers, hot molecular clumps, and UC H II regions, along a linear structure of ~0.6 pc, is produced by a shock front, associated with the expansion of nearby more evolved H II regions, that has compressed the molecular gas and triggered star formation along the front.

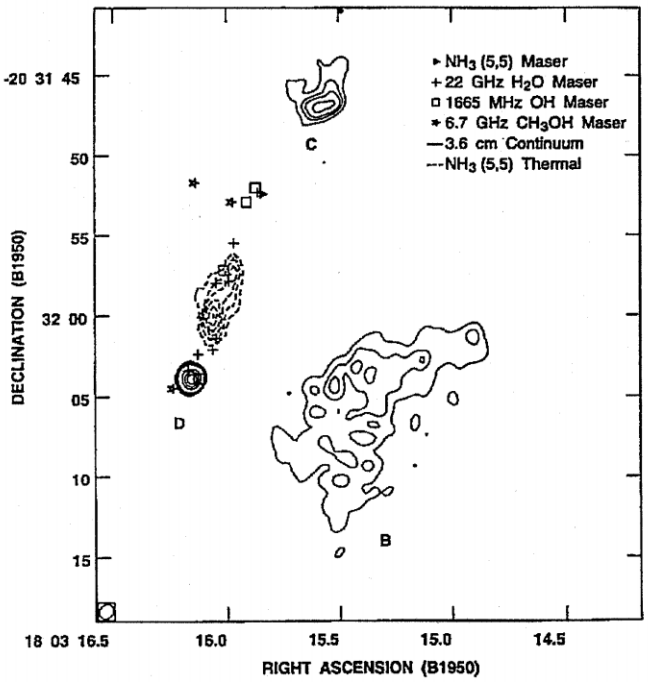

FIG. 11.—Maser spots (H_2O: *crosses*; OH: *boxes*; CH_3OH: *five-pointed stars*; NH_3: *filled triangle*) toward the G9.62+0.19 region of massive star formation, superposed on contour maps of the hot molecular gas [NH_3(5, 5) emission: *dashed line*] and ionized gas (radio continuum emission: *solid line*).

The lack of positional coincidence between different maser species suggests that they might indicate different evolutionary stages in the formation of massive stars (e.g., Lo, Burke, & Haschick 1975; Genzel & Downes 1977). The fact that H_2O masers are found located near, but not coincident with, compact radio continuum sources, whereas OH masers often coincide with UC H II regions, might indicate that H_2O masers are generally associated with stellar objects at an earlier stage of evolution than OH masers. It is thought that H_2O masers appear in the earliest stages of protostellar evolution, being excited in a high-density medium close to a deeply embedded protostar. They may arise either from a disk around a central protostar or from condensations or density enhancements in the outflow from a young stellar object which has not yet ionized a region large enough to be detectable. Methanol masers, which also seem to be signposts of disks around young massive objects, are in most cases associated with a detectable radio continuum source. This suggests that methanol masers indicate a later evolutionary stage than H_2O masers, in which the central protostar is currently developing a detectable UC H II region. OH masers, which are always associated with UC H II regions, appear last. They exist in a compressed, possibly infalling, shell of molecular gas just outside the Strömgren sphere of a very young star. The whole maser phenomenon ocurrs during the earlier phases of evolution

of massive stars and fades away as the H II region evolves into the diffuse stage (Codella et al. 1994b).

The relationship between masers and the sequence of maser events asserted above may not be unique, however. In some cases there is a close association between several types of masers and UC H II regions, which has been attributed to the presence of shocks. An example of this is the positional agreement between the H_2O, OH, and NH_3 masers and the ultracompact radio source E in G9.62+0.19, which is thought to correspond to a partially ionized stellar wind (Hofner et al. 1996). The masers toward this deeply embedded object are thought to mark an extremely young massive star in the process of destroying the remnant molecular material from which it formed. The CH_3OH masers near this source are displaced from the center of activity defined by the other masers and are probably excited by the collisions of dense clumps in the wind with clumps in the ambient gas.

5. THE FORMATION OF MASSIVE STARS

According to current ideas the first stage in the formation of massive OB stars is initiated by contraction and fragmentation of a giant molecular cloud leading to the formation of dense molecular cores in approximate hydrostatic equilibrium. This premise is supported by observations which show that GMCs are composed of numerous dense cores and have small volume filling factors (e.g., Blitz 1993). The cores appear to have a considerable range of physical parameters. The distribution of core mass follows a power-law relation with an index of -1.6 (see Blitz 1991 and references therein), close to the value of -1.5 predicted as the result of an equilibrium between coagulation and fragmentation (Spitzer 1982; Genzel 1991). Little is known, however, about the relationship between the mass spectrum of the cores and the initial mass function of the massive stars. The most massive stars appear to form in the dense cores of massive clouds, and the mass of the most massive young star increases systematically with the mass of the associated molecular cloud (Larson 1982). In addition, the average star formation efficiency increases with cloud mass (Williams & McKee 1997).

The discussion presented in the preceding sections raises a host of questions related to the structure of molecular cores and the formation of massive stars, such as: Once a molecular core forms, how does it evolve to produce massive stars? What are the roles of fragmentation and accretion? Do the more massive cores lead to a simultaneous formation of a group of massive stars or does the formation of massive stars proceed individually from well-separated dense smaller clumps? Is there a basic unit within dense cores that will eventually produce a single massive star? How often does the collapse of massive molecular cores lead to the formation of clusters of massive stars rather than to a single high-mass star? Are accretion disks and bipolar outflows present in the formation of massive stars? Although no definite answer to these questions have been given yet, partial answers are beginning to emerge. In the following discussion we first summarize the main observational properties that have been gathered about the formation of massive stars, then discuss basic theoretical principles of a few physical phenomena that are relevant for the development of a theory of massive star formation, and finally speculate on a possible scenario for the formation of massive stars.

5.1. Observational Characteristics

5.1.1. Clustering, Gregariousness, and Segregation

A wealth of radio continuum observations of deeply embedded star-forming regions in our Galaxy have shown that massive stars are gregarious, namely, that they tend to be born in groups (e.g., Ho & Haschick 1981; Welch et al. 1987; Rudolph et al. 1990; Garay et al. 1993b). As discussed in § 2.4, Garay et al. (1993b) found that most of the luminous *IRAS* point sources associated with compact regions of ionized gas exhibit complex structure in their radio continuum emission, suggesting that the complex morphologies are produced by excitation from multiple stars and thus implying that a cluster of OB stars have been formed. The radio free-free observations can only detect massive, luminous stars within the region, and thus they do not provide information regarding the less luminous nonionizing stars.

The ability to investigate the population of newly formed stars deeply embedded in molecular clouds has recently improved with the advent of infrared array detectors. Several regions containing high-mass stars have been extensively studied: W3 (Megeath et al. 1996), Mon R2 (Carpenter et al. 1997), Orion-Trapezium (Hillenbrand & Hartmann 1998), and NGC 2024 (Lada et al. 1991), giving valuable clues to the mechanism of formation of massive stars. These observations show that massive stars do not form in isolation but are instead born in relatively rich clusters. The young embedded clusters have typically stellar volume densities of $\sim 10^4$ stars pc^{-3} and sizes of 0.2–0.4 pc. Furthermore, they provide clear evidence that the most massive stars within the dense cluster are preferentially formed near its central region. The concentration of OB stars near the center of young stellar clusters is unlikely to be the result of dynamical evolution since the ages of the stars are smaller than the required collisional relaxation times (Hillenbrand & Hartmann 1998; Bonnell & Davies 1998). In addition, the gravitational potential of the cluster still has a significant contribution from molecular gas that is usually thought to impede the process of dynamical mass segregation. The preference for high-mass stars to be

located in dense, central cluster regions is thus likely to be a primordial feature, namely, an indication of where massive stars are formed. The mass segregation in young stellar clusters would then reflect their formation scenario and the cluster initial conditions.

5.1.2. *Bipolar Molecular Outflows*

Bipolar molecular outflows represent an important evolutionary stage in the formation of low-mass stars (see Shu 1991 and Bachiller 1996 for reviews on theory and observations, respectively). Although systematic studies to identify bipolar outflows from massive young stellar objects (YSOs) have begun only recently, there is growing evidence that bipolar molecular outflows are also associated with massive stars (Snell et al. 1984; Scoville et al. 1986; Garden et al. 1991; Harvey & Forveille 1988; Bachiller & Cernicharo 1990; Kastner et al. 1994; Shepherd & Churchwell 1996b; Acord, Walmsley, & Churchwell 1997; Shepherd, Churchwell, & Wilner 1997), showing that this phenomenon is also a basic component of the formation process of massive stars. To investigate the frequency of occurrence, Shepherd & Churchwell (1996a) searched for high-velocity (HV) line wings toward $\sim$120 high-mass star-forming regions and found that the presence of HV gas is quite common ($\sim$90%). If the HV gas is due to bipolar outflows, then these results indicate that molecular outflows are a common property of newly formed massive stars.

A list with most of the currently known massive bipolar outflows detected toward young massive star-forming regions and their properties has been recently compiled by Churchwell (1999). The bipolar outflow masses range from about 10 to 4800 $M_\odot$, with a mean value of 130 $M_\odot$; the mass outflow rates range from 3×10^{-5} to 3×10^{-2} $M_\odot$ yr^{-1}, and the kinetic energies range from 1×10^{46} to 6×10^{48} ergs. Whereas the dynamical ages of outflows in massive star-forming regions are similar to those associated with low-mass YSOs, their masses, outflow rates, and energetics are substantially larger (Churchwell 1997). In particular, the mean mass and luminosity of outflows in massive star-forming regions are roughly a factor of 100 times greater than those from low-mass stars (Churchwell 1999). These results indicate that the luminous outflows are driven by massive stars which are indeed more energetic and hence are able to inject more energy into their surroundings than low-mass stars. In fact, it has been found that the mass outflow rate, force, and mechanical luminosity of the molecular outflows are tightly correlated with the stellar luminosity of the driving source (Cabrit & Bertout 1992; Shepherd & Churchwell 1996b).

Although most of the massive outflows are found in the immediate vicinity of UC H II regions, the identification of the driving source is not straightforward since in many cases, if not always, a cluster of emerging massive stars is present in these regions. Possibly the best way to identify the energy source would be through observations of the radio continuum emission from the stellar jet that is expected to be associated with the driving source (e.g., Rodríguez et al. 1994). We note that a few massive outflows do not show the presence of compact sources of radio continuum emission that could be identified as the driver of the bipolar outflow. In these cases the driver of the flow is probably a massive protostar that has not yet been able to form a detectable H II region because of rapid mass accretion (see § 3.6.1). Particularly notable are the luminous objects IRAS 20126+4104 ($L_{\rm bol} \sim 1.3 \times 10^4$ $L_\odot$) and IRAS 23385+6053 ($L_{\rm bol} \sim 1.6 \times 10^4$ $L_\odot$), which are associated with outflows, are luminous in the millimeter-wavelength range, but are undetected in the continuum at centimeter wavelengths (Cesaroni et al. 1997; Molinari et al. 1998), suggesting that they are bona fide massive Class 0 objects, namely, massive protostars in a very early accretion phase (André, Ward-Thompson, & Barsony 1993).

The observational results described above are of invaluable importance, implying that bipolar molecular outflows are a basic component of the formation process of all stars. However, the large masses and energetics associated with the luminous outflows raise several questions which have not yet been answered, such as: What is the origin of the mass in massive outflows? and What is the driving mechanism of the luminous outflows? Although the physics of the high-mass outflows remain to be addressed, it has been suggested that a common driving mechanism could operate across the entire mass or luminosity range (Richer et al. 1999).

5.1.3. *Disks*

Most of the flattened structures detected within high-mass star-forming regions have diameters in the range 0.1–1 pc, corresponding to interstellar, rather than circumstellar, disks (Vogel & Welch 1983; Jackson et al. 1988; Gaume & Claussen 1990; Nakamura et al. 1991; Ho, Terebey, & Turner 1994; Kraemer et al. 1997). A large fraction of these elongated structures exhibit smooth velocity gradients, suggesting that they correspond to rotating disks. Their masses range from 10 to 2000 $M_\odot$. In some cases rotation in combination with collapse or expansion motions are detected. The massive rotating interstellar disks may provide the natural environment for the formation of a cluster of stars. Whether they correspond to dynamically bound disks is not yet known.

The evidence for the presence of circumstellar disks ($<10^4$ AU) around young massive stars was, until recently, null. However, sensitive, high angular resolution observations of dust and molecular gas emission are beginning to change this state of affairs. Synthesis observations of the SiO maser emission from IRc2, a young star with a lumi-

nosity of $\sim 10^5\ L_\odot$ in the Orion KL region, provide strong evidence for the presence of an 80 AU diameter rotating and expanding circumstellar disk (Plambeck, Wright, & Carlstrom 1990). Dust emission from this disk has been detected at mid-IR wavelengths (7.8 and 12.5 μm: Lester et al. 1985; 3.6 μm: Dougados et al. 1993). An elongated dust feature of $\sim 10^2$ AU is detected at near-infrared wavelengths toward the luminous ($\sim 3 \times 10^4\ L_\odot$) star MWC 349A (Lienert 1986). Zhang et al. (1998b) found that the flattened disklike structure around the young high-mass star IRAS 20126+4104 ($\mathscr{L} \sim 1.3 \times 10^4\ L_\odot$), first detected by Cesaroni et al. (1997) in CH_3CN, exhibits a velocity gradient across the major axis. The kinematics of the disk, which has a radius of $\sim 5 \times 10^3$ AU, are consistent with Keplerian rotation around a 20 $M_\odot$ star.

A new and exciting probe that is providing distinct evidence of the presence of circumstellar disks rotating around a massive OB star is methanol maser emission. Interferometric observations towards a few southern massive star-forming regions show that the CH_3OH masers lie along lines or curves and have linear velocity gradients (Norris et al. 1998). The line of masers within source G339.88−1.2, a compact H II region excited by a B0.5 star, lies across the diameter of the H II region, suggesting that they are tracing a circumstellar photoevaporated disk (Ellingsen, Norris, & McCulloch 1996). This has been confirmed by observations at 10 μm which show a disklike dust feature aligned with the methanol masers (Stecklum et al. 1998). In sources G309.92+0.48 and G336.42−0.26 the motions of the methanol maser spots are essentially Keplerian, implying the presence of bound disks, with diameters of 4×10^3 and 3×10^3 AU, around central masses of 10 and 14 $M_\odot$, respectively (Norris et al. 1998). Interestingly, Natta, Grinin, & Mannings (1999) found that Herbig Be stars, which are in a later stage of evolution than the above objects, are not associated with the compact continuum emission in the millimeter expected from circumstellar disks, suggesting that the disks may have been eroded by the strong radiation fields.

5.2. Physical Processes

The sequence of processes leading to the formation of massive stars from the parental molecular cloud is not yet well understood and is one of the most important challenges in the field of star formation. Clustered star formation is a complex hydrodynamic problem which, in addition to gravity, angular momentum, magnetic fields, and heating and cooling, should include feedback effects from dense protostellar cores and newly formed stars.

Since the formation of massive stars occurs simultaneously on a number of gravitating centers, implying some kind of global synchronization of the process, a comprehensive theory of massive star formation must necessarily provide a thorough account of the progression of molecular gas over several decades in spatial scales (see Larson 1999). It should yield a detailed description of all stages of evolution, beginning with the initial stage in which the large-scale fragmentation of a molecular cloud, containing clumps and dense filaments, leads to the formation of dense massive cores, proceeding through intermediate stages in which the fragmentation of dense cores leads to the formation of multiple prestellar cores, and ending with the final stage of evolution of a protostar which accretes from its surrounding dense core, and possibly interacts with other prestellar cores through winds, radiation, and/or dynamically, leading to the formation of a massive star. The stages of building stars from the collapse of their parent molecular clouds is thought to involve two main processes: fragmentation and accretion. In what follows we discuss the importance of these processes in forming massive stars.

5.2.1. *Fragmentation*

Fragmentation processes are believed to be important in the initial stage of the collapse of large clouds of molecular gas. The details of the mechanism of gravitational fragmentation are poorly known. Theoretical studies indicate that gravitational fragmentation during three-dimensional collapse is a highly inefficient process but that fragmentation will occur in flattened or filamentary structures (Layzer 1963; Larson 1972, 1985). Fragmentation can also become significant if large density perturbations are present initially, the small perturbations being damped out during the collapse (e.g., Tohline 1980a, 1980b).

Numerical simulations of the fragmentation of an isothermal collapsing cloud show that condensations can indeed be formed on a dynamical timescale as a result of gravitational fragmentation (e.g., Larson 1978; Monaghan & Lattanzio 1991). In particular, Larson (1978) found that the number of condensations formed in the collapse of an isolated cloud is comparable to the number of Jeans masses initially present. For a cloud with gas temperature T and molecular hydrogen density n_{H_2}, the Jeans mass, M_J, representing the minimum mass of gas that is required for gravitational collapse, is

$$M_J = 5.6 \left(\frac{T}{10\ \mathrm{K}} \right)^{3/2} \left(\frac{n_{H_2}}{10^4\ \mathrm{cm}^{-3}} \right)^{-1/2} M_\odot\ ,$$

which decreases with increasing density. To assess the validity of Larson's result under different initial conditions, Klessen, Burkert, & Bate (1998) followed the isothermal collapse and fragmentation of a small highly gravitationally unstable region, consisting of a hierarchy of clumps and filaments. They find that the large-scale density fluctuations within the region under consideration collapse onto them-

selves and into filaments and knots in about a free-fall time of the isolated region. Dense cores are formed in the center of the most massive Jeans-unstable clumps, soon followed by the collapse of clumps of lower initial mass, altogether creating a hierarchical structured cluster of highly condensed cores. The mass distribution of the resulting cores peaks at about twice the initial Jeans mass in the system and ranges from 0.3 to 15 Jeans masses. Thus, at the end of the fragmentation phase a fragment's mass is typically of the order of the initial Jeans mass, roughly independent of the initial conditions.

Nevertheless, a wealth of observations shows that giant molecular clouds and massive cores are supported against gravity by turbulent motions and magnetic fields rather than by thermal pressure (McKee 1989; Bertoldi & McKee 1992). Thus, the concept of Jeans mass may be of little use in the definition of the appropriate initial conditions in the context of fragmentation of molecular clouds. Furthermore, the above results, whereby a collapsing cloud fragments into clumps with masses of the order of the initial Jeans mass, do not easily explain the formation of massive stars. Massive stars appear to form in the dense ($n_{H_2} \sim 3 \times 10^5$ cm^{-3}) cores of massive cold clouds where the Jeans mass is only $\sim 1.0\ M_\odot$, considerable smaller than those of OB stars. This conclusion rests, however, on the assumption that the cloud temperature is similar to that observed in dark clouds producing low-mass stars, $T \sim 10$ K. It has been argued that more massive fragments could form if the gas temperature in high-mass star-forming regions were higher. As discussed in § 3.3.1, temperatures of 100–200 K are now routinely measured toward hot cores near H II regions, suggesting that fragments with masses of the order of a massive star can be produced in such environments. However, hot cores might be or are influenced by the presence of a nearby, or embedded, massive star, whose large luminosity raises the temperature of the ambient dust and gas. Thus, it is not clear if this temperature is the same as that before the formation of massive stars. It might be possible that the temperature of massive cores increases gradually with time as energy is injected in the surrounding medium by low- and intermediate-mass stars formed during an initial stage of star formation and that the massive stars are formed last, during a late "hot" stage of star formation. Nevertheless, we stress that the effects of magnetic fields and turbulence at large scales in molecular clouds will dominate the cloud structure. In particular, their support allows the clouds to achieve much higher densities than with thermal pressure support alone before becoming gravitationally unstable (Caselli & Myers 1995; Crutcher 1999).

Another mechanism of fragmentation might occur in turbulent flows. Based on two-dimensional hydrodynamical simulations of the interstellar medium at kiloparsec scales, Ballesteros-Paredes, Vázquez-Semadeni, & Scalo (1999) proposed that GMCs and their substructures form as density fluctuations induced by large-scale interstellar turbulence due to colliding streams of gas (see also Vázquez-Semadeni, Passot, & Pouquet 1996). However, in these simulations quasi-hydrostatic configurations like the observed ammonia cores have not yet been produced.

5.2.2. *Coalescence and Accretion*

It is believed that accumulation processes, such as interactions among clumps or forming stars (e.g., Larson 1978, 1982, 1990), and/or accretion processes play a crucial role in the formation of massive stars. If most of the gas in a massive molecular core is in clumps, a clump may gain mass through coagulation with other clumps or through accretion from residual gas. Larson (1992) suggested that core coalescence can account for the observed power law of the stellar initial mass function (see also Silk & Takahashi 1979). A key issue is to identify a mechanism that increases the efficiency of accretion processes in dense protocluster cores. Larson (1982) suggested that tidal forces from an association of stars produce the disruption of incipient condensations within the remaining gas, with the gas settling toward the center of the forming cluster and becoming progressively more dense. Much of this dense gas may then give rise to a few massive stars. Bonnell et al. (1997) investigated the effects of accretion of gas in a cloud containing initially a number of nucleating centers and found the accretion process to be highly nonuniform, with a few nucleating centers accreting significantly more than the rest. A large dynamic range in the final core masses is obtained, with the nucleating structures near the cloud center accreting, due to their location at the bottom of the potential well, most of the material and hence giving rise to the most massive stars. There are then two possible stages of accumulation of gas: an initial stage of coalescence in which dense cores grow by accretion and interactions with other cores and become progressively more massive and condensed, and a final accretion stage in which a protostar mainly accretes from its surroundings.

Recently, Stahler et al. (1999) suggested that OB stars could form inside dense clusters by coalescence of already existing stars of lower mass. Since the cross section for these type of encounters is too small for naked stars, they suggested that the coagulation occurs when the low-mass stars are still surrounded by dense molecular cores which increases the effective cross sections.

An alternative scenario for the formation of massive stars is direct accretion onto a central object from a surrounding prestellar dense, massive ($M \geq 100\ M_\odot$) core. This accretion scenario assumes the existence of such structures but does not address the problem of their formation. A potential problem in forming massive stars by accretion from an infalling envelope is the difficulty of accreting once the protostar has attained a mass $\geq 10\ M_\odot$. The large radiation

pressure on dust grains, produced by the intense radiation field of such a protostar, can halt the collapse and reverse the infall (Larson & Starrfield 1971; Kahn 1974; Yorke & Krügel 1977). This problem may be circumvented in two ways. First, the above limit applies to accretion in a spherically symmetric collapse. However, the prestellar core is likely to have some angular momentum resulting in the formation of a protostellar disk. Accretion onto the massive protostar may then proceed from the disk. In this case, Jijina & Adams (1996) found that the maximun luminosity-to-mass ratio for radiation pressure on dust grains to reverse the infall is much less restrictive. Second, Wolfire & Cassinelli (1987) showed that for inflows with mass accretion rates $\dot{M} \geq 10^{-3}\ M_{\odot}\ \mathrm{yr}^{-1}$, the ram pressure is sufficiently strong to overcome the radiative forces on dust by the luminous central star, allowing continuous accretion to form massive stars.

Recently, Osorio et al. (1999) developed models of collapsing hot molecular cores assuming that the cores collapse from an initial singular logatropic density distribution characterized by a logatropic equation of state $P = P_0 \ln(\rho/\rho_0)$, where ρ_0 is an arbitrary reference density and P_0 is the pressure at this density. This type of structure has been invoked by several authors (Lizano & Shu 1989; Myers & Fuller 1992; McLaughlin & Pudritz 1996) to explain the line width–density relation observed in molecular clouds ($\Delta v \propto \rho^{-1/2}$; e.g., Larson 1981) since in logatropes the sound speed, c_s, given by $c_s = (dP/d\rho)^{1/2} = (P_0/\rho)^{1/2}$, depends on density like the observed relationship. The mass-weighted quadratic velocity dispersion of a logatropic core is

$$c_s^2 = \left(\frac{8\pi G P_0}{9}\right)^{1/2} R_{\mathrm{core}}\, F(x)\ ,$$

where R_{core} is the core size and $F(x) = (1 + x + x^2)/(1 + x)$, where $x = s/R_{\mathrm{core}}$ is the fraction of the core size that is actually probed by observations in a given molecular line. The distance s is measured from the outer boundary of the core, R_{core}, toward the center of the core. For an optically thin transition, $x \sim 1$ and $F(x) \simeq 3/2$, whereas for an optically thick transition, like NH_3 lines, $x \ll 1$ and $F(x) \simeq 1$. This velocity dispersion corresponds to the virial speed that provides the hydrostatic support of the logatropic core. Appreciable free-fall speeds are expected only at scales of a few tens of AU from the core center. The expected line width (FWHM) averaged over the source is

$$\Delta v = 6.8\left(\frac{P_0}{4\times 10^{-7}\ \mathrm{dyn\ cm^{-2}}}\right)^{1/4} \times \left(\frac{R_{\mathrm{core}}}{0.1\ \mathrm{pc}}\right)^{1/2} [F(x)]^{1/2}\ \mathrm{km\ s^{-1}}\ ,$$

where the normalization factors in P_0 and R_{core} are typical of the cores modeled by Osorio et al. (1999). Thus, this type of models can account for the large line widths observed in hot molecular cores as shown in Figure 10.

5.2.3. *Magnetic Fields*

Magnetic fields are believed to play an important role in the formation process of stars. They may initially provide the support of molecular clouds against gravity (e.g., see reviews of Heiles et al. 1993; McKee et al. 1993). A molecular cloud can be supported against its self-gravity by magnetic fields alone provided its mass is less than the magnetic critical mass, M_{Φ},

$$M_{\Phi} = \frac{1}{2\pi}\frac{\Phi}{G^{1/2}}\ ,$$

where $\Phi(=\int B dA)$ is the magnetic flux threaded by the cloud (Mestel & Spitzer 1956; Mouschovias & Spitzer 1976; Tomisaka, Ikeuchi, & Nakamura 1988, 1989; Li & Shu 1996). For a cloud with radius R and magnetic field of strength B, $\Phi \simeq \pi R^2 B$. If the cloud mass is greater than the critical mass, $M > M_{\Phi}$, the cloud is called supercritical. It has been suggested that, in the absence of other substantial means of support, supercritical clouds will collapse to form a closely packed group of stars. Instead, subcritical clouds with $M < M_{\Phi}$ will condense locally as the magnetic field support is lost via ambipolar diffusion. This dichotomy is the basis of the proposed mechanism of bimodal star formation in which "loosely aggregated" versus "closely packed" star formation occurs (Shu et al. 1987, 1993).

Since molecular clouds are lightly ionized, the predominantly neutral (molecular) matter feels the Lorentz force through collisions with ions that slip past the neutrals in the process known as ambipolar diffusion, first studied by Mestel & Spitzer (1956). This causes a local weakening of the magnetic support that allows the condensation of dense cloud cores with subcritical masses. The evolution of axisymmetric clouds and dense cores to a centrally condensed state via ambipolar difusion of the magnetic field has been investigated by several authors (e.g., Nakano 1979, 1982; Lizano & Shu 1989; Tomisaka, Ikeuchi, & Nakamura 1990; Basu & Mouschovias 1994; Ciolek & Mouschovias 1994). As a result of the loss of magnetic field support, the cloud core reaches a "gravo-magneto catastrophe" where the central density tries to reach infinite values (Shu 1995). To describe the transition between quasi-static evolution by ambipolar diffusion and dynamical gravitational collapse, Li & Shu (1996) introduced the idea of a pivotal state with a scale-free, magnetostatic, density distribution approaching $\rho \propto r^{-2}$, for an isothermal equation of state, when the mass-to-flux ratio has a constant

value, a condition they termed "isopedic." These pivotal states flatten as the degree of magnetic support is increased. Although small, dense cores that give rise to low-mass star formation are effectively isothermal, the situation may be different for larger and denser regions that yield high-mass or clustered star formation. Recently, Galli et al. (1999) have generalized these pivotal states to self-gravitating isopedic clouds with a polytropic equation of state with negative index n. These polytropic equations of state try to mimic the support due to the observed nonthermal motions in molecular clouds. In particular, the associated sound speed increases with decreasing density as the observed line width–density relation for molecular clouds (see § 3.4). These pivotal states may represent the initial states for dynamical collapse to form a star or group of stars.

5.3. Collapse Models

Theoretical studies of gravitational collapse, intended to model the collapse of a dense molecular cloud to form a star, have been made by several authors. In particular, the problem of finding self-similar solutions for the gravitational collapse of isothermal spheres has been investigated by Larson (1969), Penston (1969), Shu (1977), Hunter (1977), Whitworth & Summers (1985), and Foster & Chevalier (1993). Larson (1969) and Penston (1969) studied the collapse of an isothermal sphere with initial uniform density which evolves to a central region of homologous inflow. In their similarity solution, the central flow tends to a free-fall collapse with velocity proportional to $r^{-1/2}$ and density proportional to $r^{-3/2}$, whereas in the outer parts the inflow velocity is constant at 3.3 times the sound speed and the density is proportional to r^{-2}. On the other hand, Shu (1977) derived a self-similar solution for the collapse of a singular isothermal sphere with an initial density distribution of the form

$$\rho = \frac{Aa^2}{4\pi G}\frac{1}{r^2},$$

where a is the local sound speed and A is a dimensionless constant. If $A = 2$ the sphere is initially in hydrostatic equilibrium and the cloud collapse begins at the center and spreads outward. In this case the mass accretion rate is constant in time and equal to $\dot{M} = m_0(a^3/G)$, where m_0 is a constant ($=0.975$). In the Larson-Penston (LP) solution, the initial accretion rate onto the central object is ~ 47 times higher than in Shu's solution and declines monotonically. Hunter (1977) and Whitworth & Summers (1985) showed that there is a continuum set of similarity solutions for the collapse of an isothermal sphere, the LP ($A = 8.85$, $m_0 = 46.9$) and Shu ($A = 2$, $m_0 = 0.975$) solutions being the extreme cases (the fastest and slowest collapse, respectively). In particular, models of the condensation of cloud cores via ambipolar diffusion discussed in the previous section do show a tendency of the core's density to acquire a scale-free profile $\rho \propto r^{-2}$.

Models that include the effects of magnetic fields have been investigated by several authors. Galli & Shu (1993a, 1993b) followed the collapse of a magnetized isothermal cloud and found that strong magnetic pinching forces deviate the infalling gas to the equatorial plane to form a flattened disequilibrium structure around the star (a "pseudodisk"). Tomisaka (1995, 1996) and Nakamura, Hanawa, & Nakano (1995) studied the collapse and fragmentation of magnetized cylindrical clouds and found that geometrically thin disks perpendicular to the symmetry axis are formed which evolve toward a central singularity. Shu & Li (1997) found that in isopedic thin disks, the magnetic tension exerts a force that acts to dilute the disk self-gravity, while magnetic pressure is proportional to the gas pressure that gives support to the disk in the vertical direction. They found that fragmentation of the disk does not occur, but instead the disk collapses inside-out to form a single compact object (Li & Shu 1997; see also Nakamura et al. 1995). Chiueh & Chou (1994) considered the collapse of a spherical magnetized cloud, taking into account only the isotropic pressure of a tangled magnetic field, and found that the collapse proceeds in an inside-out fashion, as in the unmagnetized case. A similar approach was followed by Safier, McKee, & Stahler (1997), who investigated the quasi-static evolution of spherical magnetized clouds due to ambipolar diffusion of the magnetic field and the subsequent inside-out collapse of the envelope to a central mass, ignoring magnetic tension and thermal pressure. Li (1998a) extended the work of Safier et al. (1997) to include thermal pressure and followed the evolution of the core through the formation of a point mass at the center (see also Li 1998b). Ciolek & Königl (1998) calculated the evolution through the central point-mass formation including the magnetic tension (see also Contopoulos, Ciolek, & Königl 1998). Recently, Allen & Shu (1999) followed the self-similar collapse of the isothermal pivotal states studied by Li & Shu (1996). All these calculations show that for magnetized clouds, the mass accretion rates increase with respect to that in the unmagnetized case. This happens because of the higher densities supported by magnetic fields in the equilibrium state, and also, as found by Galli & Shu (1993b), because the slowing down of the infall speed by magnetic forces is largely offset by the increase of the signal speed at which the wave of infall propagates outward.

5.4. Star Formation

Shu's solution provided the basis for the development of the current paradigm of the gravitational collapse of low-mass cores leading to the formation of low-mass stars (Shu et al. 1987, 1993). In this model a self-gravitating core ini-

tially supported by magnetic fields gradually contracts and becomes centrally condensed as the magnetic field is lost via ambipolar diffusion, producing an unstable isothermal core with an r^{-2} density distribution. Finally, gravity predominates over magnetic forces and an inside-out dynamical collapse occurs. The collapse begins at the center of the core and propagates outward at the effective sound speed, $a_{\rm eff}$,

$$a_{\rm eff} = (1 + 2\alpha + \beta)^{1/2}\left(\frac{kT}{\mu m_{\rm H_2}}\right)^{1/2}, \qquad (15)$$

where α and β are the ratios of the magnetic pressure ($B^2/8\pi$) and turbulent pressure ($\rho\langle\delta v^2\rangle$) to thermal pressure ($\rho kT/m$), respectively, producing a density distribution of $r^{-3/2}$ close to the central point mass, behind the expansion wave. The rate, $\dot{M}$, at which the central object accumulates matter is

$$\dot{M} = 0.975\,\frac{a_{\rm eff}^3}{G}\,. \qquad (16)$$

As a result of the initial rotation of the core, a flattened disk is produced at the center of the collapsing structure (cf. Terebey, Shu, & Cassen 1984). There follows an outflow stage in which the protostar deposits linear momentum, angular momentum, and mechanical energy into its surroundings through jets and molecular outflows, while still accreting mass. Finally, the protostar settles onto the ZAMS. The predictions of this model are in good agreement with observations of collapse in several low-mass cores (e.g., Zhou et al. 1990) and has become the paradigm of low-mass star formation. Nonetheless, Mardones (1998) and Tafalla et al. (1998) recently claimed that the strong molecular line asymmetries found in dense cores around low-mass YSOs require infall speeds at large distances from the YSOs, which, even though subsonic, are inconsistent with pure inside-out collapse models. On the other hand, the theory of gravitational collapse of high-mass cores leading to the formation of massive stars has not yet been well developed. The recent observational results are providing valuable constraints for theoretical models.

5.5. Formation Scenario

The initial evolution of molecular clouds to form dense prestellar massive cores is perhaps the most poorly understood aspect of massive star formation (cf. Larson 1999). Also, the dynamical processes taking place within massive cores to form massive stars are yet to be understood. The observational evidence gathered during the last decade suggests that in clouds with masses above a certain value, the formation of a cluster is favored instead of isolated star formation. In particular, the largest ($\sim$few parsecs) massive cores seems to give rise to stellar clusters and OB associations. The simultaneous process of formation of massive stars on a number of gravitating centers is thought to be related to the initial stage of gravitational fragmentation which leads to the synchronized formation of prestellar cores. Magnetic fields are thought to play an important role in the support of the cloud before collapse, allowing high densities in the cores to be achieved.

Some authors have argued that the first stage in the formation of massive stars is the overall collapse of a massive core. A spectacular case where large-scale, seemingly organized, massive star formation has taken place is that of the central region of the W49A massive molecular cloud core (Welch et al. 1987). W49A exhibits a remarkable ring of compact H II regions, lying within a region of 2 pc in diameter, made of 10 distinct ionized regions each containing at least an O star. The ring is apparently rotating with an angular velocity of 13 km s^{-1} pc^{-1}, implying a total mass within the ring of $\sim 5 \times 10^4\ M_\odot$. In addition, it appears that over a spatial extent of $\sim$3 pc the molecular gas is moving toward the H II regions, on both the near and far side of the ring. Welch et al. (1987) suggest that the rotating ring of UC H II regions indicates a cluster of OB stars that was formed by gravitational fragmentation of the flattened rotating structure associated with the collapse of a single molecular cloud. Other star-forming regions in which the presence of overall gravitational collapse on large size scales involving large ($>10^4\ M_\odot$) masses has been proposed are G34.3+0.15 (Carral & Welch 1992; Heaton et al. 1993), W51 (Rudolph et al. 1990), and G5.89 (Wilner 1993). The hypothesis of global collapse in W49A has, however, been challenged by Serabyn, Güsten, & Schultz (1993), who instead suggest that the enhanced O-star formation has been triggered by a collision of two clouds composed of several clumps (see also Mufson & Liszt 1977). In addition, De Pree et al. (1997) found that the UC H II regions in the ring do not have systematic velocities as a function of position, the individual regions appearing to be associated with distinct molecular clouds observed toward this region.

It is probable that the early evolution of a massive core involves the gravitational contraction of subregions, accompanied by the dissipation of turbulent motions, to finally produce the observed dense hot cores. Nakano's (1998) suggestion that the decay of turbulence in molecular clouds may trigger the formation of stars is supported by recent numerical simulations of MHD waves which show that magnetohydrodynamic turbulence is short-lived and must be constantly replenished (MacLow et al. 1998; Stone, Ostriker, & Gammie 1998). Generalized subsonic motions observed toward low-mass cores have been explained as due to decay of turbulence (Myers & Lazarian 1998). Recently, Shu et al. (1999) proposed that either ambipolar diffusion or turbulent decay will produce scale-free, cen-

trally condensed pivotal states. These pivotal states may correspond to the massive prestellar cores and will dynamically collapse to form massive stars.

The new observational evidence presented in the previous sections shows that accretion disks and molecular outflows appear to be intrinsic to the formation process of high-mass stars. A list of massive young objects associated with both disks and outflows is given in Table 3. This evidence suggests that massive stars are formed in a similar manner as low-mass stars, although in a medium of much larger density. We propose that the formation process of massive stars from prestellar cores, left by a still not well understood combination of accretion, turbulent, and fragmentation processes, is analogous to that of low-mass stars. The clumps giving rise to massive stars are, however, considerably denser and possibly hotter than the dark cores giving rise to low-mass stars. Besides the shorter timescale of the dynamical process involved in the collapse of a massive star, a key difference is in the mass accretion rate. Mass accretion rates as high as $6 \times 10^{-3}\ M_{\odot}\ \mathrm{yr}^{-1}$ have been estimated in collapsing cores associated with high-mass star-forming regions (e.g., W51e2; Zhang & Ho 1997), whereas those associated with the formation of low-mass stars are typically $\sim 10^{-6}\ M_{\odot}\ \mathrm{yr}^{-1}$. The problem posed by the radiative forces on dust halting the accretion inflow can be overcome through the high accretion rates (Wolfire & Cassinelli 1987). Assuming that all the infalling mass reaches the stellar surface, the timescale to form a 30 $M_{\odot}$ star under this infall rate is about 5×10^3 yr. The large values of the mass accretion rates are consistent with the predictions of the inside-out collapse model for a medium with a large amount of initial hydrostatic support, such as in the logatropic cores (see § 5.2.2), and with the large observed mass outflow rates. Using the typically observed line widths of the ammonia emission of $\sim 7\ \mathrm{km\ s}^{-1}$ (FWHM), implying initial turbulent or Alfvenic velocity dispersion of $\sim 3\ \mathrm{km\ s}^{-1}$, equation (16) predicts that $\dot{M}$ should be of the order of $6 \times 10^{-3}\ M_{\odot}\ \mathrm{yr}^{-1}$.

6. SUMMARY

We reviewed the results of recent high spatial resolution observations of free-free emission and molecular line emission made toward regions of high-mass star formation which have significantly contributed to the understanding of the physical conditions, morphologies, and dynamics of the ionized and molecular gas in the immediate vicinity of recently formed massive stars. The main results that are relevant for the study of the formation process of massive stars are summarized as follows.

The radio continuum observations of UC H II regions show that massive stars are formed in clusters. The recombination line observations, which show broad profiles and that the line width increases as size decreases, imply that winds are present from a very early stage in the evolution of newly formed stars. They also provide definitive evidence for the presence of collimated ionized bipolar outflows and indirect evidence of the presence of circumstellar disks.

The observations of ammonia thermal emission show the existence of dense ($>10^5\ \mathrm{cm}^{-3}$), hot (>50 K), and small (<0.1 pc) structures embedded within larger, less dense, and cooler structures of molecular gas. These hot ammonia cores are invariably located near, and in several cases intimately associated with, UC H II regions. The observed kinematics and derived physical conditions of the hot molecular cores have permitted researchers to establish an evolutionary sequence among them. Hot cores in the earliest stage of evolution are undergoing gravitational collapse, with mass accretion rates as high as $6 \times 10^{-3}\ M_{\odot}\ \mathrm{yr}^{-1}$. They exhibit densities up to a few $10^8\ \mathrm{cm}^{-3}$, suggesting that massive

TABLE 3

YOUNG MASSIVE OBJECTS ASSOCIATED WITH DISKS AND OUTFLOWS

Source	Luminosity ($L_{\odot}$)	M_{disk} ($M_{\odot}$)	R_{disk} (AU)	Molecular Outflow?	Jet?	Reference
W3(H_2O).....	(1–10) $\times 10^3$	10–20	<500	Y	Y	1, 2
GL 490.....	2×10^3	10	8500	Y	N	3, 4, 5
AFGL 5142.....	4×10^3	150	6000	Y	N	6
G192.16−3.82.....	3×10^3	15	1000	Y	Y	7, 8
HH 80–81.....	1.7×10^4	30	<4000	Y	Y	9, 10, 11
IRAS 20126+4104.....	1.3×10^4	10	850	Y	Y	12, 13, 14
Cep A HW2	1×10^4	200	750	Y	Y	15, 16
IRAS 23385+6053.....	1.6×10^4	370	10000	Y	N	17

REFERENCES.—(1) Wilner et al. 1995; (2) Reid et al. 1995; (3) Nakamura et al. 1991; (4) Snell et al. 1984; (5) Chini, Henning, & Pfau 1991; (6) Hunter et al. 1999; (7) Shepherd & Kurtz 1999; (8) Shepherd et al. 1998; (9) Yamashita et al. 1991; (10) Yamashita et al. 1989; (11) Martí, Rodríguez, & Reipurth 1993; (12) Cesaroni et al. 1997; (13) Hofner et al. 1999; (14) Zhang et al. 1998b; (15) Gómez et al. 1999; (16) Torrelles et al. 1996; (17) Molinari et al. 1998.

stars form in regions of molecular clouds of exceptionally high density, high temperatures, up to ~ 250 K, and masses of typically a few 10^2 $M_\odot$. Their luminosities imply that they are heated by a recently formed massive star embedded at their centers, but due to the high mass accretion rates they have not yet produced a detectable UC H II region. Hot molecular cores in the latest stage of evolution are intimately associated with UC H II regions and are undergoing outflowing motions, which might be produced either by the expansion of the recently formed H II region or by the presence of molecular outflows. These cores, whose densities and masses are lower than those in early stages and whose luminosities are consistent with heating by the star exciting the UC H II region, are likely to represent remnant structures of molecular gas before being disrupted by the expansion of the H II region.

The observations of methanol and water maser emission show the presence, within dense and hot molecular cores, of linear molecular structures with Keplerian rotation, which provide the most direct evidence of the existence of circumstellar disks around young massive OB stars. The disks may provide intense mass accretion and play an essential role in the formation of massive stars.

The observations of thermal CO emission show the presence of collimated bipolar outflows associated with massive stars, implying that this phenomenon is also a basic component of the formation process of massive stars. The bipolar outflows driven by massive stars are considerably more massive, luminous, and energetic than those associated with low-mass stars. The ionized bipolar outflows associated with UC H II regions are likely to mark a late stage of the massive outflow phenomenon.

To summarize, the observational evidence discussed in this review, showing the existence of hot and very dense molecular structures undergoing large mass accretion rates and attesting that during the process of collapse of massive stars massive disks are formed and that bipolar outflows appear, indicates that the formation of massive stars from massive prestellar cores shares similar characteristics with those of low-mass stars. Although the massive prestellar cores appear in clusters and could be formed by a complex accumulation process starting with smaller clumps within massive clouds, the new observational evidence suggests that massive stars are formed by the collapse of single massive prestellar cores, rather than by an accumulation process, and suggests that the paradigm of low-mass star formation is more universal than previously thought.

We are very grateful to our colleagues E. Churchwell, R. Larson, D. Mardones, J. Moran, and L. F. Rodríguez for many stimulating discussions and comments on the manuscript. G. G. gratefully acknowledges support from a Chilean Presidential Science Fellowship and from the Chilean Fondecyt Project 1980660. S. L. gratefully acknowledges the support of the John Simon Guggenheim Memorial Foundation, of CONACyT and DGAPA/UNAM.

REFERENCES

Acord, J. M., Churchwell, E., & Wood, D. O. S. 1998, ApJ, 495, L107
Acord, J. M., Walmsley, C. M., & Churchwell, E. 1997, ApJ, 475, 693
Afflerbach, A., Churchwell, E., Hofner, P., & Kurtz, S. 1994, ApJ, 437, 697
Allen, A., & Shu, F. H. 1999, in preparation
Andersson, M., & Garay, G. 1986, A&A, 167, L1
André, P., Ward-Thompson, D., & Barsony, M. 1993, ApJ, 406, 122
Arons, J., & Max, C. E. 1975, ApJ, 196, L77
Arthur, S. J., & Lizano, S. 1997, ApJ, 484, 810
Bachiller, R. 1996, ARA&A, 34, 111
Bachiller, R., & Cernicharo, J. 1990, A&A, 239, 276
Ballesteros-Paredes, J., Vázquez-Semadeni, E., & Scalo, J. 1999, ApJ, 515, 286
Barrett, A. H., Ho, P. T. P., & Martin, R. N. 1975, ApJ, 198, L119
Barrett, A. H., Schwartz, P. R., & Waters, J. W. 1971, ApJ, 168, L101
Basu, S., & Mouschovias, T. Ch. 1994, ApJ, 432, 720
Batrla, W., Matthews, H. E., Menten, K. M., & Walmsley, C. M. 1987, Nature, 326, 49
Batrla, W., & Menten, K. M. 1988, ApJ, 329, L117
Bertoldi, F., & McKee, C. F. 1992, ApJ, 395, 140
Berulis, I. I., & Ershow, A. A. 1983, Soviet Astron. Lett., 9, 341
Blitz, L. 1991, in The Physics of Star Formation and Early Stellar Evolution, ed. C. J. Lada & N. D. Kylafis (Dordrecht: Kluwer), 3
———. 1993, in Protostars and Planets III, ed. E. H. Levy & J. I. Lunine (Tucson: Univ. Arizona Press), 125
Bloemhof, E. E., Reid, M. J., & Moran, J. M. 1992, ApJ, 397, 500
Bodenheimer, P., Tenorio-Tagle, G., & Yorke, H. W. 1979, ApJ, 233, 85
Bonnell, I. A., Bate, M. R., Clarke, C. J., & Pringle, J. E. 1997, MNRAS, 285, 201
Bonnell, I. A., & Davies, M. B. 1998, MNRAS, 295, 691
Brown, R. L., Lockman, F. J., & Knapp, G. R. 1978, ARA&A, 16, 445
Cabrit, S., & Bertout, C. 1992, A&A, 261, 274
Campbell, B. 1984, ApJ, 282, L27
Carpenter, J. M., Meyer, M. R., Dougados, C., Strom, S. E., & Hillenbrand, L. A. 1997, AJ, 114, 198
Carral, P., Kurtz, S. E., Rodríguez, L. F., De Pree, C., & Hofner, P. 1997, ApJ, 486, L103
Carral, P., & Welch, W. J. 1992, ApJ, 385, 244
Caselli, P., & Myers, P. 1995, ApJ, 446, 665
Castor, J., McCray, R., & Weaver, R. 1975, ApJ, 200, L107
Caswell, J. L., Vaile, R. A., Ellingsen, S. P., Whiteoak, J. B., & Norris, R. P. 1995a, MNRAS, 272, 96

Caswell, J. L., Vaile, R. A., & Forster, J. R. 1995b, MNRAS, 277, 210
Cesaroni, R., Churchwell, E., Hofner, P., Walmsley, C. M., & Kurtz, S. 1994a, A&A, 288, 903
Cesaroni, R., Felli, M., Testi, L., Walmsley, C. M., & Olmi, L. 1997, A&A, 325, 725
Cesaroni, R., Hofner, P., Walmsley, C. M., & Churchwell, E. 1998, A&A, 331, 709
Cesaroni, R., Olmi, L., Walmsley, C. M., Churchwell, E., & Hofner, P. 1994b, ApJ, 435, L137
Cesaroni, R., Walmsley, C. M., & Churchwell, E. 1992, A&A, 256, 618
Cesaroni, R., Walmsley, C. M., Kömpe, C., & Churchwell, E. 1991, A&A, 252, 278
Chini, R., Henning, Th., & Pfau, W. 1991, A&A, 247, 157
Chiueh, T., & Chou, J. 1994, ApJ, 431, 380
Churchwell, E. 1990, A&A Rev., 2, 79
———. 1991, in The Physics of Star Formation and Early Stellar Evolution, ed. C. J. Lada & N. D. Kylafis (Dordrecht: Kluwer), 221
———. 1993, in ASP Conf. Ser. 35, Massive Stars: Their Lives in the Interstellar Medium, ed. J. P. Casinelli & E. B. Churchwell (San Francisco: ASP), 35
———. 1997, in Herbig-Haro Flows and Low-Mass Star Formation, ed. B. Reipurth & C. Bertout (Dordrecht: Kluwer), 525
———. 1999, in Unsolved Problems in Stellar Evolution, ed. M. Livio (Cambridge: Cambridge Univ. Press), in press
Churchwell, E., Smith, L. F., Mathis, J., Mezger, P. G., & Huchtmeier, W. 1978, A&A, 70, 719
Churchwell, E., Walmsley, C. M., & Cesaroni, R. 1990, A&AS, 83, 119 (CWC90)
Ciolek, G. E., & Mouschovias, T. Ch. 1994, ApJ, 425, 142
Ciolek, G. E., & Königl, A. 1998, ApJ, 504, 257
Codella, C., & Felli, M. 1995, A&A, 302, 521
Codella, C., Felli, M., & Natale, V. 1994a, A&A, 284, 233
Codella, C., Felli, M., & Natale, V., Palagi, F., & Palla, F. 1994b, A&A, 291, 261
Colley, D. 1980, MNRAS, 193, 495
Contopoulos, I., Ciolek, G. E., & Königl, A. 1998, ApJ, 504, 247
Crutcher, R. M. 1999, ApJ, 520, 706
Danby, G., Flower, D. R., Valiron, P., Schilke, P., & Walmsley, C. M. 1988, MNRAS, 235, 229
De Pree, C. G., Gaume, R. A., Goss, W. M., & Claussen, M. J. 1995c, ApJ, 451, 284
———. 1996, ApJ, 464, 788
De Pree, C. G., Goss, W. M., Palmer, P., & Rubin, R. H. 1994, ApJ, 428, 670
De Pree, C. G., Mehringer, D. M., & Goss, W. M. 1997, ApJ, 482, 307
De Pree, C. G., Rodríguez, L. F., Dickel, H. R., & Goss, W. M. 1995a, ApJ, 447, 220
De Pree, C. G., Rodríguez, L. F., & Goss, W. M. 1995b, Rev. Mexicana Astron. Astrofis., 31, 39
Dougados, C., Lena, P., Ridgway, S. T., Christou, J. C., & Probst, R. G. 1993, ApJ, 406, 112
Downes, D. 1987, in Star Forming Regions, ed. M. Peimbert & J. Jugaku (Dordrecht: Reidel), 93
Dreher, J. W., Johnston, K. J., Welch, W. J., & Walker, R. C. 1984, ApJ, 283, 632
Dyson, J. E. 1994, in Star Formation and Techniques in Infrared and mm-Wave Astronomy, ed. T. P. Ray & S. V. W. Beckwith (Berlin: Springer-Verlag), 93
Dyson, J. E., & Williams, D. A. 1980, The Physics of the Interstellar Medium (New York: Wiley)
Dyson, J. E., Williams, R. J. R., & Redman, M. P. 1995, MNRAS, 277, 700
Elitzur, M. 1982, Rev. Mod. Phys., 54, 1225
Ellingsen, S. P., Norris, R. P., & McCulloch, P. M. 1996, MNRAS, 279, 101
Fey, A. L., Claussen, M. J., Gaume, R. A., Nedoluha, G. E., & Johnston, K. J. 1992, AJ, 103, 234
Fey, A. L., Gaume, R. A., Claussen, M. J., & Vrba, F. J. 1995, ApJ, 453, 308
Foster, P. N., & Chevalier, R. A. 1993, ApJ, 416, 303
Franco, J., Tenorio-Tagle, G., & Bodenheimer, P. 1990, ApJ, 349, 126
Fuller, G. A., & Myers, P. C. 1987, in Physical Processes in Interstellar Clouds, ed. M. Scholer (Dordrecht: Reidel), 137
———. 1992, ApJ, 384, 523
Galli, D., Lizano, S., Li, Z.-Y., Adams, F. C., & Shu, F. H. 1999, ApJ, 521, 630
Galli, D., & Shu, F. H. 1993a, ApJ, 417, 220
———. 1993b, ApJ, 417, 243
Garay, G., Lizano, S., & Gómez, Y. 1994, ApJ, 429, 268
Garay, G., Moran, J. M., & Rodríguez, L. F. 1993a, ApJ, 413, 582
Garay, G., Moran, J. M., Rodríguez, L. F., & Reid, M. J. 1998, ApJ, 492, 635
Garay, G., Reid, M. J., & Moran, J. M. 1985, ApJ, 289, 681
Garay, G., & Rodríguez, L. F. 1983, ApJ, 266, 263
———. 1990, ApJ, 362, 191
Garay, G., Rodríguez, L. F., Moran, J. M., & Churchwell, E. 1993b, ApJ, 418, 368
Garay, G., Rodríguez, L. F., & van Gorkom, J. H. 1986, ApJ, 309, 553
García-Segura, G., & Franco, J. 1996, ApJ, 469, 171
Garden, R. P., Hayashi, M., Gatley, I., & Hasegawa, T. 1991, ApJ, 374, 540
Gaume, R. A., & Claussen, M. J. 1990, ApJ, 351, 538
Gaume, R. A., Claussen, M. J., De Pree, C. G., Goss, W. M., & Mehringer, D. M. 1995a, ApJ, 449, 663
Gaume, R. A., Fey, A. L., & Claussen, M. J. 1994, ApJ, 432, 648
Gaume, R. A., Goss, W. M., Dickel, H. R., Wilson, T. L., & Johnston, K. J. 1995b, ApJ, 438, 776
Gaume, R. A., Johnston, K. J., Nguyen, H. A., Wilson, T. L., Dickel, H. R., Goss, W. M., & Wright, M. C. H. 1991, ApJ, 376, 608
Gaume, R. A., Johnston, K. J., & Wilson, T. L. 1993, ApJ, 417, 645
Gaume, R. A., & Mutel, R. L. 1987, ApJS, 65, 193
Genzel, R. 1991, in The Physics of Star Formation and Early Stellar Evolution, ed. C. J. Lada & N. D. Kylafis (Dordrecht: Kluwer), 155
Genzel, R., & Downes, D. 1977, A&AS, 30, 145
Genzel, R., Downes, D., Ho, P. T. P., & Bieging, J. 1982, ApJ, 259, L103
Genzel, R., et al. 1978, A&A, 66, 13
Genzel, R., Reid, M. J., Moran, J. M., & Downes, D. 1981, ApJ, 244, 884
Gómez, Y., Garay, G., & Lizano, S. 1995, ApJ, 453, 727
Gómez, Y., Rodríguez, L. F., Garay, G., & Moran, J. M. 1991, ApJ, 377, 519
Gómez, J. F., Sargent, A., Torrelles, J. M., Ho, P. T. P., Rodríguez, L. F., Cantó, J., & Garay, G. 1999, ApJ, 514, 287
Gordon, M. A. 1988, in Galactic and Extra-galactic Radio Astronomy, ed. G. L. Verschuur & K. I. Kellerman (New York: Springer), 37
Güsten, R., & Mezger, P. G. 1983, Vistas Astron., 26, 159
Habing, H. J., & Israel, F. P. 1979, ARA&A, 17, 345

Hartquist, T. W., & Dyson, J. E. 1993, QJRAS, 34, 57
Harvey, P. M., & Forveille, T. 1988, A&A, 197, 19
Harvey, P. M., Lester, D. F. Colomé, C., Smith, B., Monin, J.-L., & Vaughlin, I. 1994, ApJ, 433, 187
Heaton, B. D., Little, L. T., & Bishop, I. S. 1989, A&A, 213, 148
Heaton, B. D., Little, L. T., Yamashita, T., Davies, S. R., Cunningham, C. T., & Monteiro, T. S. 1993, A&A, 278, 238
Heaton, B. D., Matthews, N., Little, L. T., & Dent, W. R. F. 1985, MNRAS, 217, 485
Heiles, C., Goodman, A. A., McKee, C. F., & Zweibel, E. G. 1993, in Protostars and Planets III, ed. E. H. Levy & J. I. Lunine (Tucson: Univ. Arizona Press), 279
Henkel, C., Wilson, T. L., & Johnston, K. J. 1984, ApJ, 282, L93
Henkel, C., Wilson, T. L., & Mauersberger, R. 1987, A&A, 182, 137
Hillenbrand, L. A. 1997, AJ, 113, 1733
Hillenbrand, L. A., & Hartmann, L. W. 1998, ApJ, 492, 540
Ho, P. T. P. 1972, Ph.D. thesis, Massachusetts Inst. Tech.
Ho, P. T. P., & Haschick, A. D. 1981, ApJ, 248, 622
———. 1986, ApJ, 304, 501
Ho, P. T. P., Terebey, S., & Turner, J. L. 1994, ApJ, 423, 320
Ho, P. T. P., & Townes, C. 1983, ARA&A, 21, 239
Ho, P. T. P., & Young, L. M. 1996, ApJ, 472, 742
Hofner, P., Cesaroni, R., Rodríguez, L. F., & Martí, F. 1999, A&A, 345, L43
Hofner, P., & Churchwell, E. 1996, A&AS, 120, 283
Hofner, P., Kurtz, S., Churchwell, E., Walmsley, C. M., & Cesaroni, R. 1994, ApJ, 429, L85
———. 1996, ApJ, 460, 359
Hollenbach, D., Johnstone, D., Lizano, S., & Shu, F. H. 1994, ApJ, 428, 654
Hunter, C. 1977, ApJ, 218, 834
Hunter, T. R., Neugebauer, G., Benford, D. J., Matthews, K., Lis, D. C., Serabyn, E., & Phillips, T. G. 1998, ApJ, 493, L97
Hunter, T. R., Testi, L., Zhang, Q., & Sridharan, T. K. 1999, ApJ, in press
Jackson, J. M., Ho, P. T. P., & Haschick, A. D. 1988, ApJ, 333, 73
Jijina, J., & Adams, F. C. 1996, ApJ, 462, 874
Johnson, C. O., De Pree, C. G., & Goss, W. M. 1998, ApJ, 500, 302
Kahn, F. D. 1974, A&A, 37, 149
Kastner, J. H., Weintraub, D. A., Snell, R. L., Sandell, G., Aspin, C., Hughes, D. H., & Baas, F. 1994, ApJ, 425, 695
Kaufman, M. J., Hollenbach, D. J., & Tielens, A. G. G. 1988, ApJ, 497, 276
Kawamura, J. H., & Masson, C. R. 1998, ApJ, 509, 270
Keto, E. R. 1990, ApJ, 350, 722
Keto, E. R., & Ho, P. T. P. 1989, ApJ, 347, 349
Keto, E. R., Ho, P. T. P., & Haschick, A. D. 1987a, ApJ, 318, 712
———. 1988, ApJ, 324, 920
Keto, E. R., Ho, P. T. P., & Reid, M. J. 1987b, ApJ, 323, L117
Keto, E. R., Welch, W. J., Reid, M. J., & Ho, P. T. P. 1995, ApJ, 444, 769
Klessen, R. S., Burkert, A., & Bate, M. R. 1998, ApJ, 501, L205
Kraemer, K. E., & Jackson, J. M. 1995, ApJ, 439, L9
Kraemer, K. E., Jackson, J. M., Paglione, A. D., & Bolatto, A. D. 1997, ApJ, 478, 614
Kurtz, S., Cesaroni, R., Churchwell, E., Hofner, P., & Walmsley, M. 1999b, in Protostars and Planets IV, ed. V. Mannings, A. P. Boss, & S. S. Russell (Tucson: Univ. Arizona Press), in press
Kurtz, S., Churchwell, E., & Wood, D. O. S. 1994, ApJS, 91, 659
Kurtz, S. E., Watson, A. M., Hofner, P., & Otte, B. 1999a, ApJ, 514, 232
Lada, C. J. 1991, in The Physics of Star Formation and Early Stellar Evolution, ed. C. J. Lada & N. D. Kylafis (Dordrecht: Kluwer), 329
Lada, E. A., Evans, N. J., II, Depoy, D. L., & Gatley, I. 1991, ApJ, 371, 171
Larson, R. B. 1969, MNRAS, 145, 271
———. 1972, MNRAS, 156, 437
———. 1978, MNRAS, 184, 69
———. 1981, MNRAS, 194, 809
———. 1982, MNRAS, 200, 159
———. 1985, MNRAS, 214, 379
———. 1990, in Physical Processes in Fragmentation and Star Formation, ed. R. Capuzzo-Dolcetta, C. Chiosi, & A. DiFazio (Dordrecht: Kluwer), 389
———. 1992, MNRAS, 256, 641
———. 1999, in ASP Conf. Ser., The Orion Complex Revisited, ed. M. J. McCaughrean & A. Burkert (San Francisco: ASP), in press
Larson, R. B., & Starrfield, S. 1971, A&A, 13, 190
Layzer, D. 1963, ApJ, 137, 351
Lester, D. F., Becklin, E. E., Genzel, R., & Wynn-Williams, C. G. 1985, AJ, 90, 2331
Li, Z.-Y. 1998a, ApJ, 493, 230
———. 1998b, ApJ, 497, 850
Li, Z.-Y., & Shu, F. H. 1996, ApJ, 472, 211
———. 1997, ApJ, 475, 237
Lienert, C. 1986, A&A, 155, L6
Lizano, S., & Cantó, J. 1995, Rev. Mexicana Astron. Astrofis. Conf. Ser., 1, 29
Lizano, S., Cantó, J., Garay, G., & Hollenbach, D. 1996, ApJ, 468, 739
Lizano, S., & Shu, F. H. 1989, ApJ, 342, 834
Lo, K. Y., Burke, B. F., & Haschick, A. D. 1975, ApJ, 202, 81
Lumsden, S. L., & Hoare, M. G. 1996, ApJ, 464, 272
MacLaren, I., Richardson, K. M., & Wolfendale, A. W. 1988, ApJ, 333, 821
MacLow, M.-M., Klessen, R. S., Burkert, A., Smith, M. D., & Kessel, O. 1998, Phys. Rev. Lett., 80, 2754
MacLow, M.-M., & McCray, R. 1988, ApJ, 324, 776
MacLow, M.-M., Van Buren, D., Wood, D. O. S., & Churchwell, E. 1991, ApJ, 369, 395
Madden, S. C., Irvine, W. M., Matthews, H. E., Brown, R. D., & Godfrey, P. D. 1986, ApJ, 300, L79
Mardones, D. 1998, Ph.D. thesis, Harvard Univ.
Martí, F., Rodríguez, L. F., & Reipurth, B. 1993, ApJ, 416, 208
Matthews, N., Little, L. T., Macdonald, G. H., Andersson, M., Davies, S. R., Riley, P. W., Dent, W. R. F., & Vizard, D. 1987, A&A, 184, 284
Mauersberger, R., Henkel, C., & Wilson, T. L. 1987, A&A, 173, 352
Mauersberger, R., Henkel, C., Wilson, T. L., & Walmsley, C. M. 1986, A&A, 162, 199
McCaughrean, M. J., & Stauffer, J. R. 1994, AJ, 108, 1382
McKee, C. F. 1989, ApJ, 345, 782
McKee, C. F., Zweibel, E. G., Goodman, A. A., & Heiles, C. 1993, in Protostars and Planets III, ed. E. H. Levy & J. I. Lunine (Tucson: Univ. Arizona Press), 327
McLaughlin, D. E., & Pudritz, R. E. 1996, ApJ, 469, 194
McLeod, G. C., & Gaylard, M. J. 1992, MNRAS, 256, 519
Megeath, S. T., Herter, T., Beichman, C., Gautier, N., Hester, J. J., Rayner, J., & Shupe, D. 1996, A&A, 307, 775
Menten, K. M. 1991, ApJ, 380, L75
Menten, K. M., Johnston, K. J., Wadiak, E. J., Walmsley, C. M., & Wilson, T. L. 1988, ApJ, 331, L41
Menten, K. M., Walmsley, C. M., Henkel, C., & Wilson, T. L. 1986, A&A, 157, 318
Mestel, L., & Spitzer, L., Jr. 1956, MNRAS, 116, 503

Mezger, P. G., Chini, R., Kreysa, E., Wink, J. E., & Salter, C. J. 1988, A&A, 191, 44
Mezger, P. G., & Henderson, A. P. 1967, ApJ, 147, 471
Molinari, S., Testi, L., Brand, J., Cesaroni, R., & Palla, F. 1998, ApJ, 505, L39
Monaghan, J. J., & Lattanzio, J. G. 1991, ApJ, 375, 177
Moore, T. J. T., Chandler, C. J., Gear, W. K., & Mountain, C. M. 1989, MNRAS, 237, 1p.
Moran, J. M. 1990, in Molecular Astrophysics, ed. T. Hartquist (Cambridge: Cambridge Univ. Press), 397
Mouschovias, T. C., & Spitzer, L., Jr. 1976, ApJ, 210, 326
Mufson, S. L., & Liszt, H. S. 1977, ApJ, 212, 664
Myers, P. C. 1983, ApJ, 270, 105
Myers, P. C., & Benson, P. J. 1983, ApJ, 266, 309
Myers, P. C., & Fuller, G. A. 1992, ApJ, 396, 631
Myers, P. C., & Goodman, A. A. 1988, ApJ, 329, 392
Myers, P. C., & Lazarian, A. 1998, ApJ, 507, L157
Nakamura, F., Hanawa, T., & Nakano, T. 1995, ApJ, 444, 770
Nakamura, A., Kawabe, R., Kitamura, Y., Ishiguro, M., Murata, Y., & Ohashi, N. 1991, ApJ, 383, L81
Nakano, T. 1979, PASJ, 31, 697
———. 1982, PASJ, 34, 337
———. 1998, ApJ, 494, 587
Natta, A., Grinin, V. P., & Mannings, V. 1999, in Protostars and Planets IV, ed. V. Mannings, A. P. Boss, & S. S. Russell (Tucson: Univ. Arizona Press), in press
Norris, R. P., et al. 1998, ApJ, 508, 275
Norris, R. P., Caswell, J. L., Gardner, F. F., & Wellington, K. J. 1987, ApJ, 321, L159
Norris, R. P., McCutcheon, W. H., Caswell, J. L., Wellington, K. J., Reynolds, J. E., Peng, R. S., & Kesteven, M. J. 1988, Nature, 335, 149
Norris, R. P., Whiteoak, J. B., Caswell, J. L., Wieringa, M. H., & Gough, R. G. 1993, ApJ, 412, 222
Olmi, L., Cesaroni, R., Neri, R., & Walmsley, C. M. 1996, A&A, 315, 565
Osorio, M., Lizano, S., & D'Alessio, P. 1999, ApJ, in press
Palagi, F., Cesaroni, R., Comoretto, G., Felli, M., & Natale, V. 1993, A&AS, 101, 153
Panagia, N. 1973, AJ, 78, 929
Panagia, N., & Felli, M. 1975, A&A, 39, 1
Penston, M. V. 1969, MNRAS, 144, 425
Plambeck, R. L., & Menten, K. M. 1990, ApJ, 364, 555
Plambeck, R. L., Wright, M. C. H., & Carlstrom, J. E. 1990, ApJ, 348, L65
Plume, R., Jaffe, D. T., & Evans, N. J., II. 1992, ApJS, 78, 505
Pratap, P., Menten, K. M., Reid, M. J., Moran, J. M., & Walmsley, C. M. 1991, ApJ, 373, L13
Pratap, P., Menten, K. M., & Snyder, L. E. 1994, ApJ, 430, L129
Raga, A. C. 1986, ApJ, 300, 745
Reid, M. J., Argon, A. L., Masson, C. R., Menten, K. M., & Moran, J. M. 1995, ApJ, 443, 238
Reid, M. J., & Ho, P. T. P. 1985, ApJ, 288, L17
Reid, M. J., & Moran, J. M. 1981, ARA&A, 19, 231
———. 1988, in Galactic and Extragalactic Radio Astronomy, ed. G. L. Verschuur & K. I. Kellermann (New York: Springer), 255
Reid, M. J., Myers, P. C., & Bieging, J. H. 1987, ApJ, 312, 830
Reid, M. J., Schneps, M. H., Moran, J. M., Gwinn, C. R., Genzel, R., Downes, D., & Rönnäng, B. 1988, ApJ, 330, 809
Richer, J., Shepherd, D. S., Cabrit, S., Bachiller, R., & Churchwell, E. 1999, in Protostars and Planets IV, ed. V. Mannings, A. P. Boss, & S. S. Russell (Tucson: Univ. Arizona Press), in press
Richling, S., & Yorke, H. W. 1997, A&A, 327, 317
Rodríguez, L. F., Cantó, J., & Moran, J. M. 1982, ApJ, 255, 103
Rodríguez, L. F., Cantó, J., & Moran, J. M. 1988, ApJ, 333, 801
Rodríguez, L. F., Garay, G., Curiel, S., Ramírez, S., Torrelles, J. M., Gómez, Y., & Velázquez, A. 1994, ApJ, 430, L65
Roelfsema, P. R. 1987, Ph.D. thesis, Univ. Groningen
Roth, M., Tapia, M., Gómez, Y., & Rodríguez, L. F. 1988, Rev. Mexicana Astron. Astrofis., 16, 3
Rudolph, A., Welch, W. J., Palmer, P., & Dubrulle, B. 1990, ApJ, 363, 528
Safier, P. N., McKee, C. F., & Stahler, S. W. 1997, ApJ, 485, 660
Sams, B. J., III, Moran, J. M., & Reid, M. J. 1996, ApJ, 459, 632
Scoville, N. Z., & Kwan, J. 1976, ApJ, 206, 718
Scoville, N. Z., Sargent, A. I., Sanders, D. B., Claussen, M. J., Masson, C. R., Lo, K. Y., & Phillips, T. G. 1986, ApJ, 303, 416
Serabyn, E., Güsten, R., & Schultz, A. 1993, ApJ, 413, 571
Shepherd, D. S., & Churchwell, E. 1996a, ApJ, 457, 267
———. 1996b, ApJ, 472, 225
Shepherd, D. S., Churchwell, E., & Wilner, D. J. 1997, ApJ, 482, 355
Shepherd, D. S., & Kurtz, S. E. 1999, ApJ, 523,
Shepherd, D. S., Watson, A. M., Sargent, A. I., & Churchwell, E. 1998, ApJ, 507, 861
Shu, F. H. 1977, ApJ, 214, 488
———. 1991, in The Physics of Star Formation and Early Stellar Evolution, ed. C. J. Lada & N. D. Kylafis (Dordrecht: Kluwer), 365
———. 1995, in Molecular Clouds and Star Formation, ed. C. Youan & J. H. You (Singapore: World Scientific), 97
Shu, F. H., Adams, F. C., & Lizano, S. 1987, ARA&A, 25, 23
Shu, F. H., Allen, A., Shang, H., Ostriker, E. C., & Li, Z.-Y. 1999, in Physics of Star Formation and Early Stellar Evolution II, ed. C. J. Lada & N. D. Kylafis (Dordrecht: Kluwer), in press
Shu, F. H., & Li, Z.-Y. 1997, ApJ, 475, 251
Shu, F. H., Najita, J., Galli, D., Ostriker, E., & Lizano, S. 1993, Protostars and Planets III, ed. E. H. Levy & J. I. Lunine (Tucson: Univ. Arizona Press), 3
Shull, M. J. 1980, ApJ, 238, 860
Silk, J., & Takahashi, T. 1979, ApJ, 229, 242
Slysh, V. I., Kalenskii, S. V., & Val'tts, I. E. 1995, ApJ, 442, 668
Snell, R. L., Scoville, N. Z., Sanders, D. B., & Erickson, N. R. 1984, ApJ, 284, 176
Spitzer, L. 1978, Physical Processes in the Intestellar Medium (New York: Wiley Interscience)
———. 1982, Searching between Stars (New Haven: Yale Univ. Press), 148
Stahler, S. W., Palla, F., & Ho, P. T. P. 1999, in Protostars and Planets IV, ed. V. Mannings, A. P. Boss, & S. S. Russell (Tucson: Univ. Arizona Press), in press
Stecklum, B., et al. 1998, First Circumstellar Disk around a Massive Star (ESO press release PR-08-98)
Stone, J. M., Ostriker, E. C., & Gammie, C. F. 1998, ApJ, 508, L99
Strömgren, B. 1939, ApJ, 89, 526
Tafalla, M., Mardones, D., Myers, P. C., Caselli, P., Bachiller, R., & Benson, P. J. 1998, ApJ, 504, 900
Tenorio-Tagle, G. 1979, A&A, 71, 59
Terebey, S., Shu, F. H., & Cassen, P. M. 1984, ApJ, 286, 529
Tieftrunk, A. R., Gaume, R. A., Claussen, M. J., Wilson, T. L., & Johnston, K. J. 1997, A&A, 318, 931
Tieftrunk, A. R., Gaume, R. A., & Wilson, T. L. 1998b, A&A, 340, 232
Tieftrunk, A. R., Megeath, S. T., Wilson, T. L., & Rayner, J. T. 1998a, A&A, 336, 991
Tohline, J. E. 1980a, ApJ, 235, 866
———. 1980b, ApJ, 239, 417
Tomisaka, K. 1995, ApJ, 438, 226

Tomisaka, K. 1996, PASJ, 48, 701
Tomisaka, K., Ikeuchi, S., & Nakamura, T. 1988, ApJ, 335, 239
———. 1989, ApJ, 341, 220
———. 1990, ApJ, 362, 201
Torrelles, J. M., Gómez, J. F., Garay, G., Rodríguez, L. F., Curiel, S., Cohen, R. J., & Ho, P. T. P. 1998b, ApJ, 509, 262
Torrelles, J. M., Gómez, J. F., Rodríguez, L. F., Curiel, S., Anglada, G., & Ho, P. T. P. 1998a, ApJ, 505, 756
Torrelles, J. M., Gómez, J. F., Rodríguez, L. F., Curiel, S., Ho, P. T. P., & Garay, G. 1996, ApJ, 457, L107
Torrelles, J. M., Gómez, J. F., Rodríguez, L. F., Ho, P. T. P., Curiel, S., & Vázquez, R. 1997, ApJ, 489, 744
Turner, B. E., & Matthews, H. E. 1984, ApJ, 277, 164
Ungerechts, H., Walmsley, C. M., & Winnewiser, G. 1980, A&A, 88, 259
Val'tts, I. E., Dzura, A. M., Kalenskii, S. V., Slysh, V. I., Booth, R. S., & Winnberg, A. 1995, A&A, 294, 825
Van Buren, D. 1985, ApJ, 294, 567
Van Buren, D., & Mac Low, M.-M. 1992, ApJ, 394, 534
Van Buren, D., Mac Low, M.-M., Wood, D. O. S., & Churchwell, E. 1990, ApJ, 353, 570
Van Dishoeck, E. F., & Blake, G. A. 1998, ARA&A, 36, 317
Vázquez-Semadeni, E., Passot, T., & Pouquet, A. 1996, ApJ, 473, 881
Vogel, S. N., Genzel, R., & Palmer, P. 1987, ApJ, 316, 243
Vogel, S. N., & Welch, W. J. 1983, ApJ, 269, 568
Walmsley, C. M. 1989, in Evolution of Interstellar Dust and Related Topics, ed. A. Bonetti, J. M. Greenberg, & S. Aiello (Amsterdam: Elsevier), 179
———. 1990, in Chemistry and Spectroscopy of Interstellar Molecules, ed. D. K. Bohme et al. (Tokyo: Univ. Tokyo Press), 267
———. 1995, Rev. Mexicana Astron. Astrofis. Conf. Ser., 1, 137
Walmsley, C. M., & Ungerechts, H. 1983, A&A, 122, 164
Weaver, H., Williams, R. W., Dieter, N. H., & Lum, W. T. 1965, Nature, 208, 29
Welch, W. J., Dreher, J. W., Jackson, J. M., Terebey, S., & Vogel, S. N. 1987, Science, 238, 1550
Welch, W. J., & Marr, J. 1987, ApJ, 317, L21
Whitworth, A. P., & Summers, D. 1985, MNRAS, 214, 1
Williams, J. P., & McKee, C. F. 1997, ApJ, 476, 166
Wilner, D. J. 1993, Ph.D. thesis, Univ. California, Berkeley
Wilner, D. J., Welch, W. J., & Foster, J. R. 1995, ApJ, 449, L73
Wilson, T. L., Gaume, R. A., & Johnston, K. J. 1991, A&A, 251, L7
———. 1993, ApJ, 402, 230
Wilson, T. L., Gaume, R. A., & Johnston, K. J., & Tieftrunk, A. R. 1995, ApJ, 452, 693
Wilson, T. L., & Henkel, C. 1988, A&A, 206, L26
Wilson, T. L., & Walmsley, C. M. 1989, A&A Rev., 1, 141
Wilson, T. L., Walmsley, C. M., Menten, K. M., & Hermsen, W. 1985, A&A, 147, L19
Wilson, T. L., Walmsley, C. M., Snyder, L. E., & Jewell, P. R. 1984, A&A, 134, L7
Wolfire, M. G., & Casinelli, J. P. 1987, ApJ, 319, 850
Wood, D. O. S. 1993, in ASP Conf. Ser. 35, Massive Stars: Their Lives in the Interstellar Medium, ed. J. P. Casinelli & E. Churchwell (San Francisco: ASP), 108
Wood, D. O. S., & Churchwell, E. 1989a, ApJS, 69, 831
———. 1989b, ApJ, 340, 265
———. 1991, ApJ, 372, 199
Xie, T., Mundy, L. G., Vogel, S. N., & Hofner, P. 1996, ApJ, 473, L131
Yamashita, T., Murata, Y., Kawabe, R., Kaifu, N., & Tamura, M. 1991, ApJ, 373, 560
Yamashita, T., Suzuki, H., Kaifu, N., Tamura, M., Mountain, C. M., & Moore, T. J. T. 1989, ApJ, 347, 894
Yorke, H. W. 1984, in Workshop on Star Formation, ed. R. D. Wolstencroft (Edinburgh: Royal Obs.), 63
Yorke, H. W., & Krügel, E. 1977, A&A, 54, 183
Yorke, H. W., Tenorio-Tagle, G., & Bodenheimer, P. 1983, A&A, 127, 313
———. 1984, A&A, 138, 325
Yorke, H. W., & Welz, A. 1996, A&A, 315, 555
Zhang, Q., & Ho, P. T. P. 1995, ApJ, 450, L63
———. 1997, ApJ, 488, 241
Zhang, Q., Ho, P. T. P., & Ohashi, N. 1998a, ApJ, 494, 636
Zhang, Q., Hunter, T. R., & Sridharan, T. K. 1998b, ApJ, 505, L151
Zhou, S., Evans, N. J., II, Butner, H. M., Kutner, M. L., Leung, C. M., & Mundy, L. G. 1990, ApJ, 363, 168
Zijlstra, A. A., Pottasch, S. R., Engels, D., Roelfsema, P. R., te Linkel Hekkert, P., & Umana, G. 1990, MNRAS, 246, 217